W boson mass measurements at the LHC

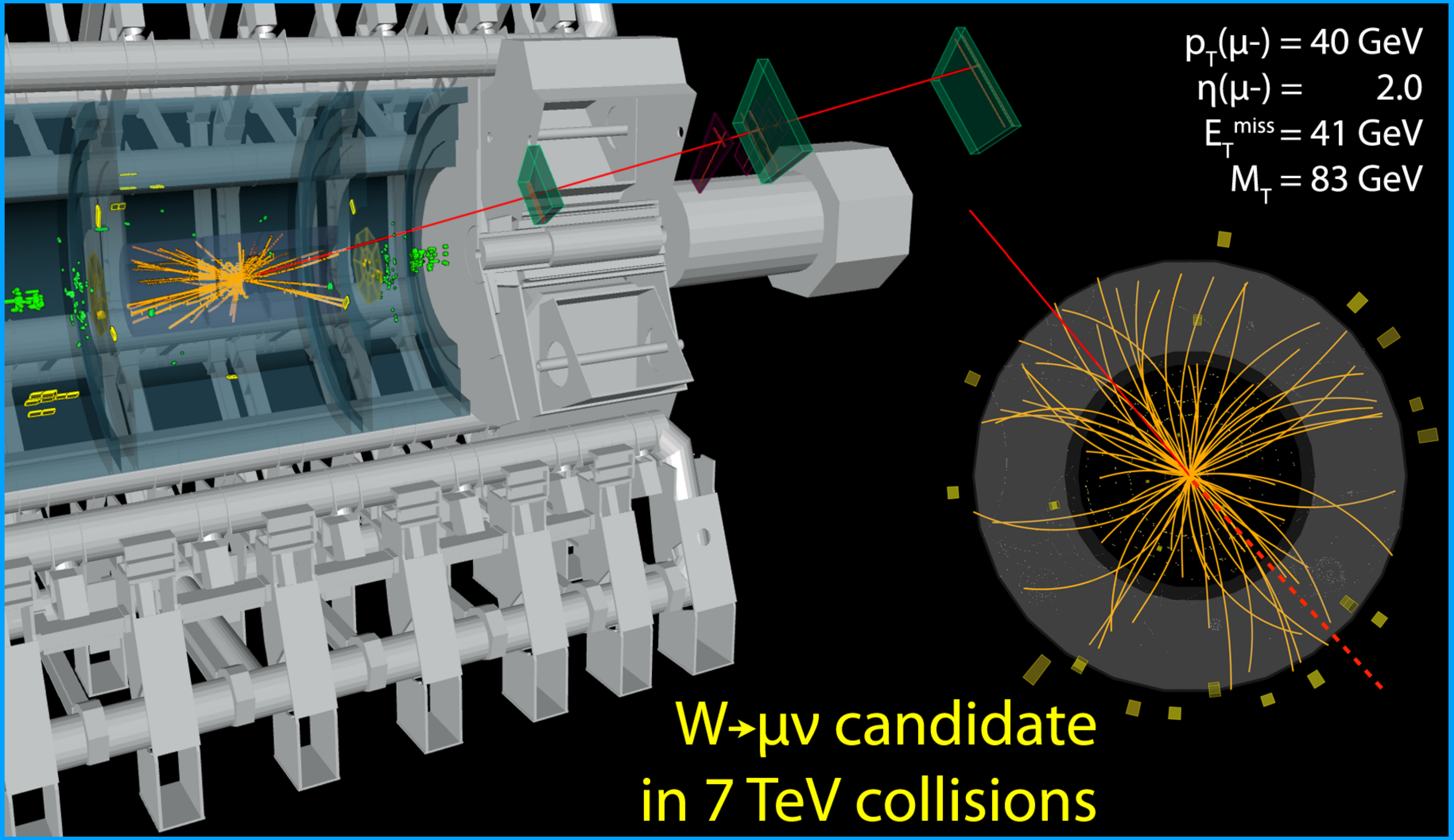

Chris Hays, Oxford University

Roma Tre Topical Seminar
13 December, 2022

Hadron-collider W boson mass measurements

$\sqrt{s} = 1.96$ TeV proton-antiproton collisions from the Fermilab Tevatron

CDF: 8.8 fb^{-1} of integrated luminosity
D0: 5.3 fb^{-1} of integrated luminosity

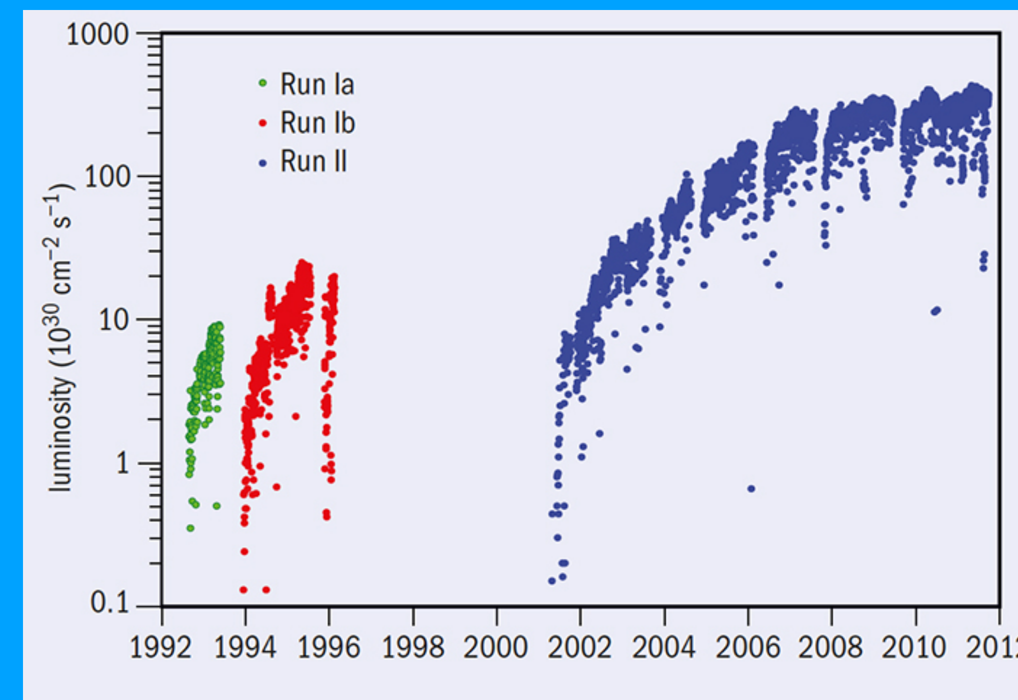

$\sqrt{s} = 7, 13$ TeV proton-proton collisions from the Large Hadron Collider

ATLAS: 4.1 fb^{-1} of integrated luminosity (7 TeV)
LHCb: 1.7 fb^{-1} of integrated luminosity (13 TeV)

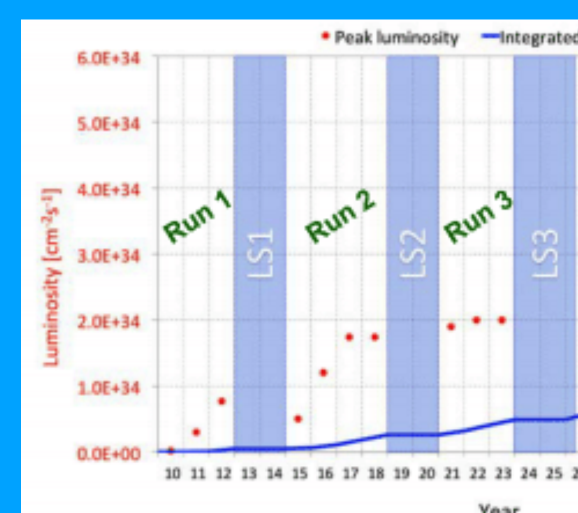

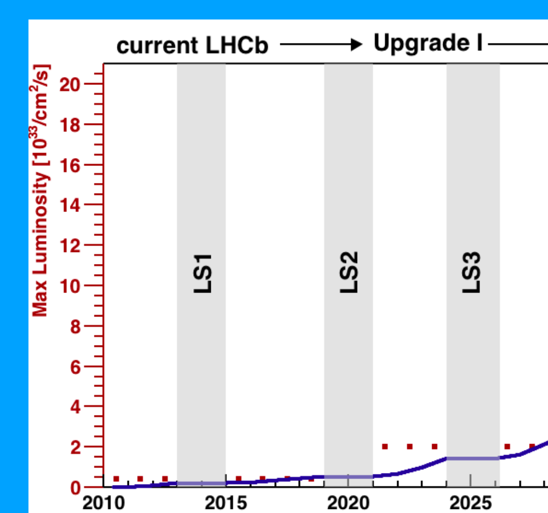

Hadron-collider W boson mass measurements

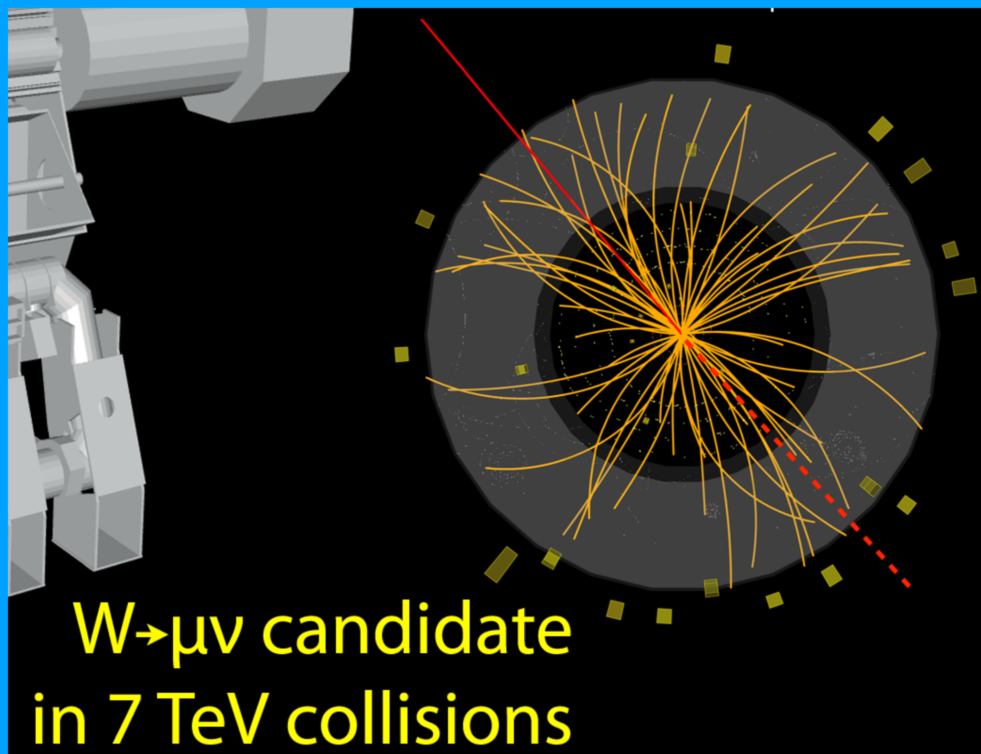

W bosons identified in their decays to $e\nu$ and/or $\mu\nu$

ATLAS both channels

LHCb & CMS $\mu\nu$ channel

D0 $e\nu$ channel

Mass measured by fitting template distributions of (inverse) transverse momentum and mass

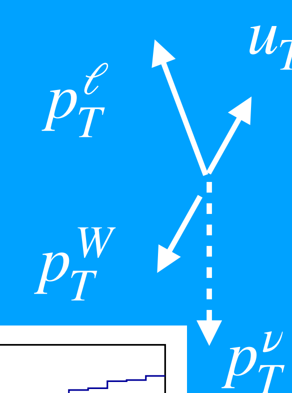

$$m_T = \sqrt{2 p_T^l \not{p}_T \left(1 - \cos\Delta\phi\right)}$$

$$\vec{\not{p}}_T = -(\vec{p}_T^{\,l} + \vec{u}_T)$$

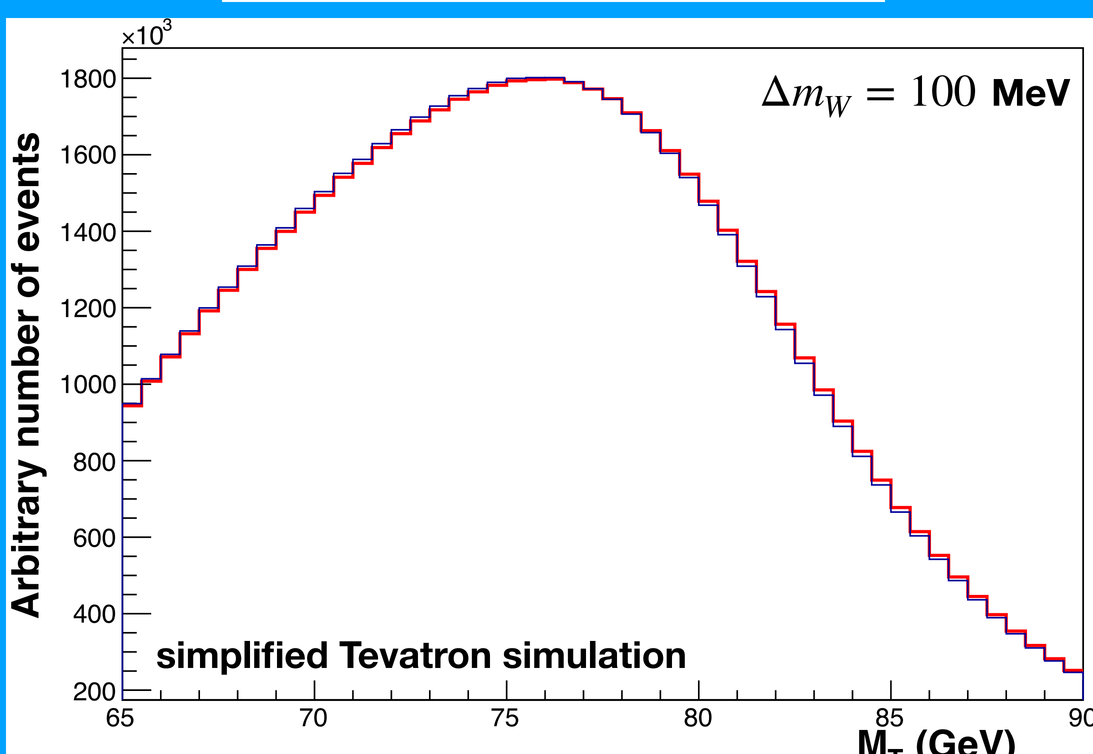

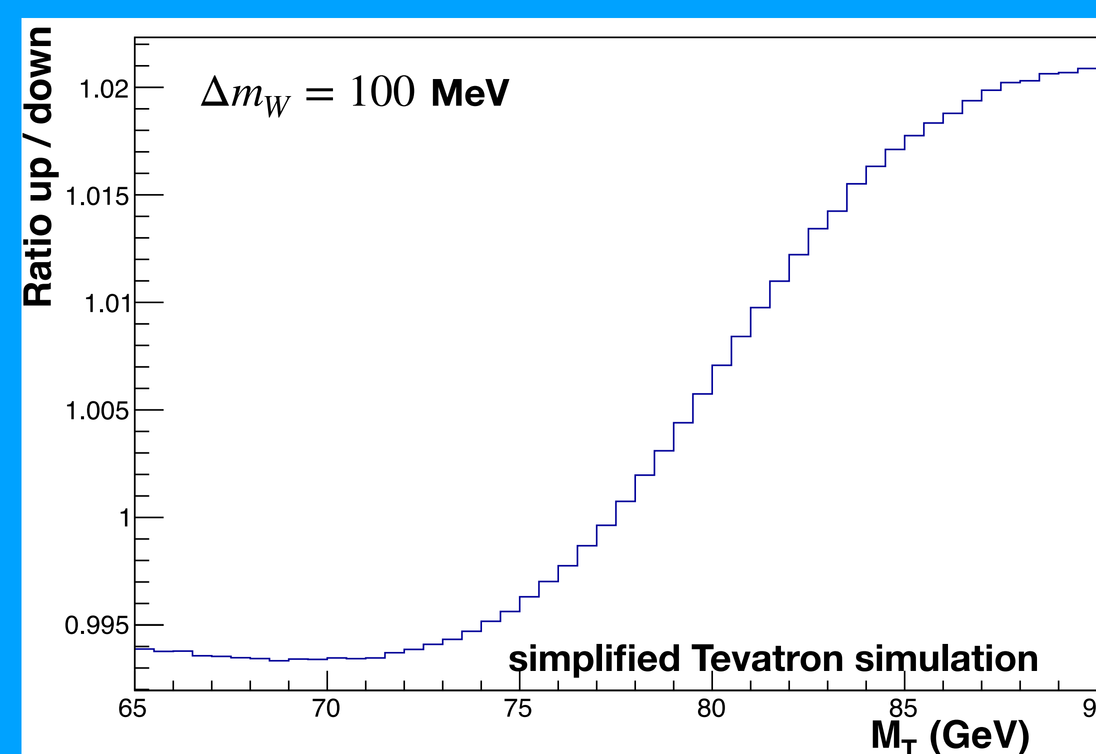

Calibrations

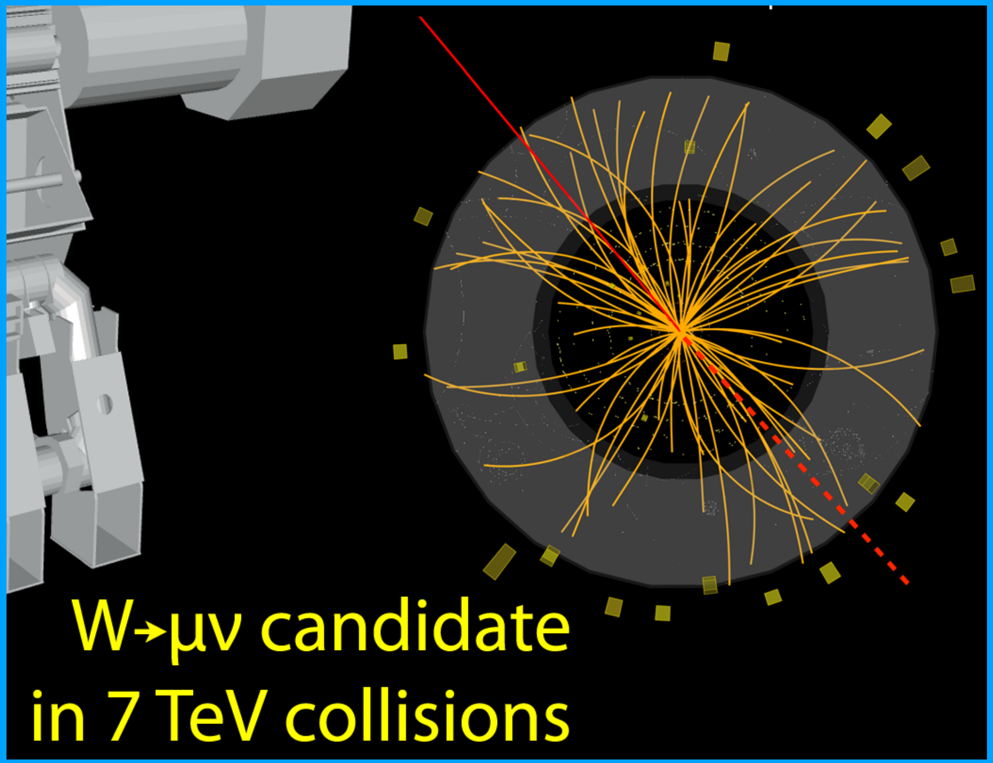

W bosons identified in their decays to $e\nu$ and/or $\mu\nu$

Dominant sensitivity from p_T^ℓ distribution @ LHC, m_T distribution @ Tevatron

Measurement requires precise calibrations of momentum scale and resolution

Charged lepton scale:

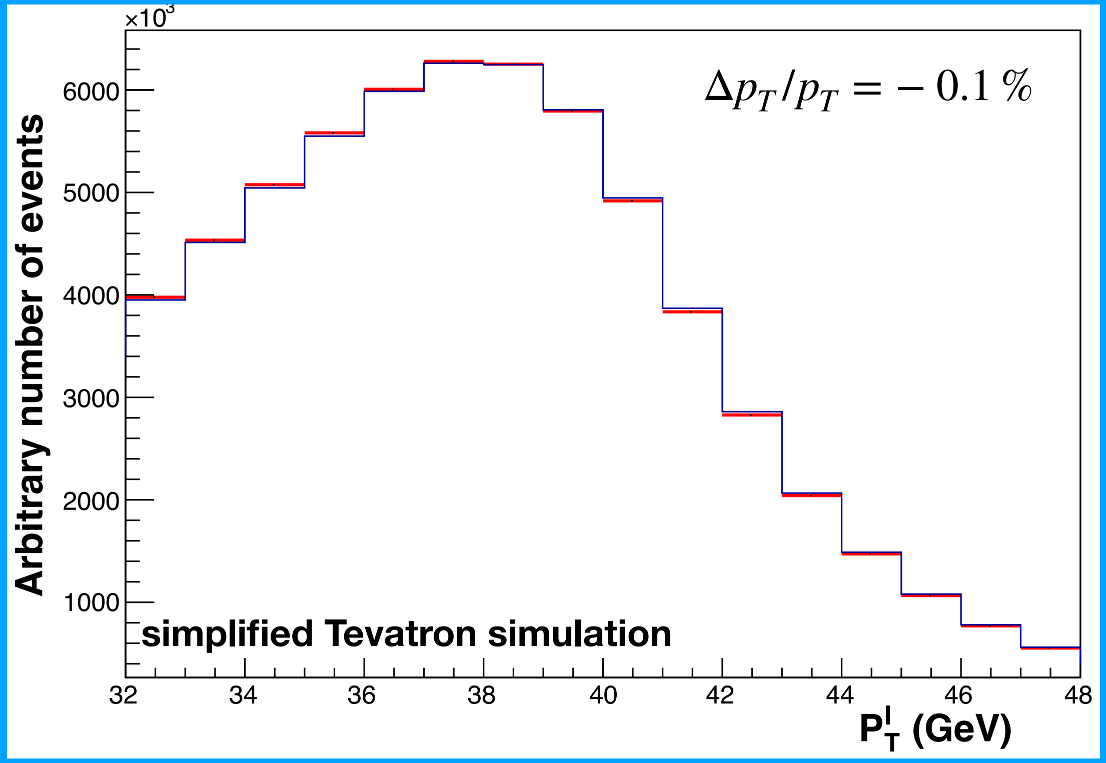

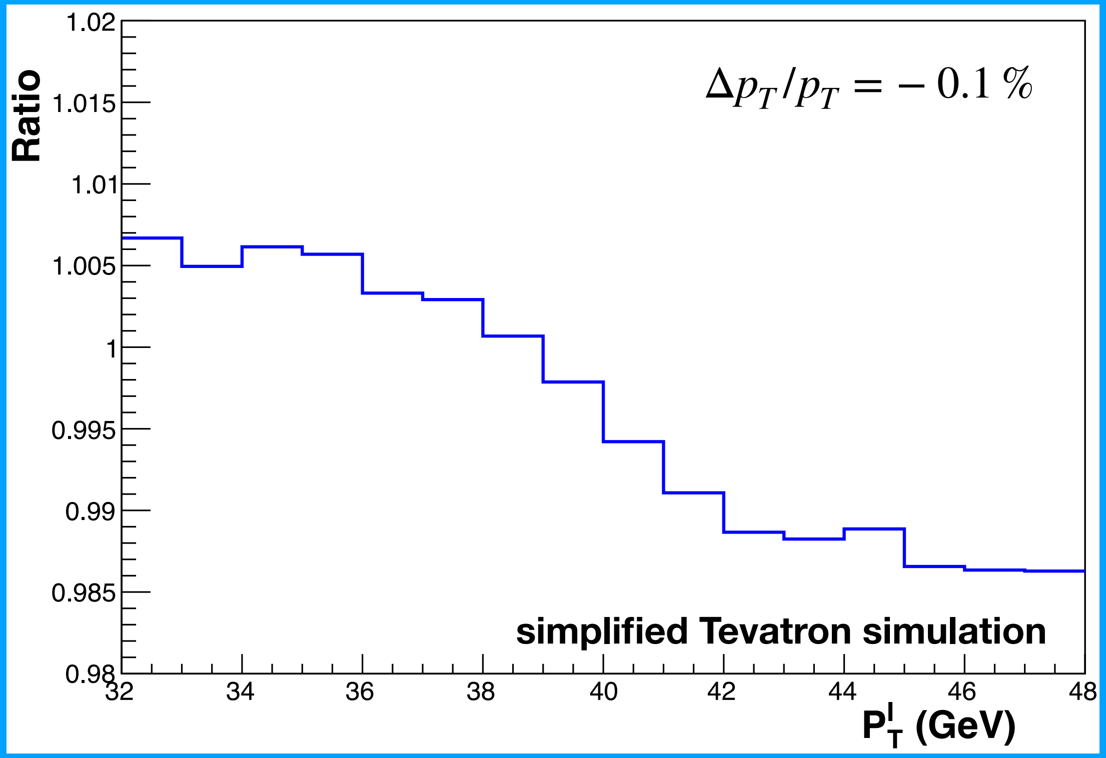

Muon momentum calibration

Detector	$\sigma_{\rm Spring}$ μm	$\sigma_{\rm Autumn}$ μm	$\sigma_{\rm Diff}$ μm
Pixel barrel	16	9	13
Pixel end-caps	17	15	8
SCT barrel	28	25	13
SCT end-caps	37	30	22
TRT barrel	124	118	38
TRT end-caps	148	132	67

First step is to align the tracker system

Determine individual 'sensor' positions by minimizing χ^2 difference between sensor and reconstructed track positions using cosmic-ray & collision data

ATLAS

Alignment level	Detector	Structures	degrees of freedom used	degrees of freedom number
Level 1	Pixel: whole detector	1	All	6
	SCT: barrel and 2 end-caps	3	All	18
	TRT: barrel	1	All (except T_z)	5
	TRT: 2 end-caps	2	All	12
	Total	7		41
Level 2	Pixel barrel: half shells	6	All	36
	Pixel end-caps: disks	6	T_x, T_y, R_z	18
	SCT barrel: layers	4	All	24
	SCT end-caps: disks	18	T_x, T_y, R_z	54
	TRT barrel: modules	96	All (except T_z)	480
	TRT end-caps: wheels	80	T_x, T_y, R_z	240
	Total	210		852
Level 3	Pixel: barrel modules	1456	All (except T_z)	7280
	Pixel: end-cap modules	288	T_x, T_y, R_z	864
	SCT: barrel modules	2112	T_x, T_y, R_z	6336
	SCT: end-cap modules	1976	T_x, T_y, R_z	5928
	TRT: barrel wires	105088	T_ϕ, R_r	210176
	TRT: end-cap wires	245760	T_ϕ, R_z	491520
	Total	356680		722104

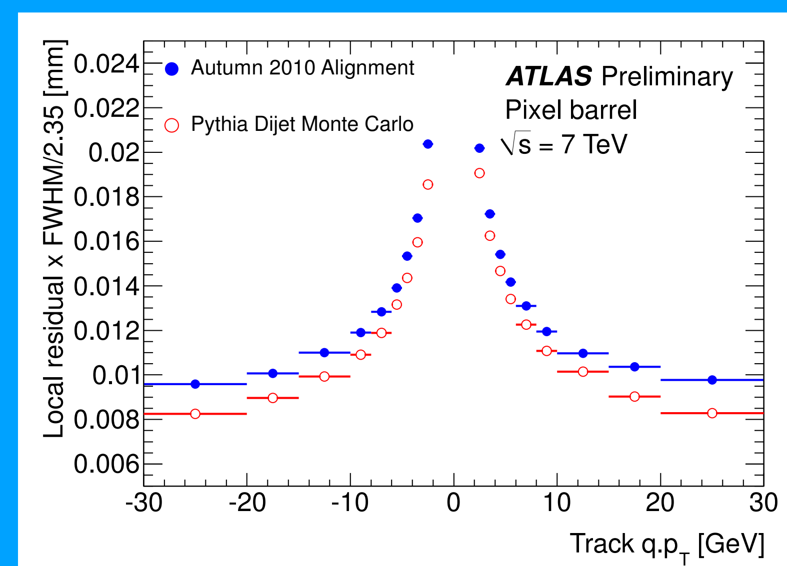

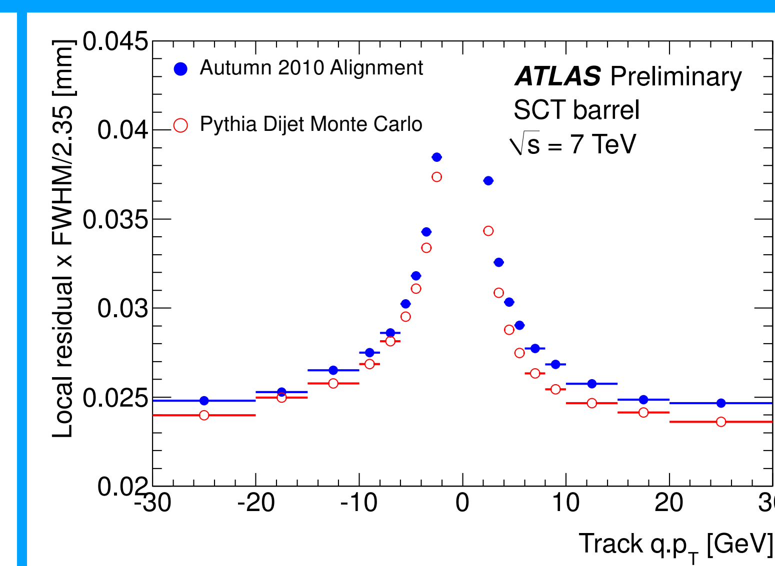

ATLAS-CONF-2011-012

Constant curvature correction determined using electron E/p & $Z \rightarrow \mu\mu$

$$c \rightarrow c + \delta$$

$$p_{\rm T}^{\rm data,corr} = \frac{p_{\rm T}^{\rm data}}{1 + q \cdot \delta(\eta,\phi) \cdot p_{\rm T}^{\rm data}},$$

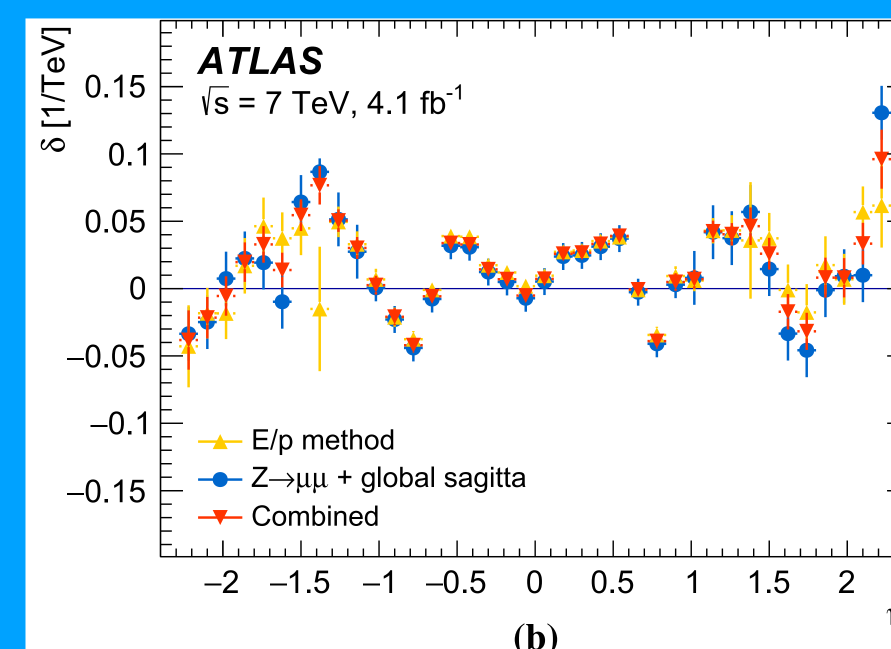

ATLAS, EPJC 78, 110 (2018)

Muon momentum calibration

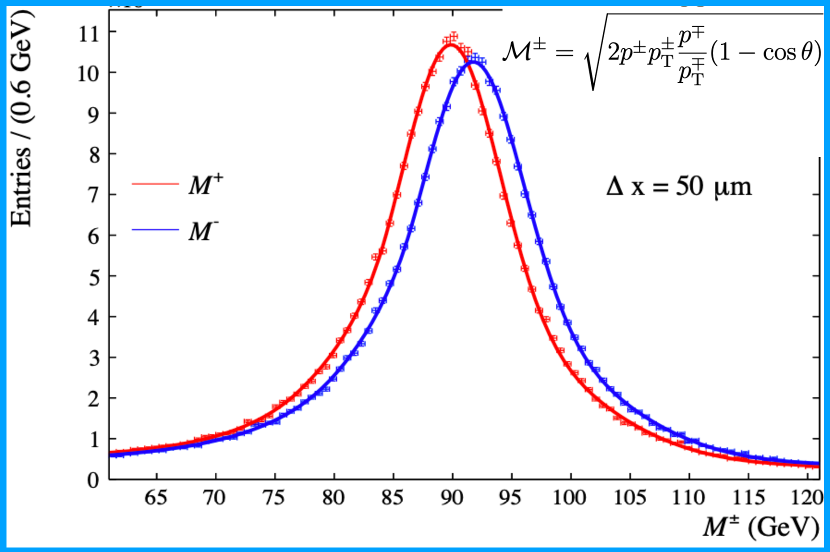

First step is to align the tracker system

Determine individual 'sensor' positions by minimizing χ^2 difference between sensor and reconstructed track positions using cosmic-ray & collision data

LHCb: 1k tracker-system degrees of freedom

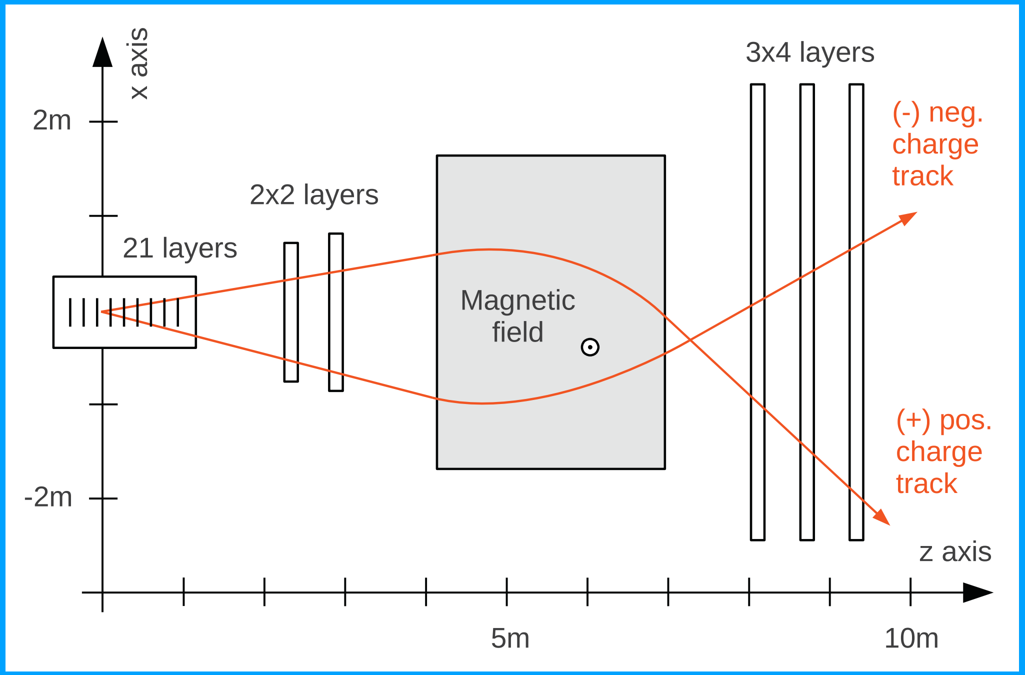

J. Amoraal et al, NIMA 712, 48 (2013)

Corrections to muon tracks from W boson decays determined using pseudomass of $Z \rightarrow \mu\mu$ decays

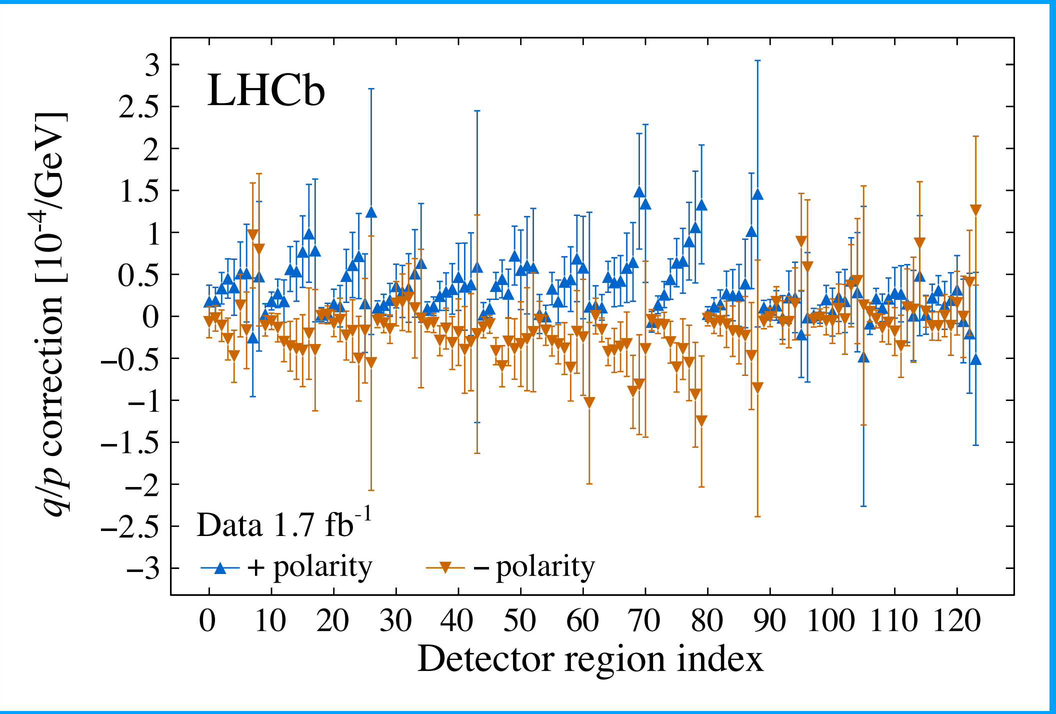

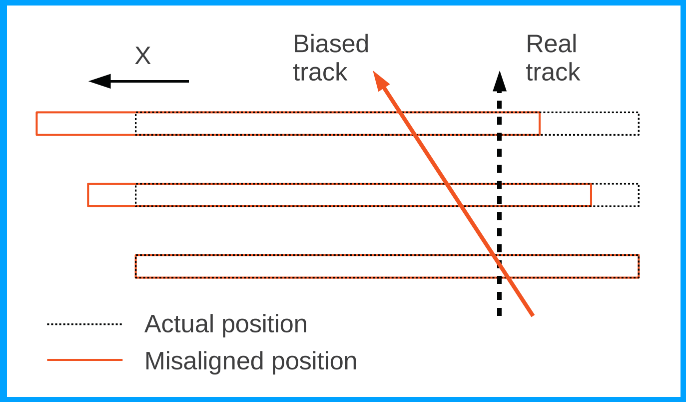

1.8 mm shift in x in outer layers determined using D^0 and J/ψ meson decays

Equivalent to 0.2 mrad rotation of vertex detector

Muon momentum calibration

Second step is to calibrate the momentum scale using J/ψ, Υ, and Z decays to muons

ATLAS: Calibration uses the Z resonance in bins of pseudorapidity and azimuthal angle

LHCb & **CMS**: Calibrations use all three resonances

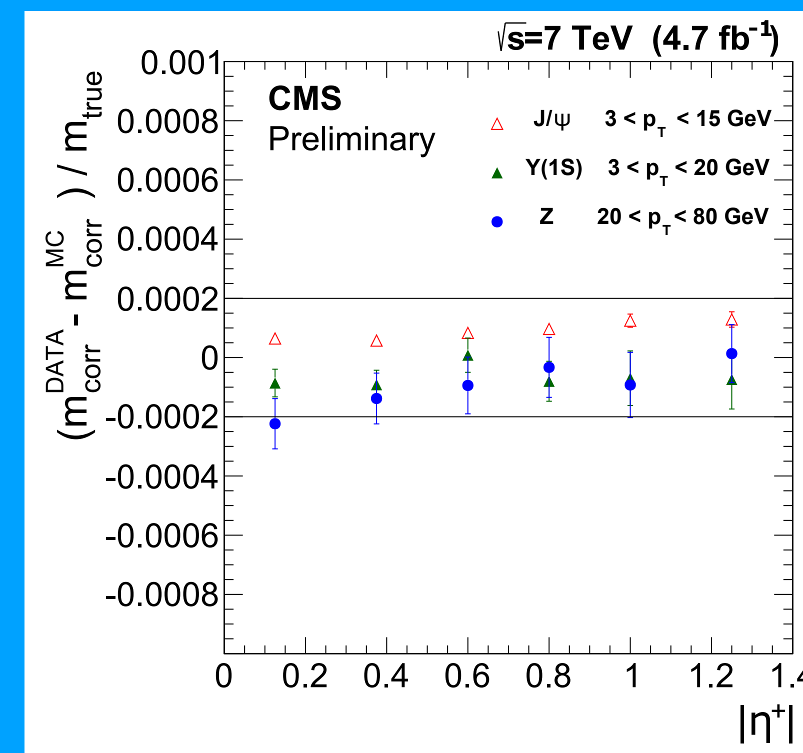

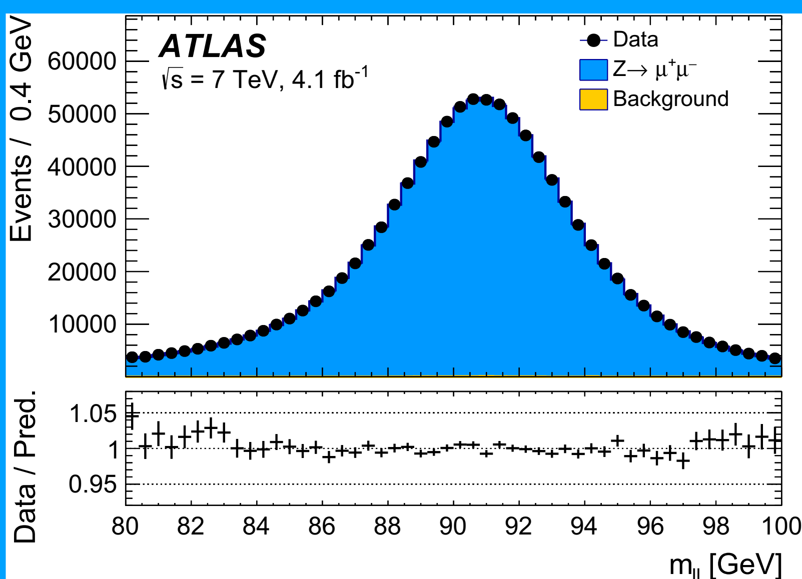

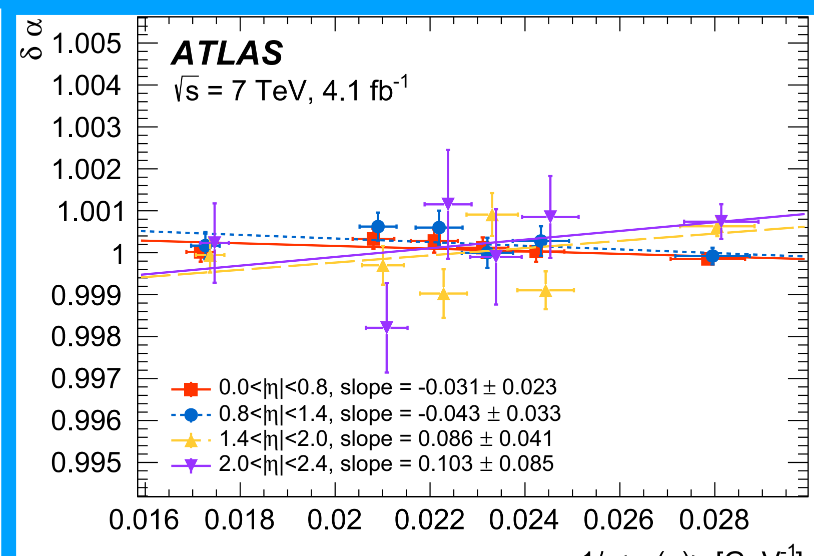

(a)

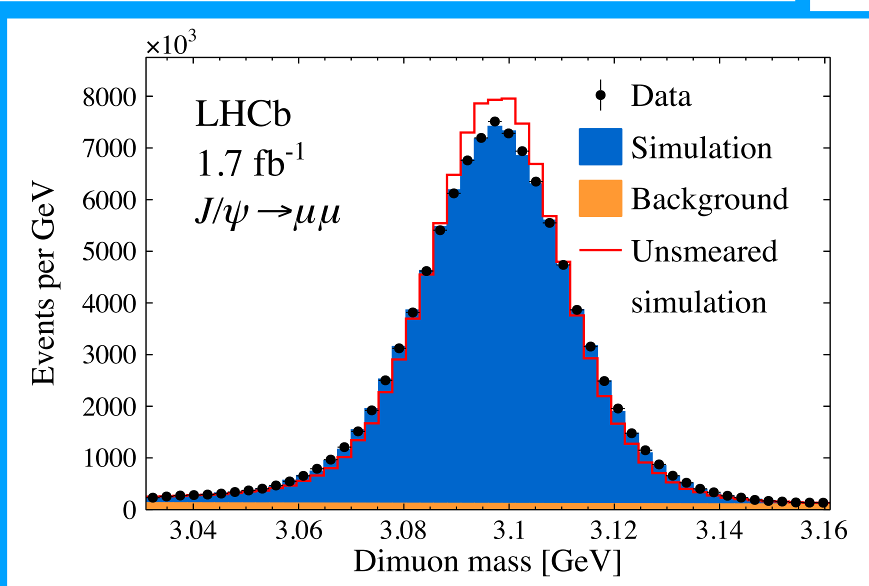

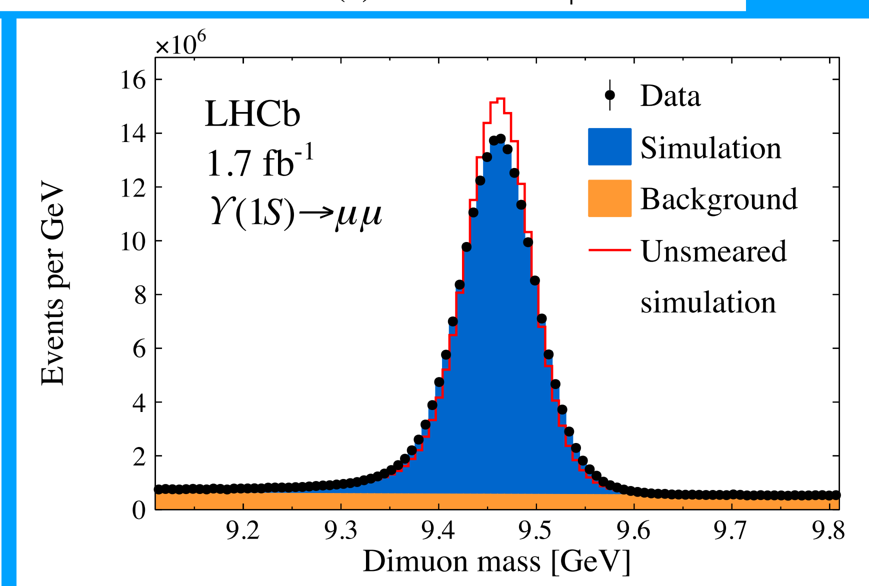

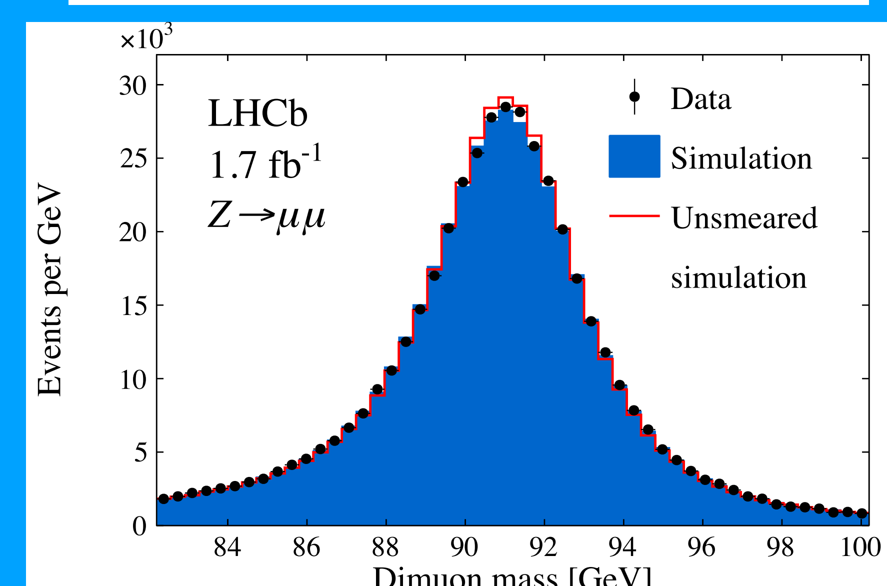

Electron momentum calibration

First step is to correct the response variations in data

ATLAS uses simulation to remove response variations due to shower losses, and uses minimum ionizing deposits from $Z \rightarrow \mu\mu$ events to correct depth dependence of the calorimeter response

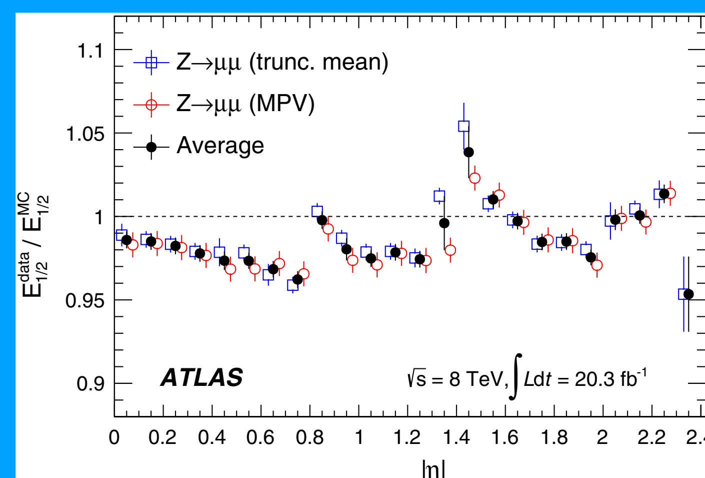

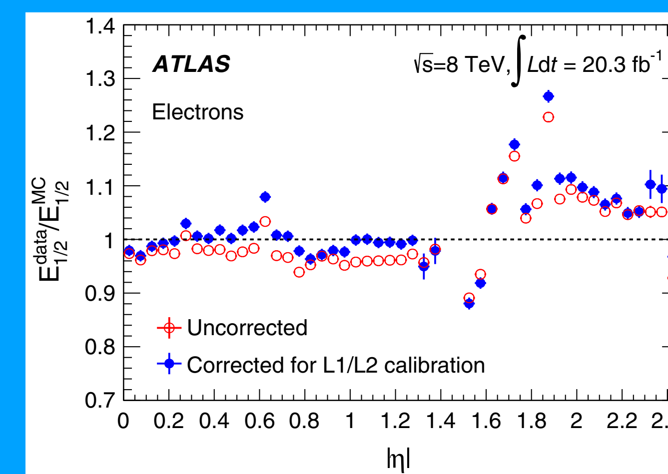

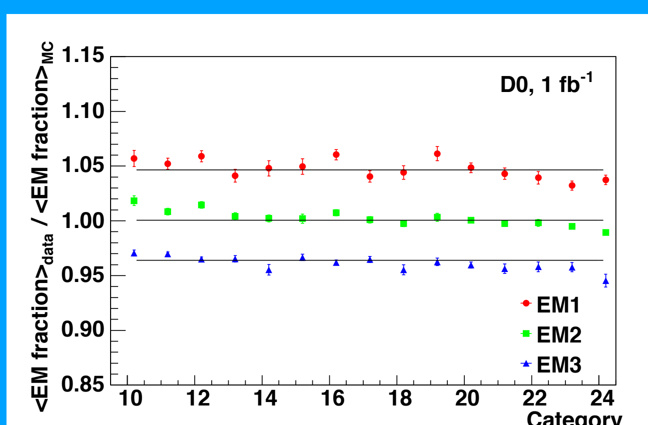

add $0.16X_0$

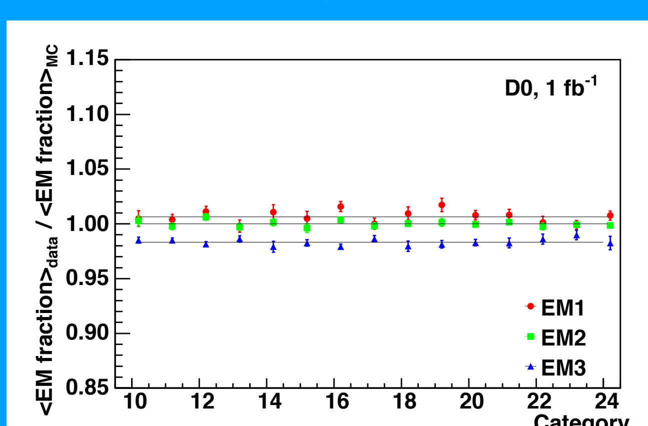

Second step is to correct the simulated energy loss

ATLAS and **D0** tune the amount of upstream material using $Z \rightarrow ee$ resonance

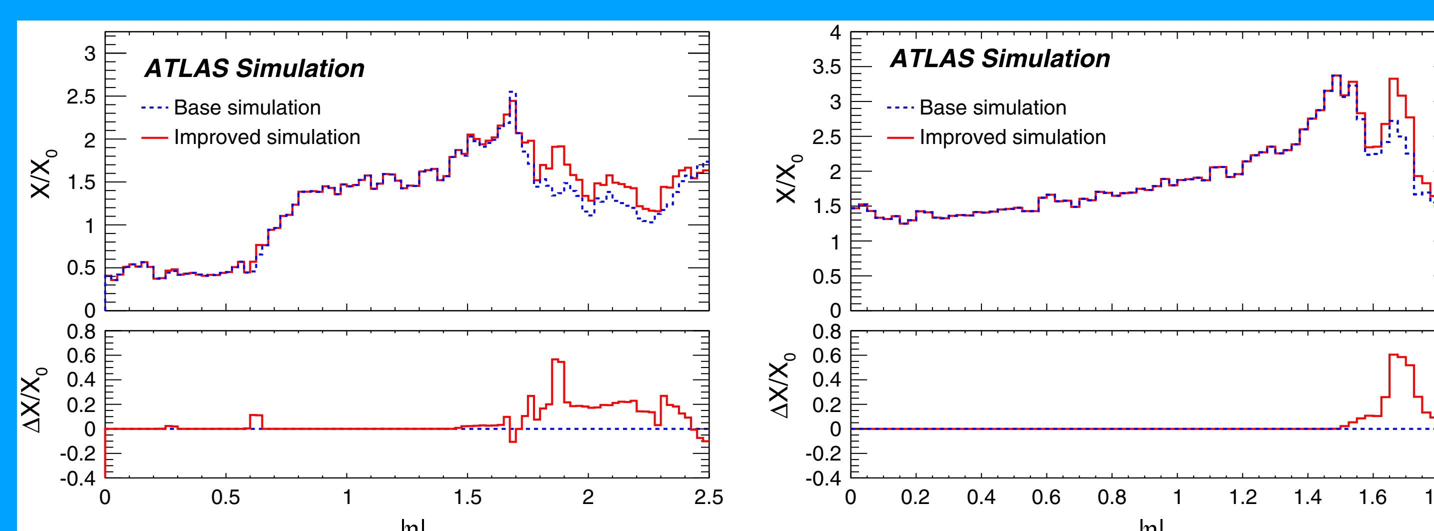

Electron momentum calibration

Third step is to calibrate the response

ATLAS & D0: Calibrate energy as a function of pseudorapidity using $Z \to ee$ decays

ATLAS validates the calibration with $J/\psi \to ee$ decays

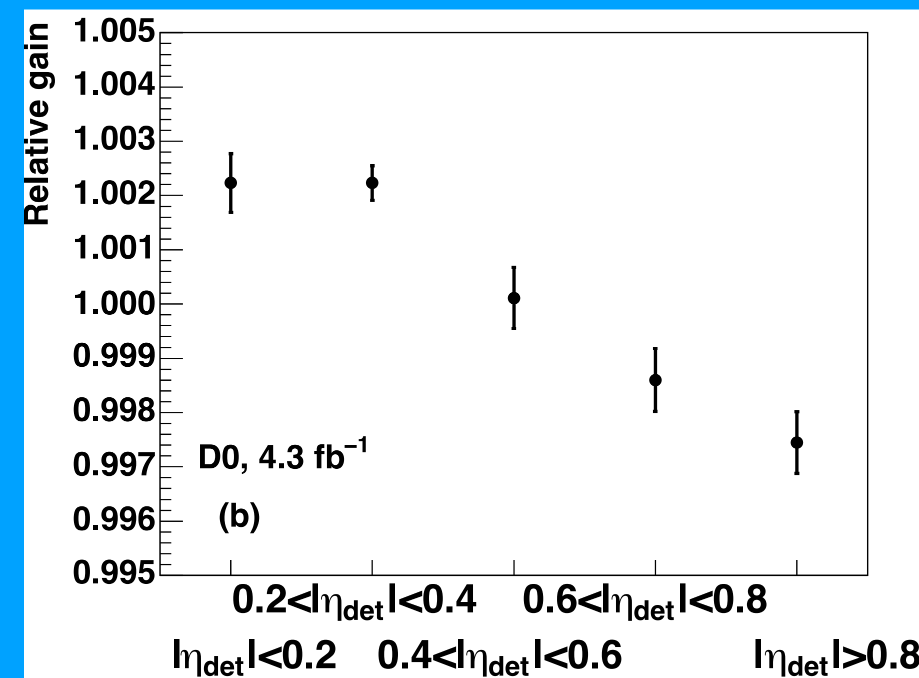

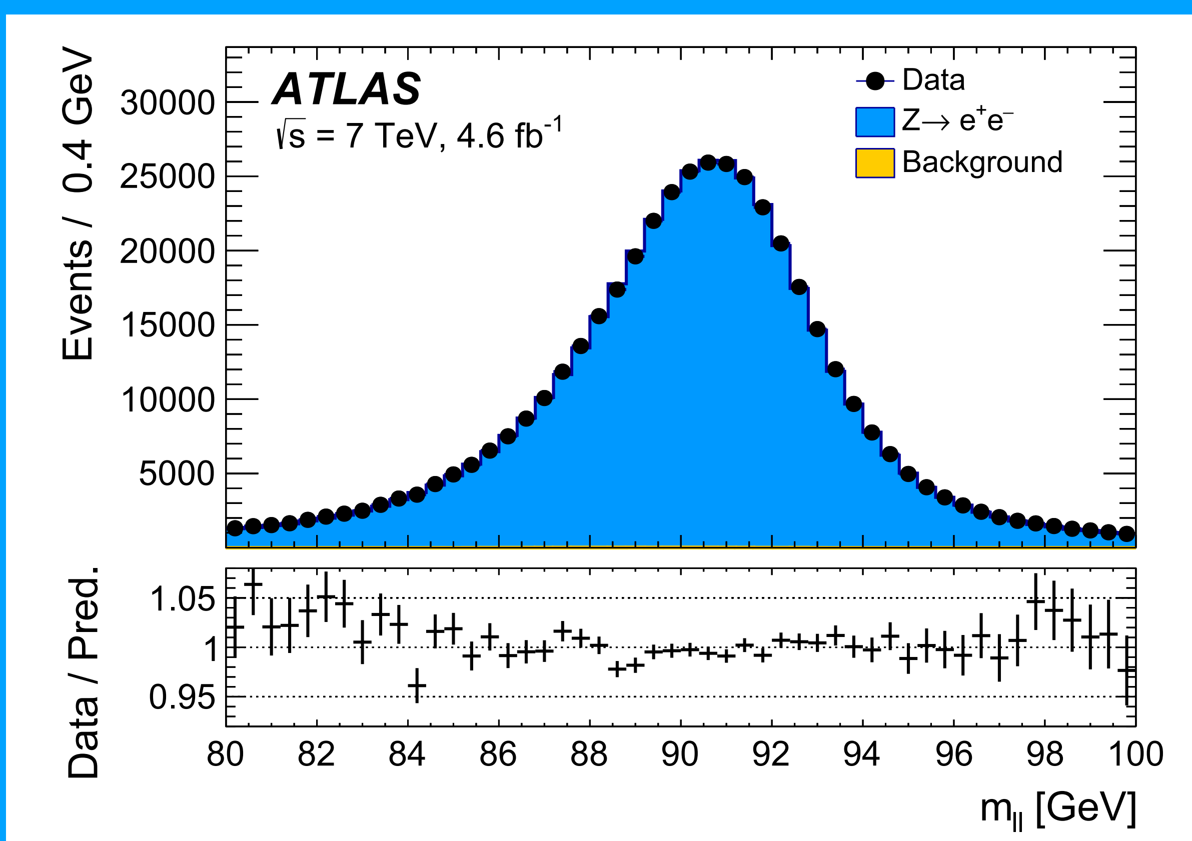

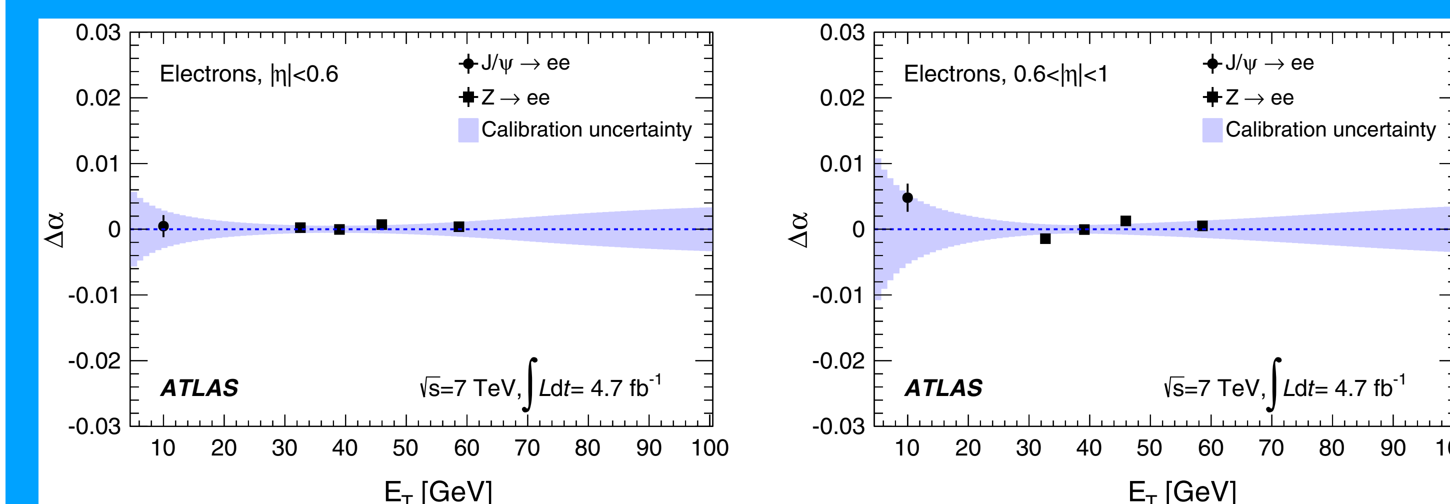

Calibrations

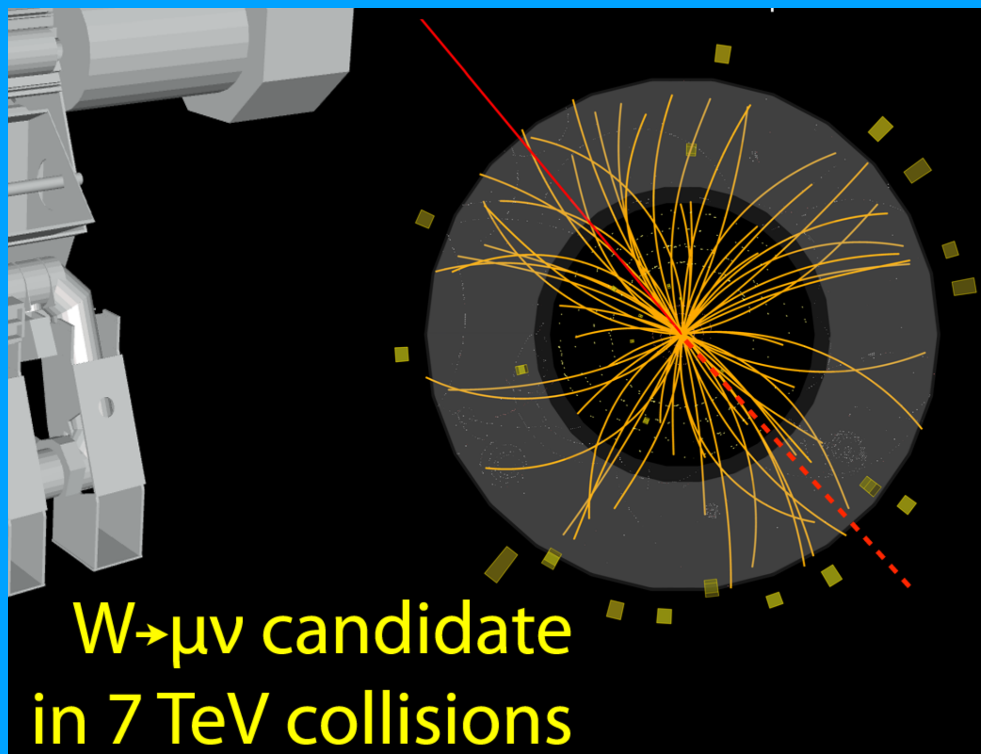

Measurement requires precise calibrations of momentum scale and resolution

$$\vec{\not{p}}_T = -(\vec{p}_T^{\,l} + \vec{u}_T)$$

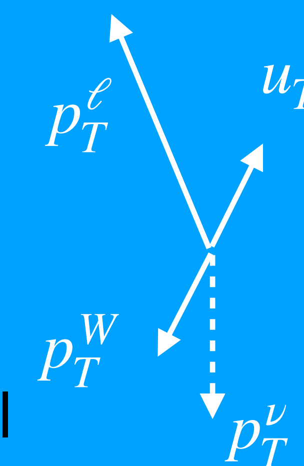

ATLAS & D0 model recoil

CMS models recoil for W-like Z mass

LHCb does not measure recoil

Recoil scale

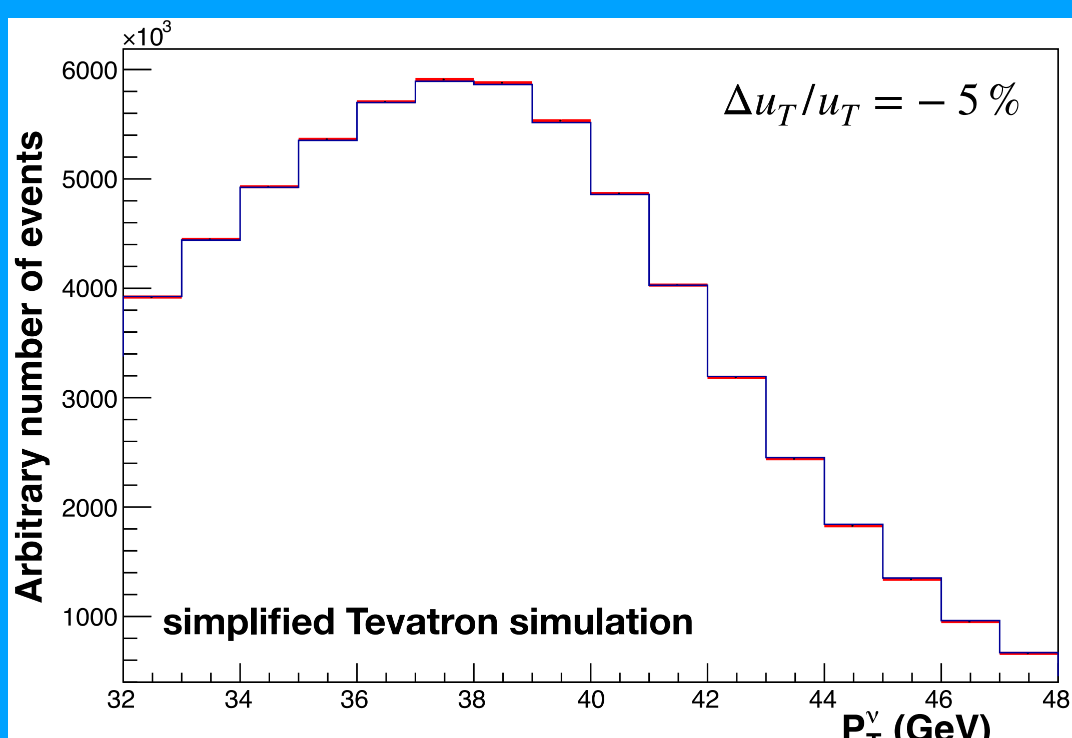

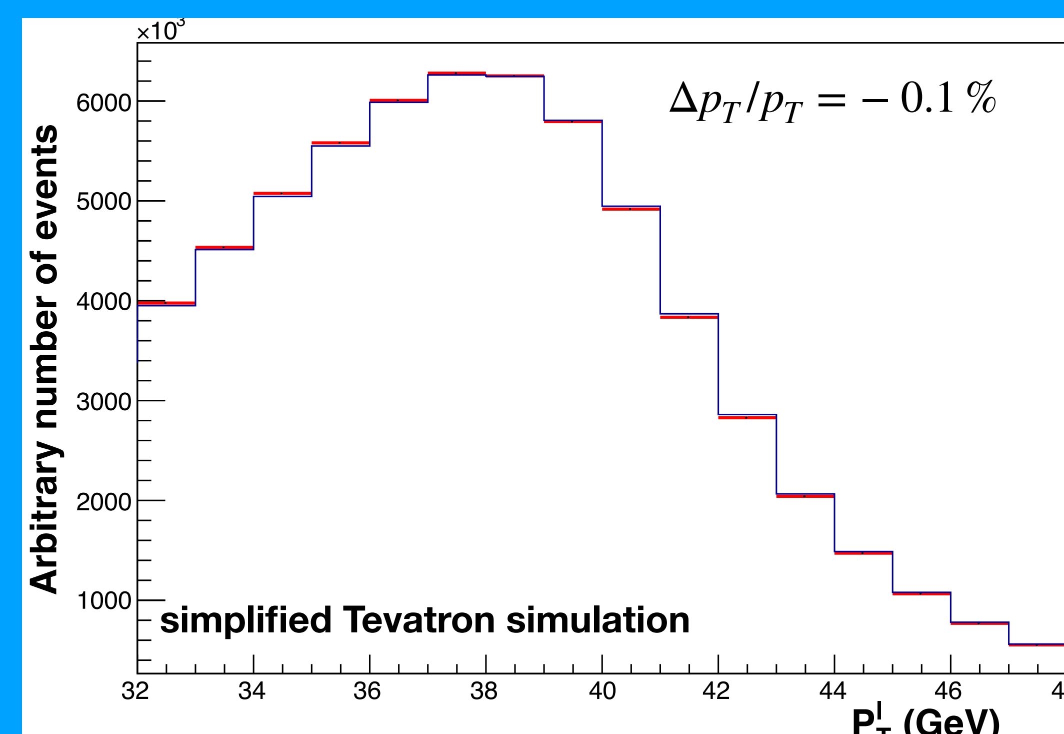

Recoil momentum calibration

First step is data uniformity corrections

ATLAS corrects measured cell energies for EM and hadronic shower differences

Second step is the reconstruction of the recoil

ATLAS and **D0** remove a common reconstruction window of $\Delta R < 0.2$

D0 removes recoil energy in simulation using a distribution derived from a random direction; also adds electron shower leakage to simulation

ATLAS adds a rotated cluster from the same event to the data recoil

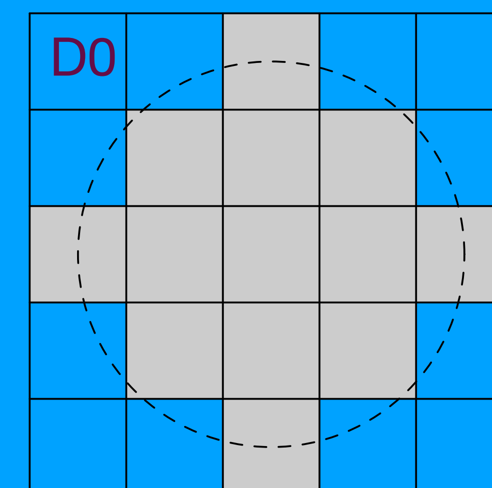

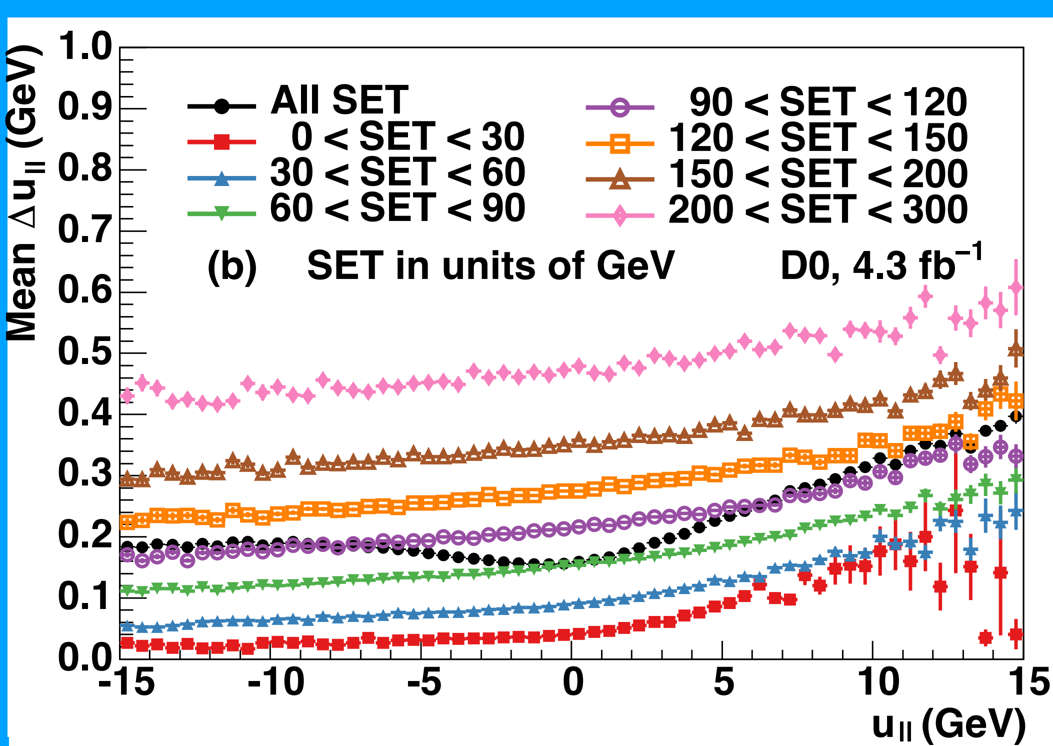

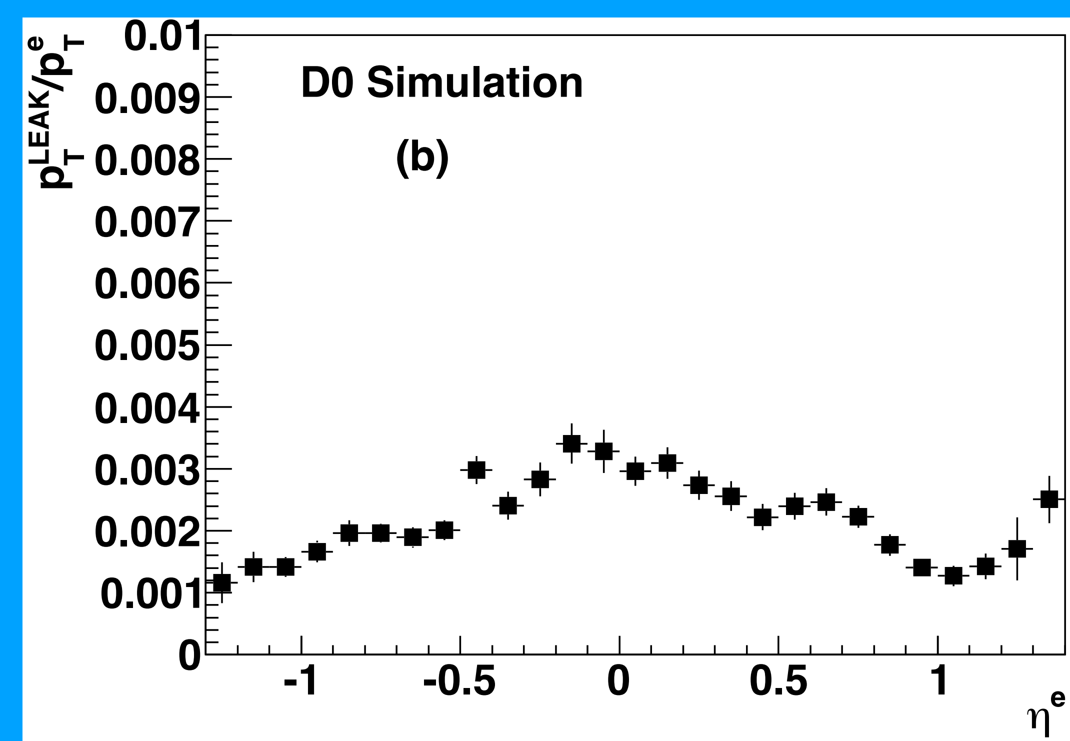

Recoil momentum calibration

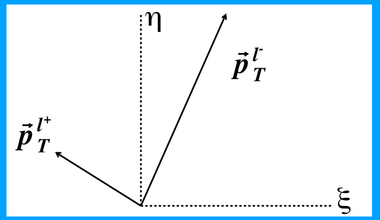

Third step is the calibration of the recoil response

ATLAS, **CMS**, & **D0** apply scale functions to fully simulated event samples

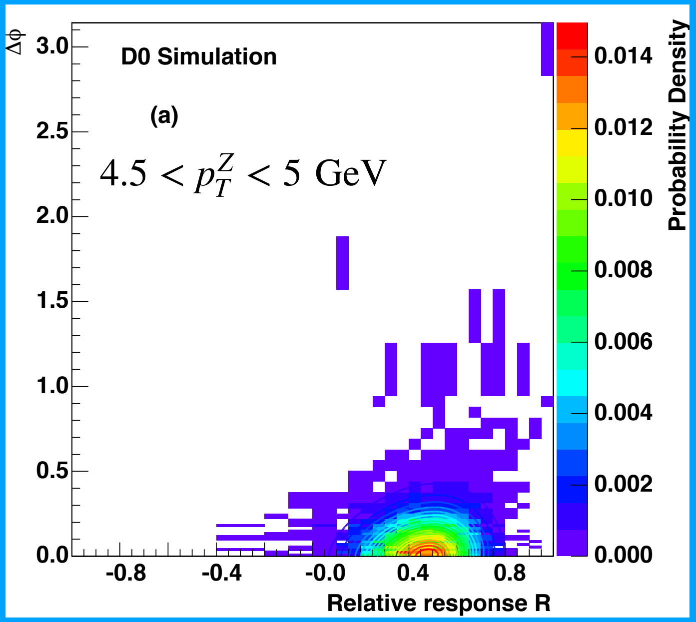

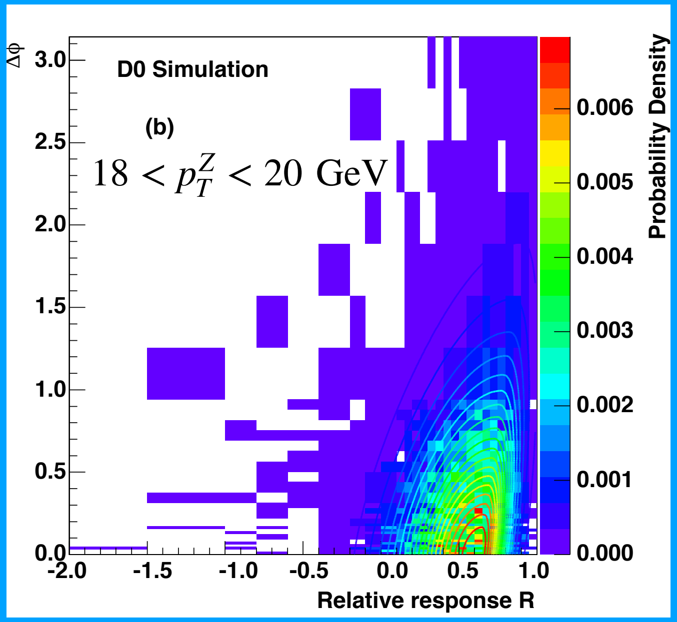

D0 simulates $Z \to \nu\nu$ decays

Smooths distribution of relative response R vs $\Delta\phi$

$$R = \frac{u_T - p_T^Z}{p_T^Z}$$

ATLAS applies ~100 MeV shifts to recoil

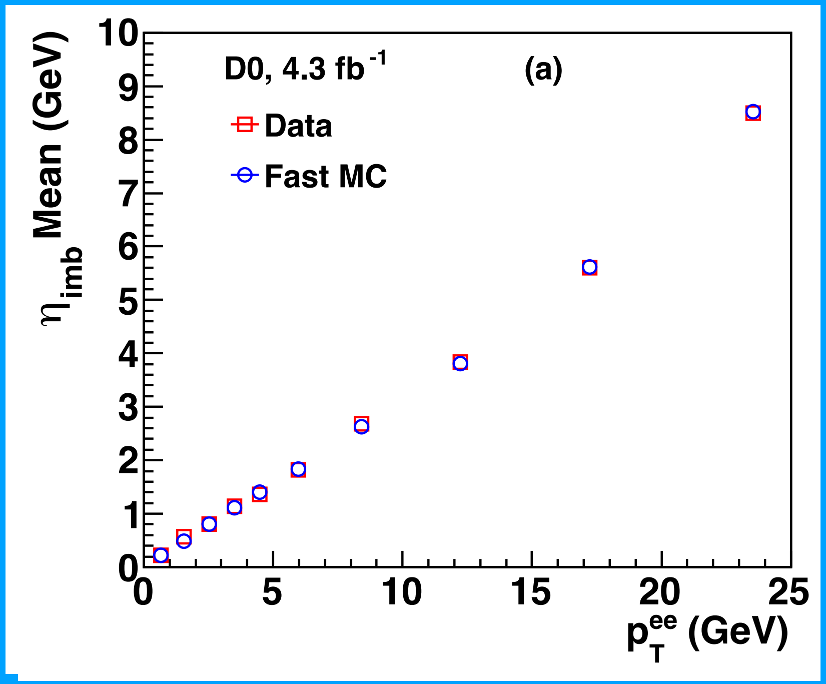

D0 corrects simulation to an empirical distribution

$$u_\parallel^{\text{HARD}}/p_T^V = (r_0 + r_1 e^{-p_T^V/\tau_{\text{HAD}}})(\overline{R}(p_T^V) + 1)$$

Corrections derived using the imbalance of recoil and p_T^Z

$$\eta_{\text{imb}} \equiv (\vec{p}_T^{\,ee} + \vec{u}_T) \cdot \hat{\eta}$$

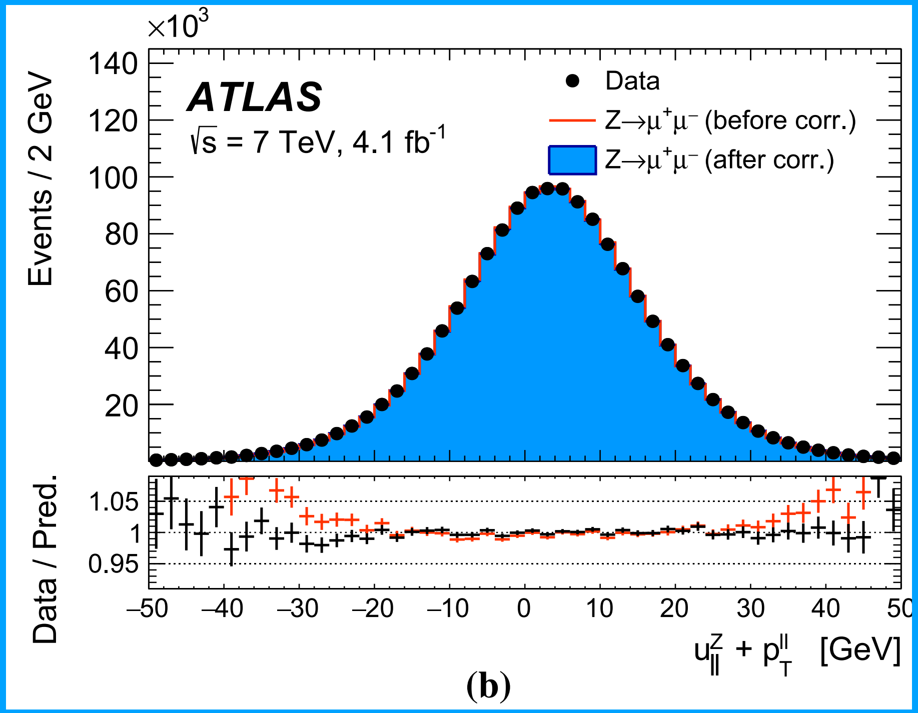

Recoil momentum calibration

Fourth step is the calibration of the recoil resolution

D0 resmears the simulation and adds pileup from measured distributions

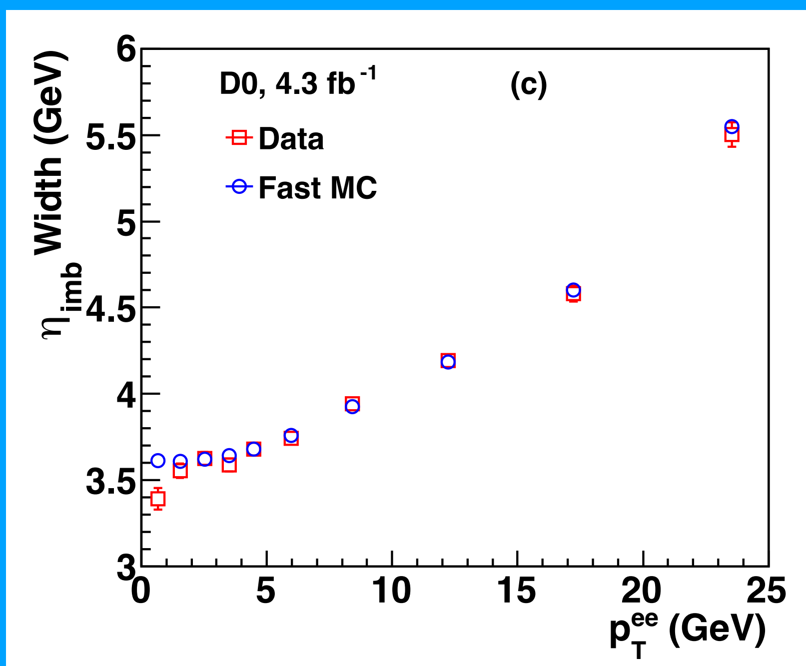

$$u_{\parallel}^{\mathrm{HARD}}/p_T^V = (r_0 + r_1 e^{-p_T^V/\tau_{\mathrm{HAD}}})(\overline{R}(p_T^V)+1)$$
$$+\sigma_0(u_{\parallel}^{\nu\nu}/p_T^V - \overline{R}(p_T^V) - 1).$$

$$\vec{u}_T^{\mathrm{SOFT}} = \sqrt{\alpha_{\mathrm{MB}}}\; \vec{u}_T^{\mathrm{MB}} + \vec{u}_T^{\mathrm{ZB}}$$

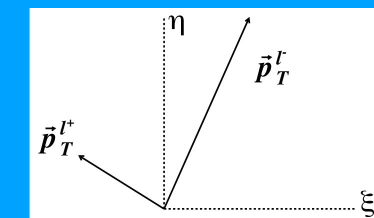

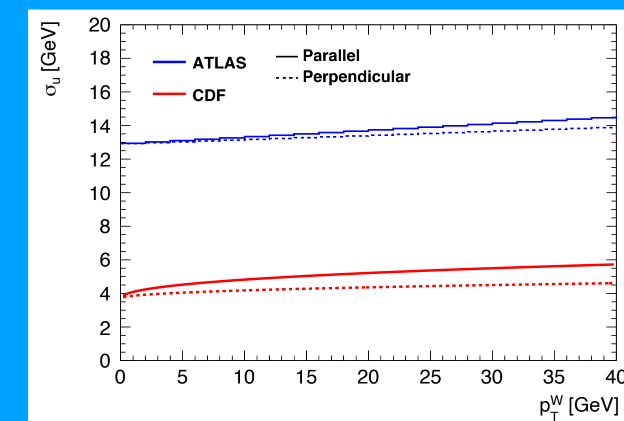

ATLAS applies transformations to the simulated sum E_T & resmears

CMS reweights simulation to a three-gaussian fit of recoil projections

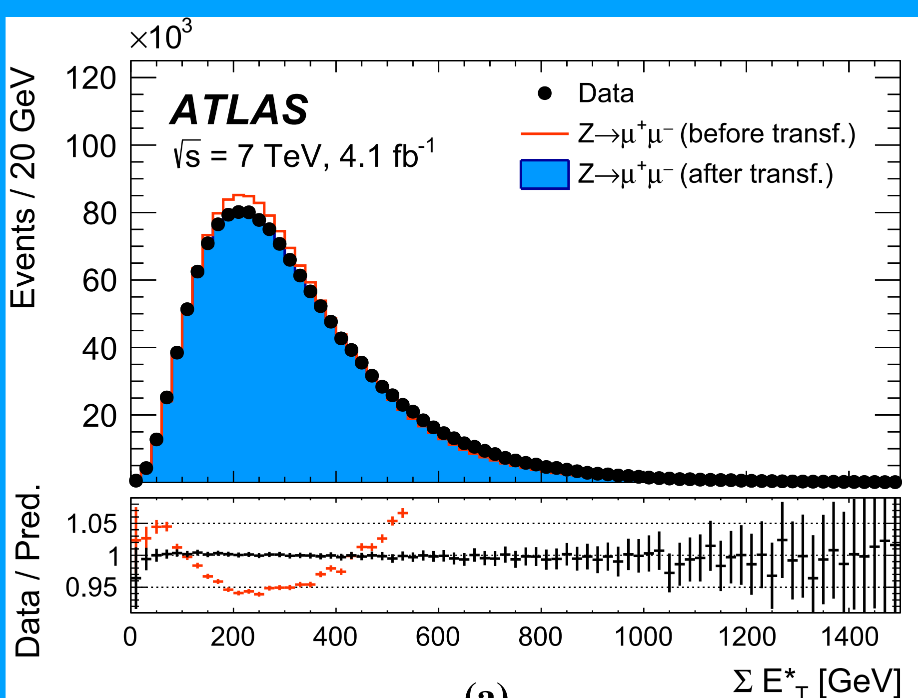

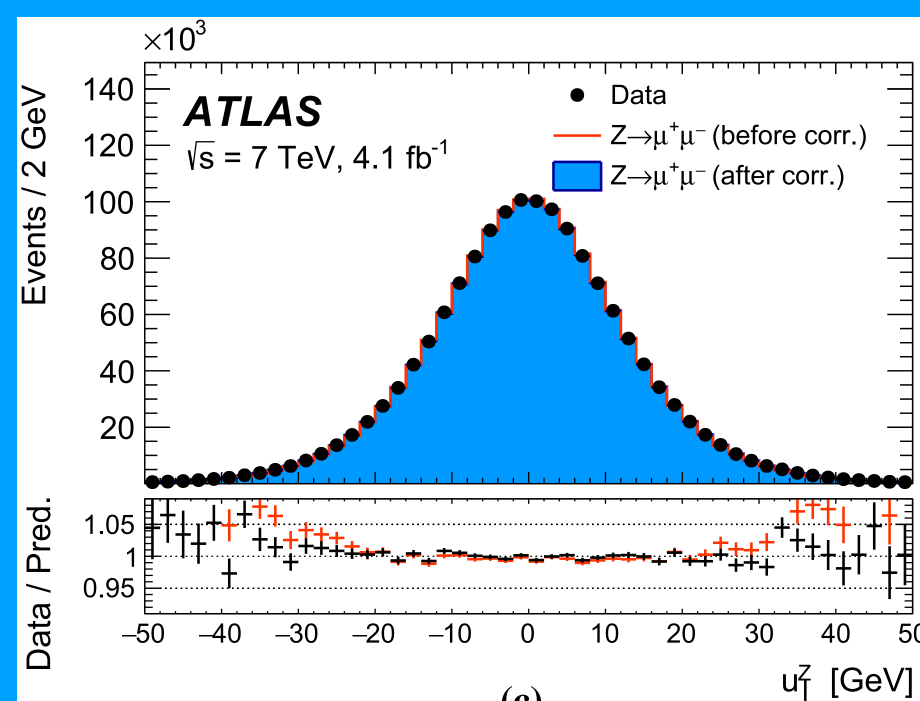

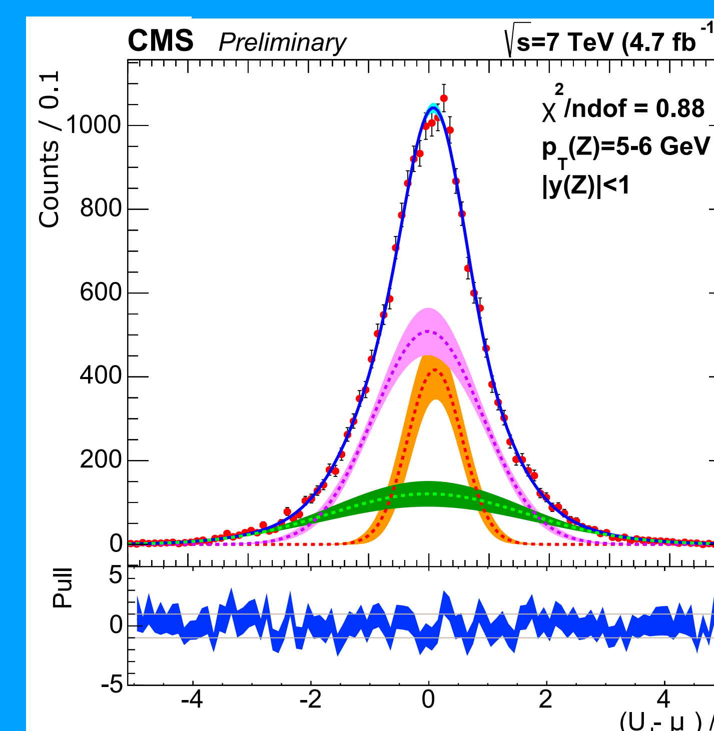

Recoil momentum validation

W boson recoil distributions validate the model

Most important is the recoil projected along the charged-lepton's momentum ($u_{||}$)

$$m_T \approx 2p_T\sqrt{1+u_{||}/p_T} \approx 2p_T + u_{||}$$

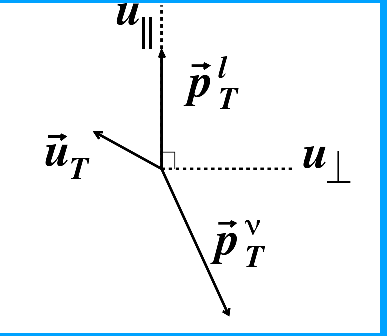

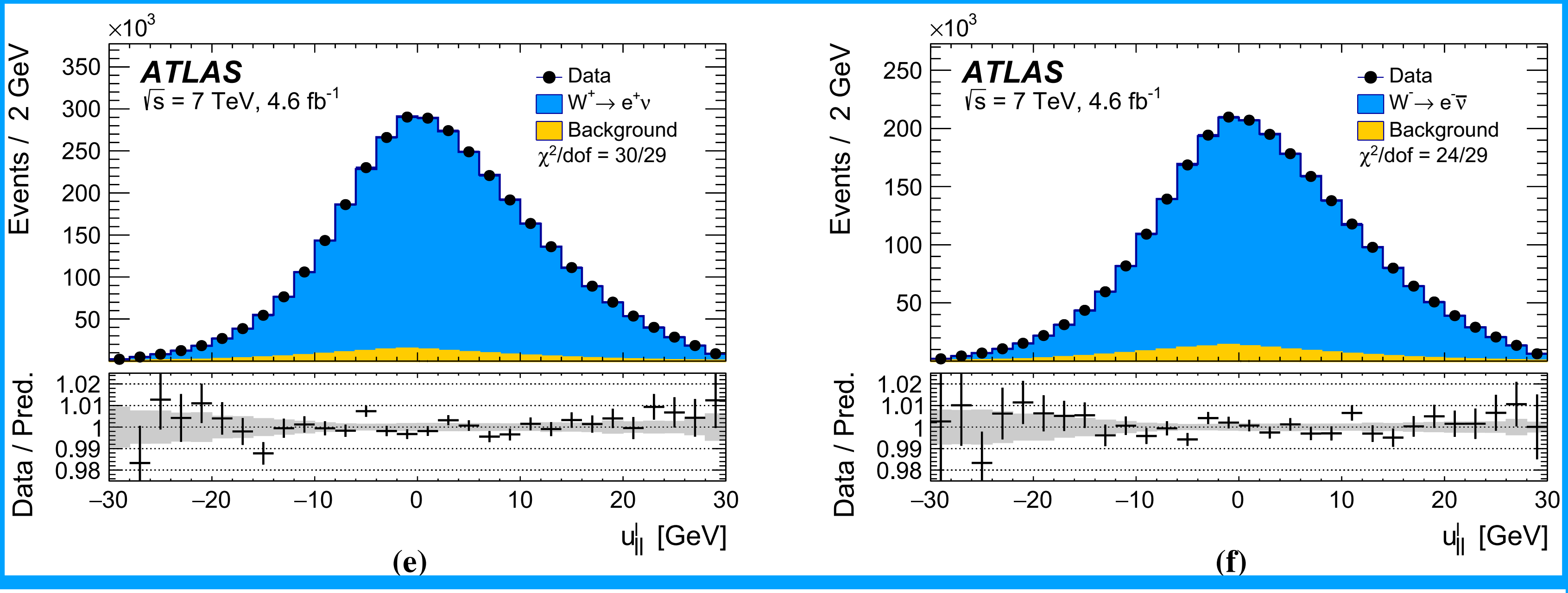

(e) (f)

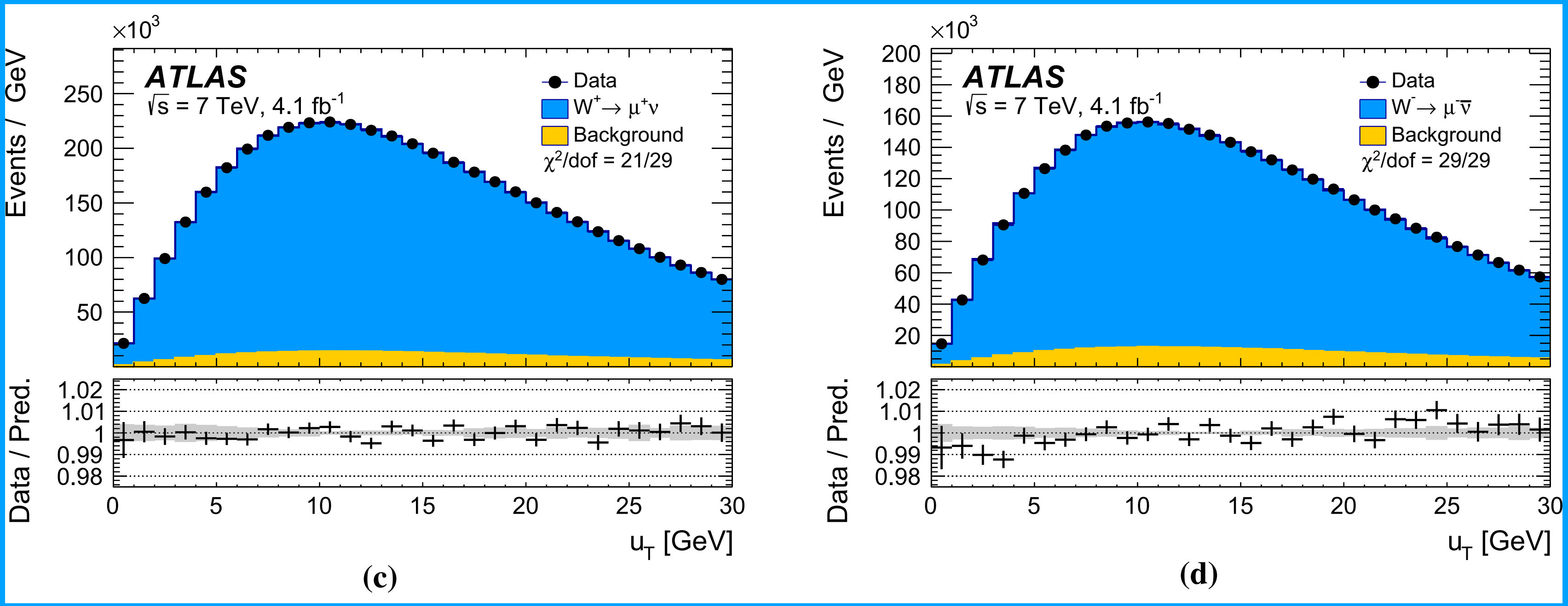

(c) (d)

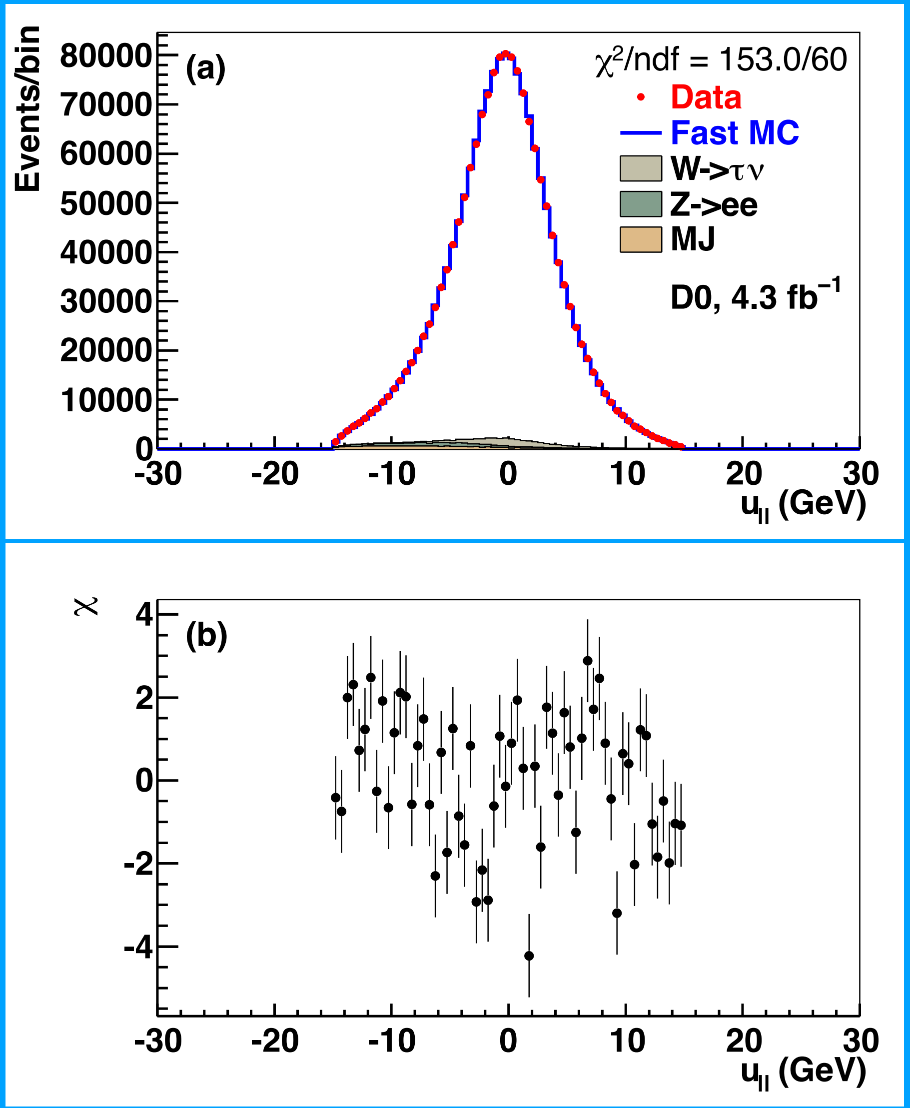

Recoil momentum validation

ATLAS validates the recoil model with single-lepton Z boson mass measurements

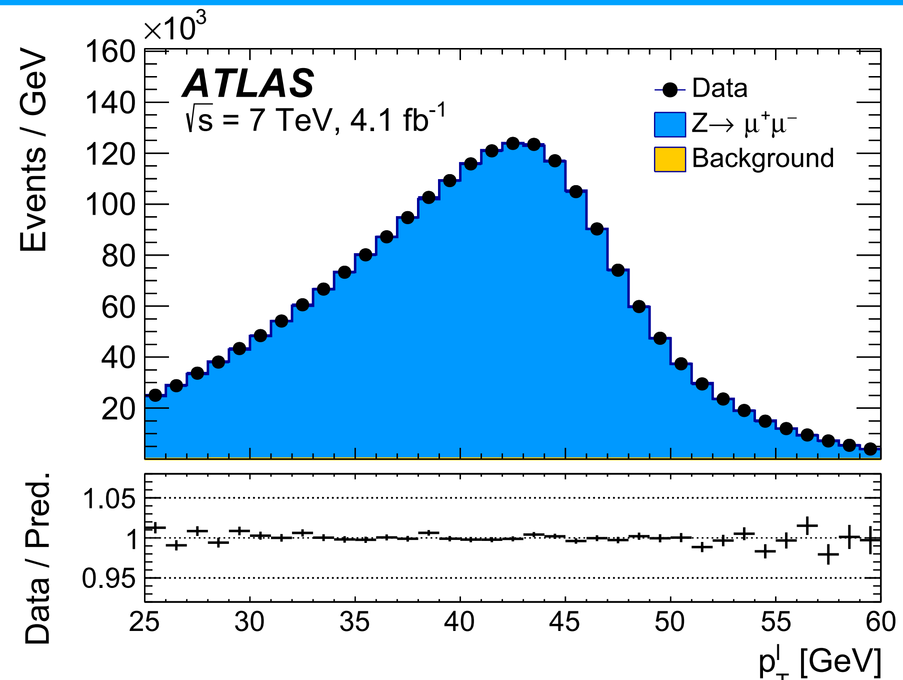

(b)

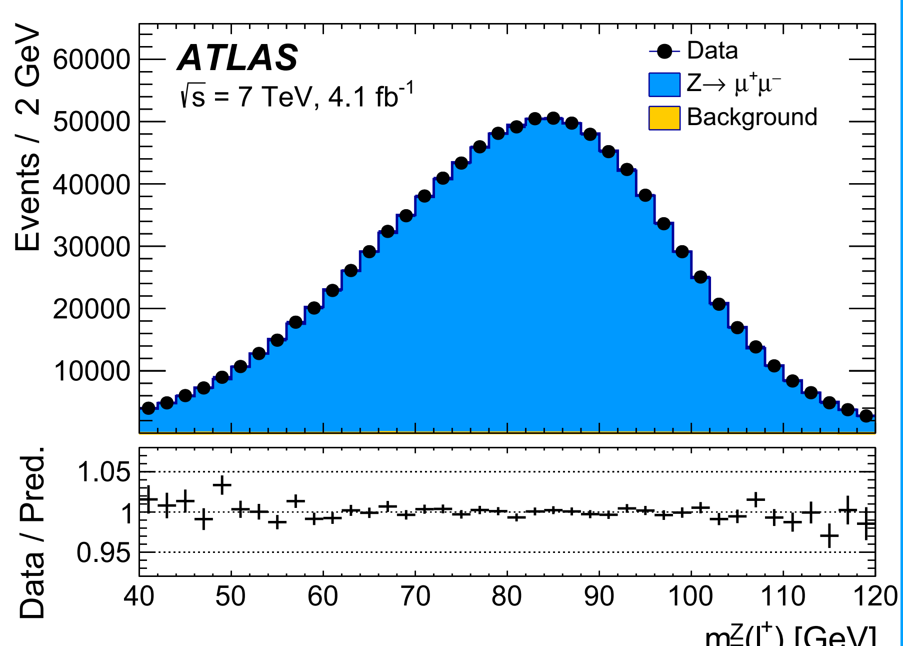

(d)

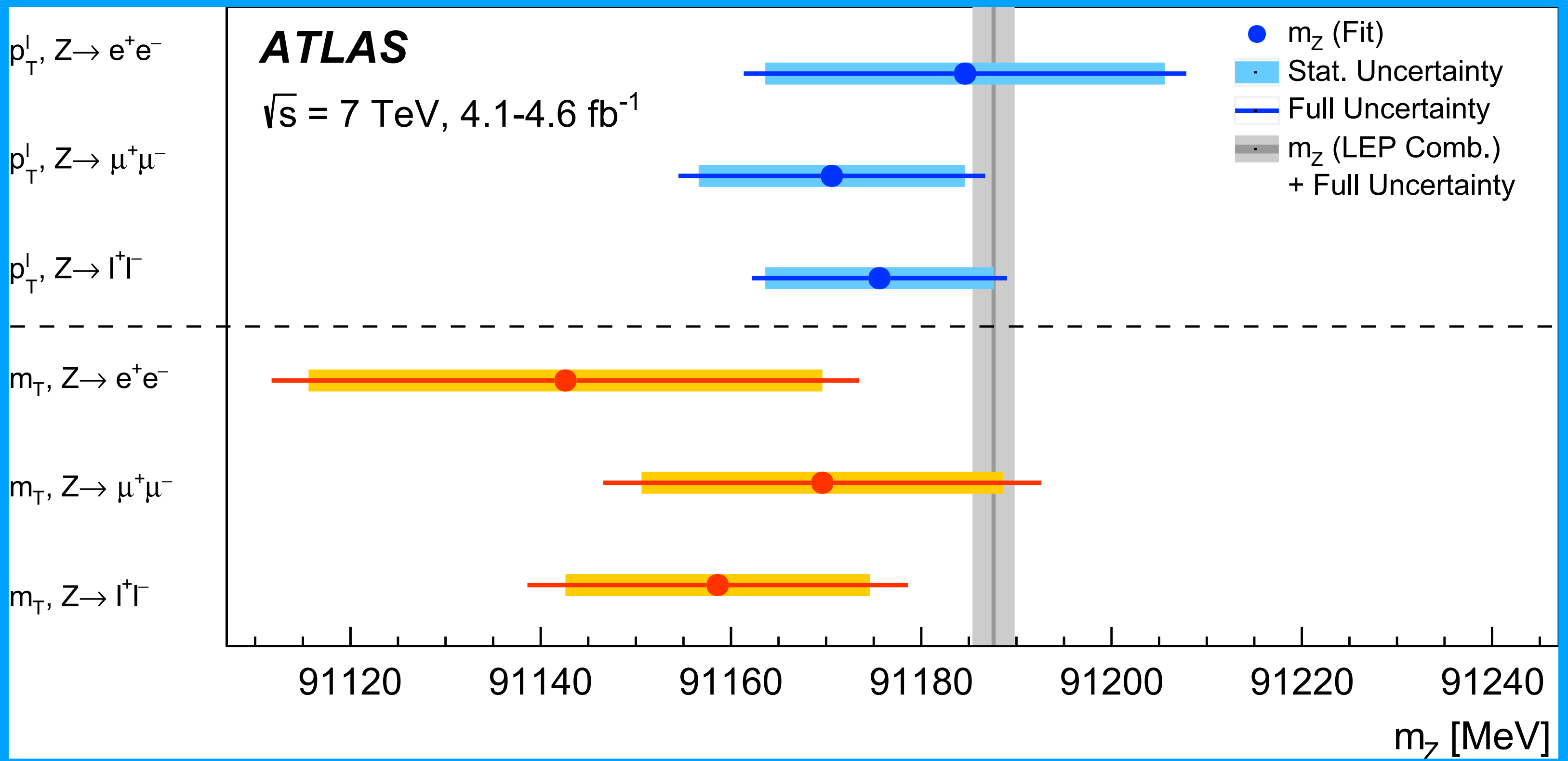

Lepton charge	ℓ^+		ℓ^-		Combined	
Kinematic distribution	p_T^ℓ	m_T	p_T^ℓ	m_T	p_T^ℓ	m_T
Δm_Z [MeV]						
$Z \to ee$	$13 \pm 31 \pm 10$	$-93 \pm 38 \pm 15$	$-20 \pm 31 \pm 10$	$4 \pm 38 \pm 15$	$-3 \pm 21 \pm 10$	$-45 \pm 27 \pm 15$
$Z \to \mu\mu$	$1 \pm 22 \pm 8$	$-35 \pm 28 \pm 13$	$-36 \pm 22 \pm 8$	$-1 \pm 27 \pm 13$	$-17 \pm 14 \pm 8$	$-18 \pm 19 \pm 13$
Combined	$5 \pm 18 \pm 6$	$-58 \pm 23 \pm 12$	$-31 \pm 18 \pm 6$	$1 \pm 22 \pm 12$	$-12 \pm 12 \pm 6$	$-29 \pm 16 \pm 12$

Recoil momentum validation

CMS has performed single-lepton Z boson mass measurements

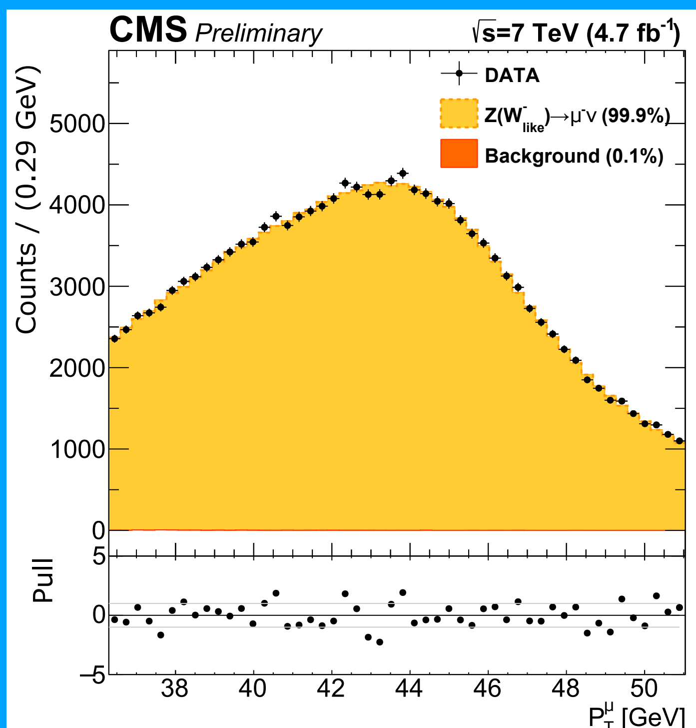

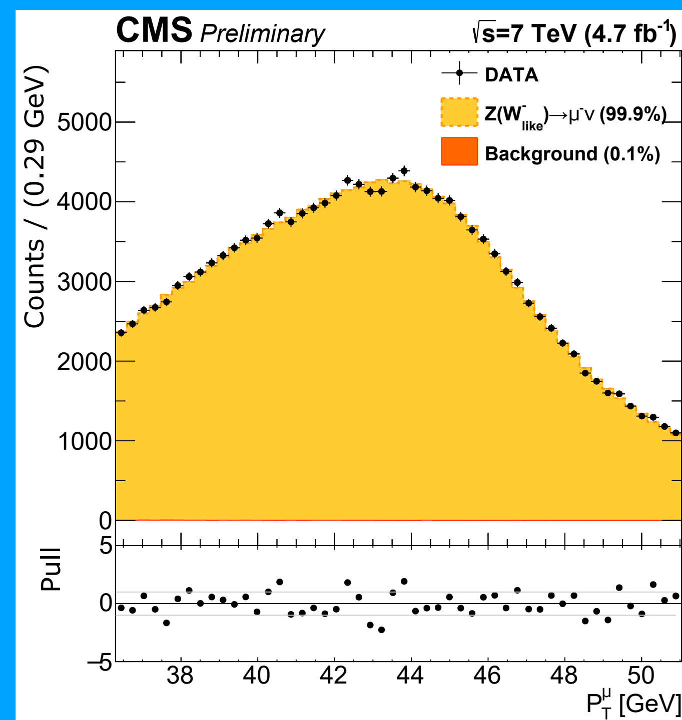

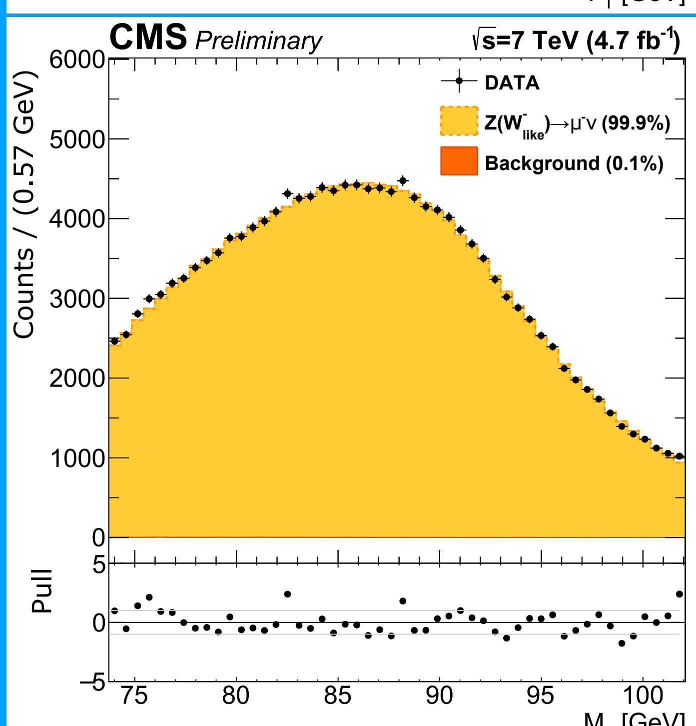

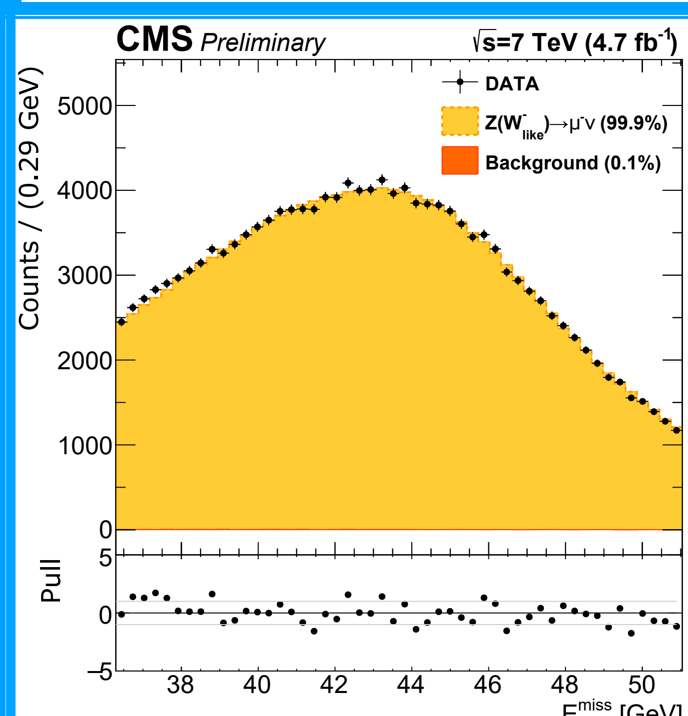

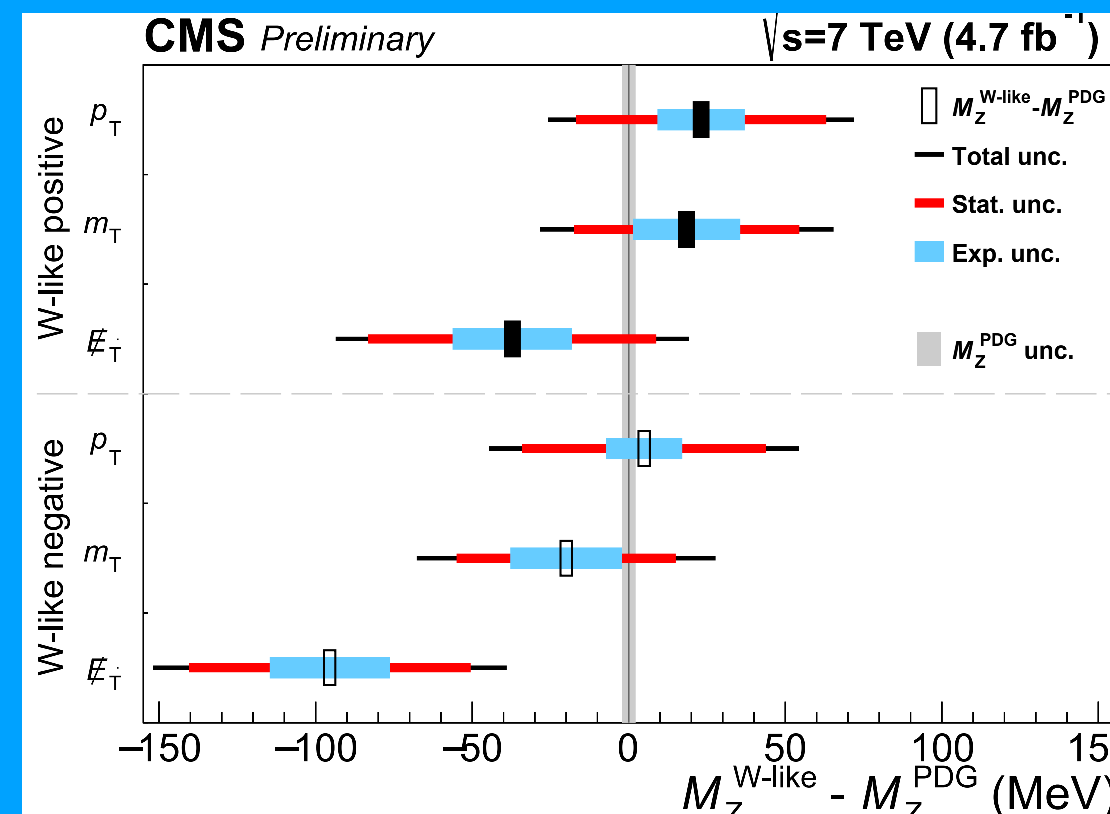

W boson p_T

Transverse mass insensitive to p_T^W to first order

O(1 MeV) change in m_W for each % change in p_T^W from 0-30 GeV

Lepton p_T distributions more sensitive to p_T^W

D0 generates events with Resbos: non-perturbative parameters & NNLL resummation

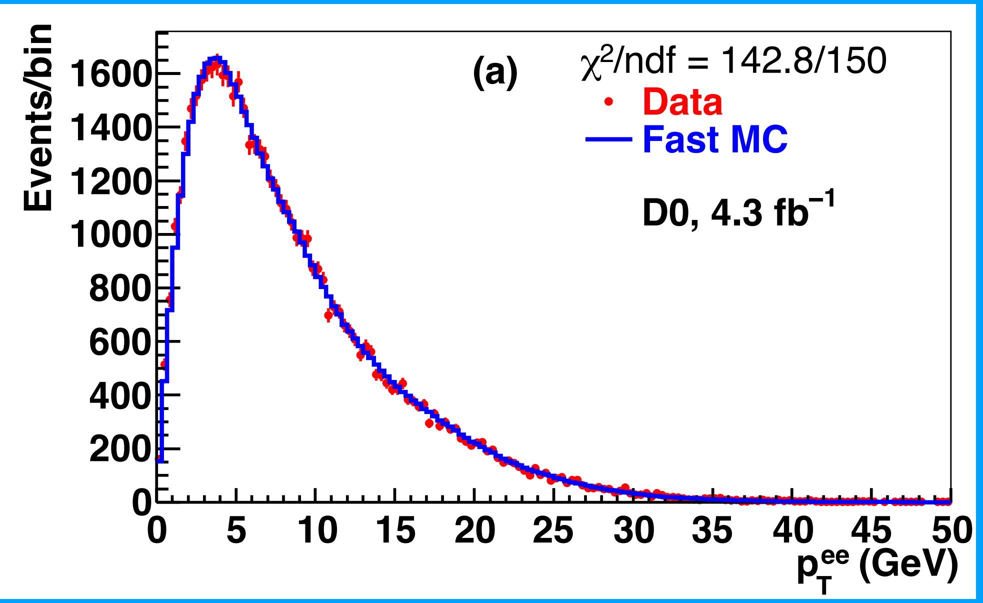

ATLAS reweights p_T^W to a tuned Pythia prediction

Variations affect negative $u_{||}$ more than u_T

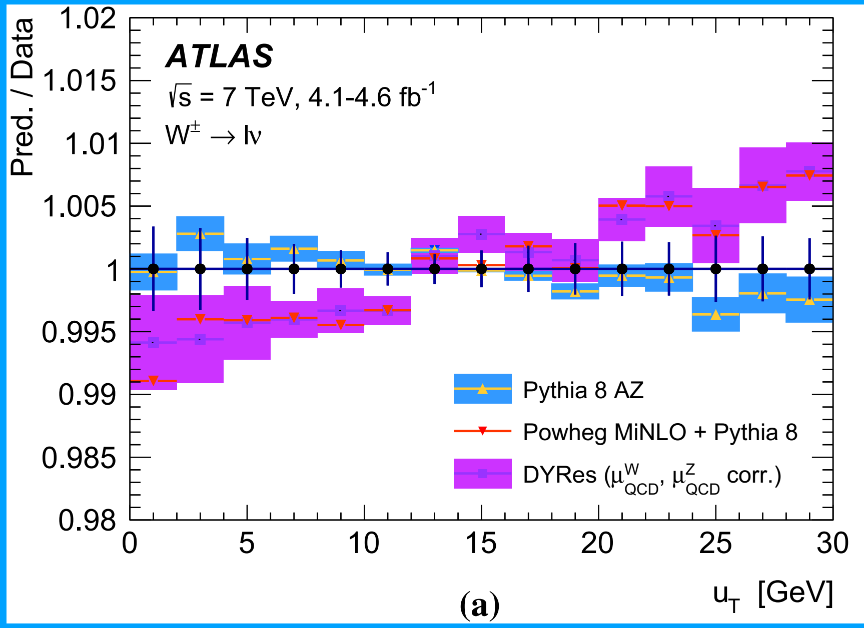

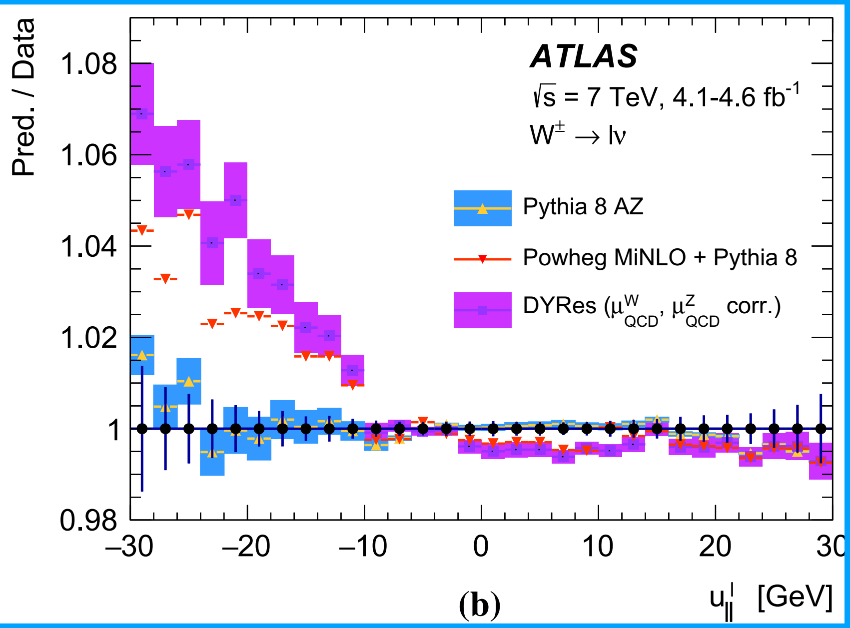

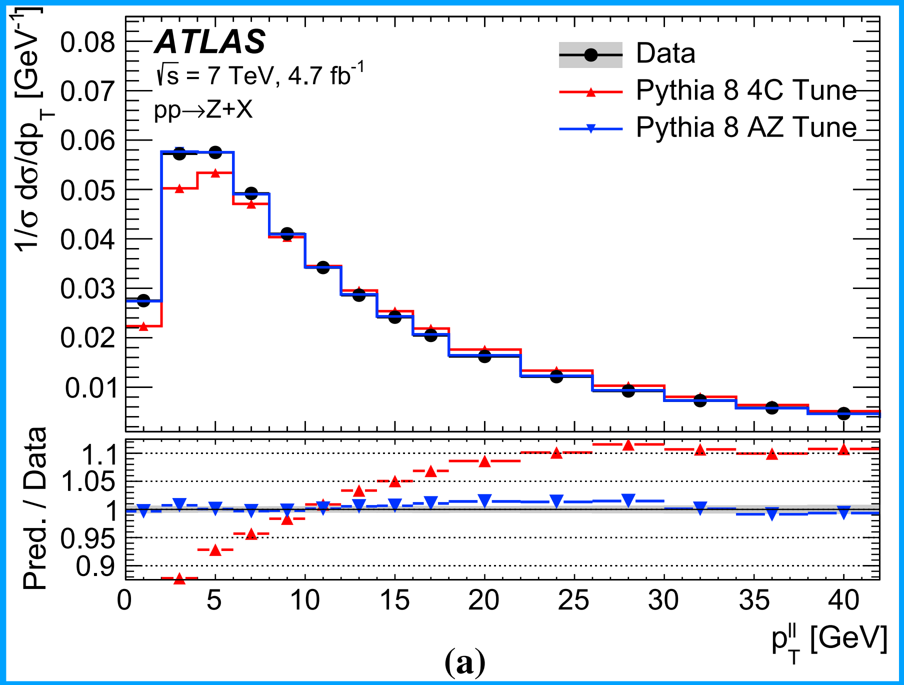

W boson p_T

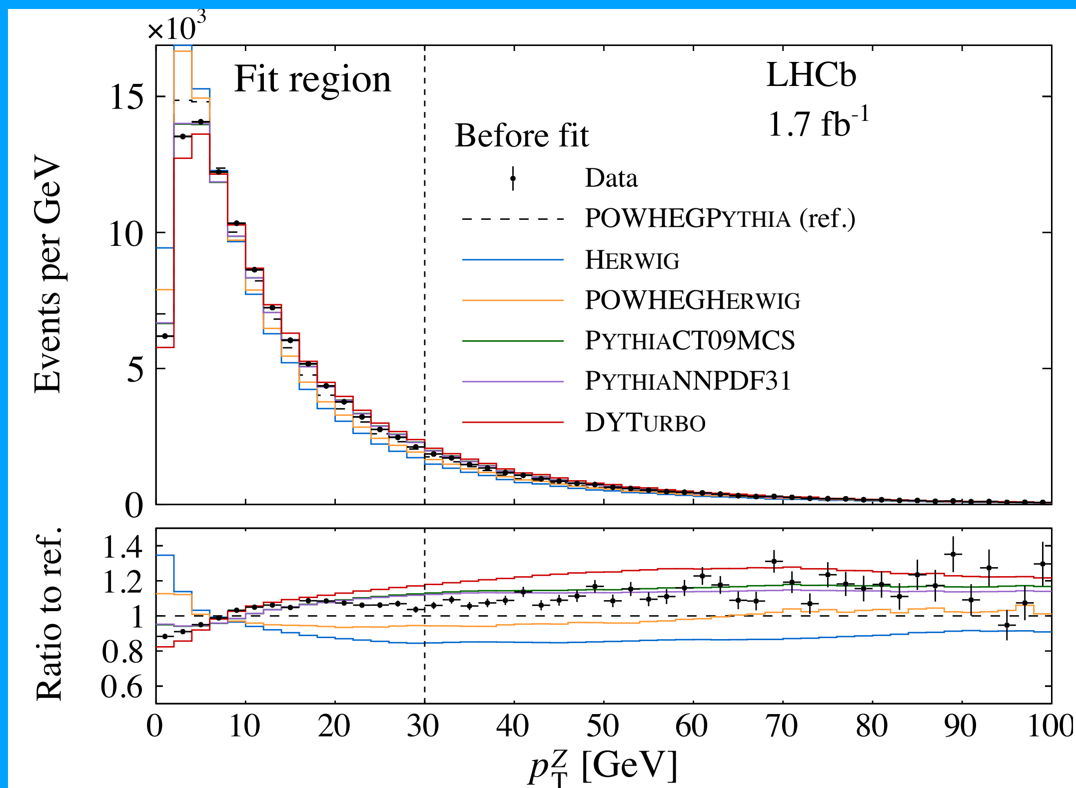

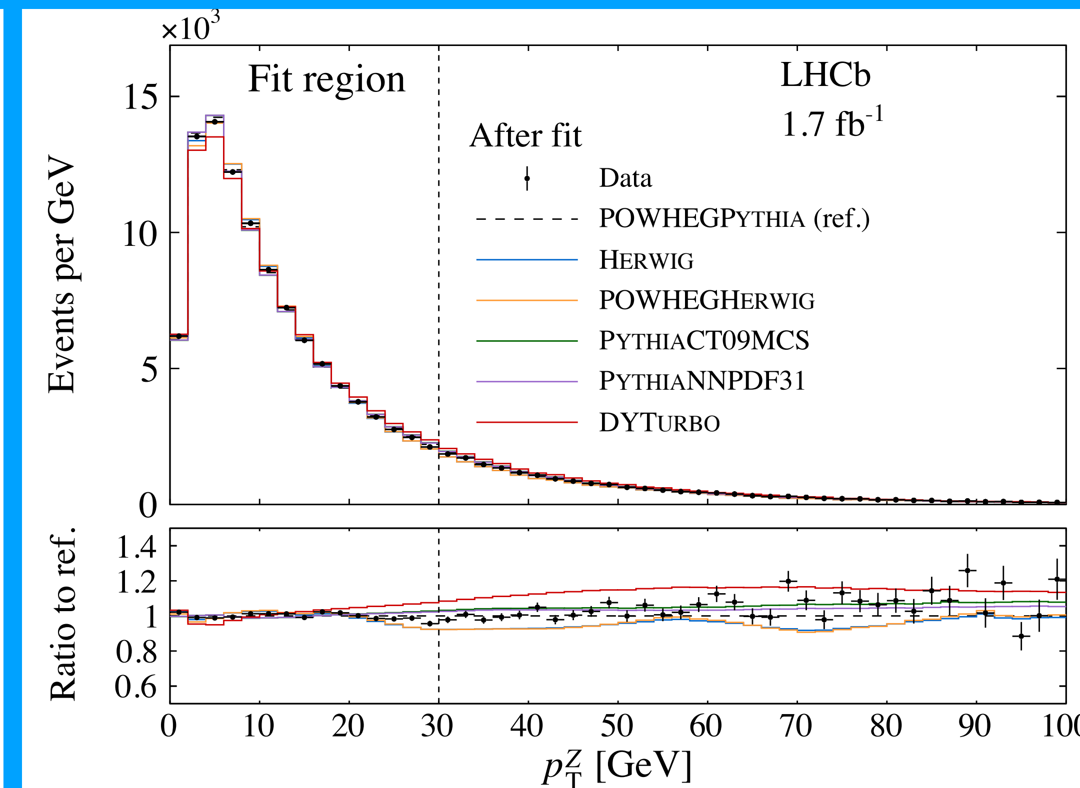

Program	χ^2/ndf	α_s	
DYTurbo	208.1/13	0.1180	$g = 0.523 \pm 0.047\,\mathrm{GeV}^2$
POWHEGPythia	30.3/12	0.1248 ± 0.0004	$k_T^{intr} = 1.470 \pm 0.130\,\mathrm{GeV}$
POWHEGHerwig	55.6/12	0.1361 ± 0.0001	$k_T^{intr} = 0.802 \pm 0.053\,\mathrm{GeV}$
Herwig	41.8/12	0.1352 ± 0.0002	$k_T^{intr} = 0.753 \pm 0.052\,\mathrm{GeV}$
Pythia, CT09MCS	69.0/12	0.1287 ± 0.0004	$k_T^{intr} = 2.113 \pm 0.032\,\mathrm{GeV}$
Pythia, NNPDF31	62.1/12	0.1289 ± 0.0004	$k_T^{intr} = 2.109 \pm 0.032\,\mathrm{GeV}$

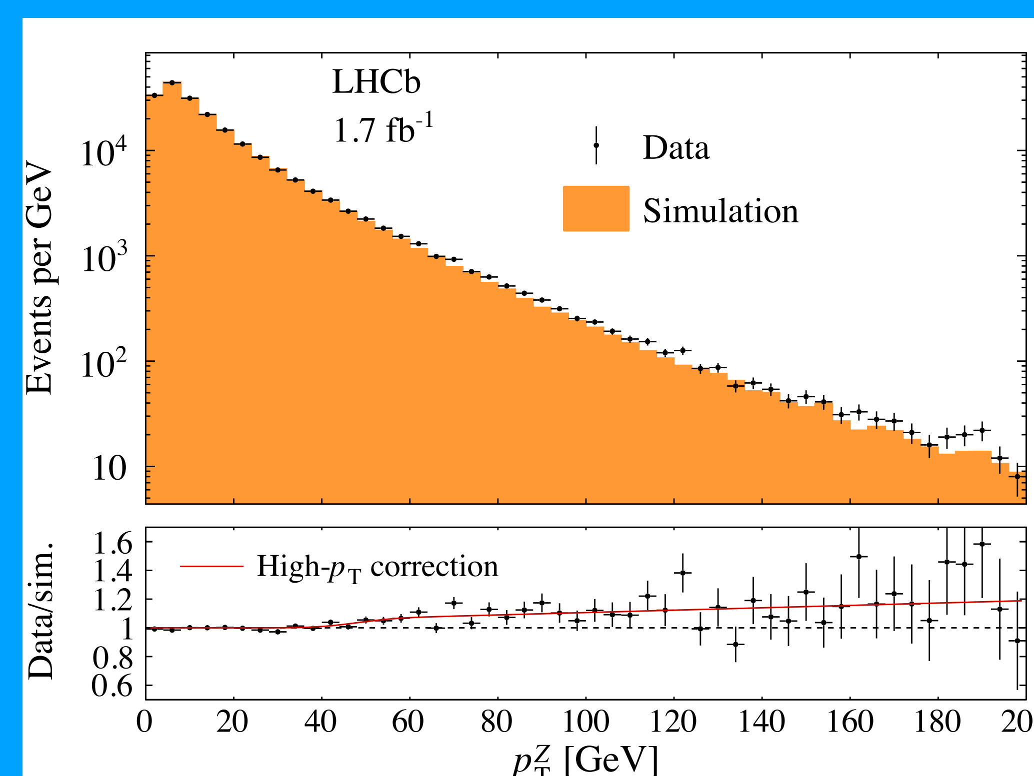

LHCb models distribution using Powheg+Pythia

Z boson data separately constrain low- and high-p_T regions

W boson polarization

$$\frac{d\sigma}{d\Omega} = \frac{d\sigma}{dm\,dp_T\,dy}\,[\,(1+\cos^2\theta) + \frac{1}{2}A_0(1-3\cos^2\theta) + A_1\sin 2\theta\cos\phi + \frac{1}{2}A_2\sin^2\theta\cos 2\phi + A_3\sin\theta\cos\phi + A_4\cos\theta + A_5\sin^2\theta\sin 2\phi + A_6\sin 2\theta\sin\phi + A_7\sin\theta\sin\phi\,]\,,$$

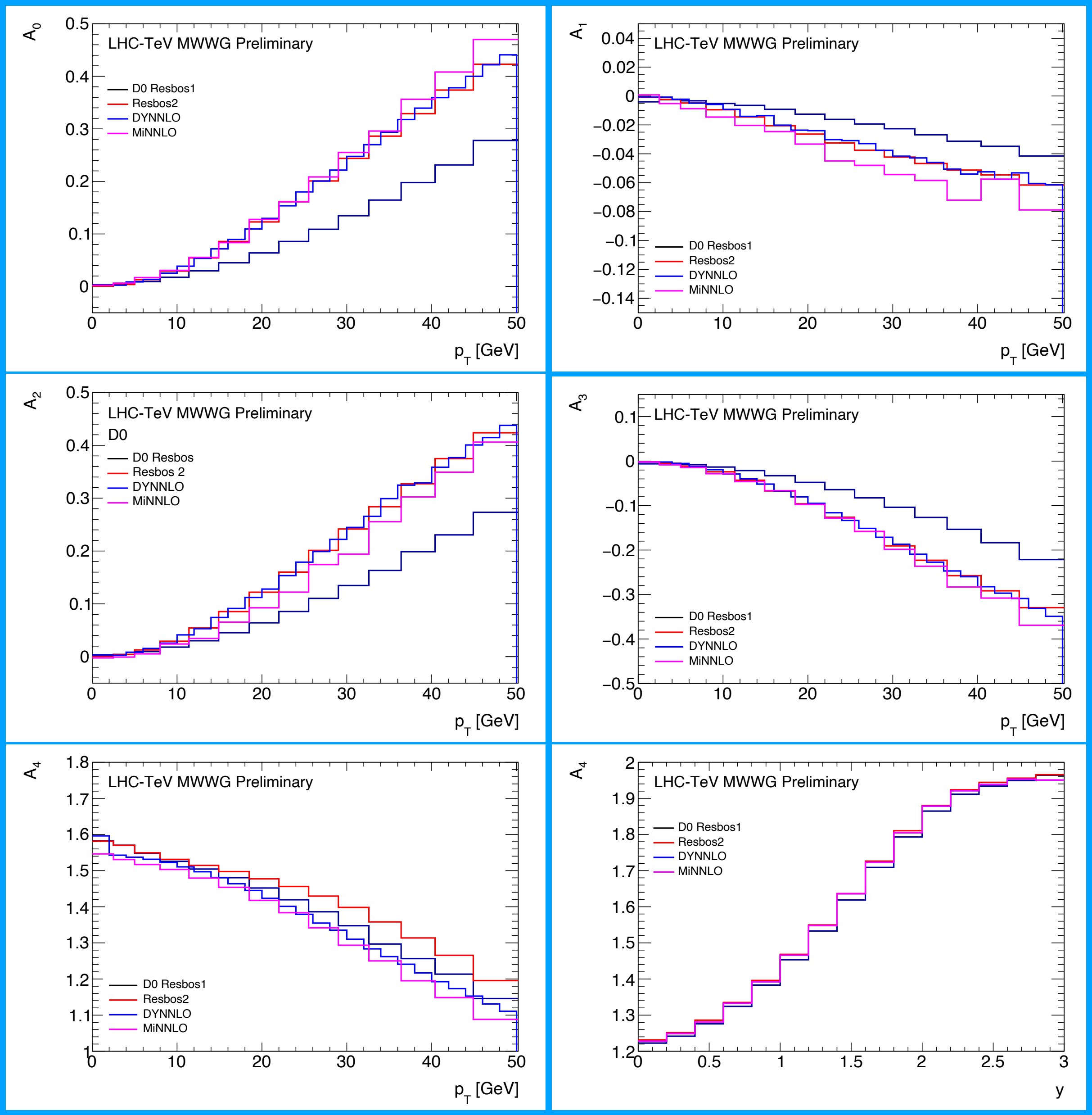

D0 version of Resbos resums the first term and the A_4 term

Fully resummed calculation shifts measurement by -8 MeV

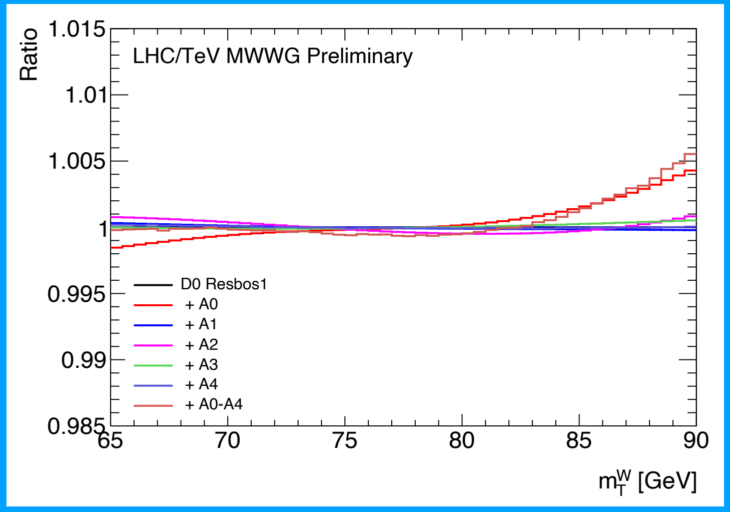

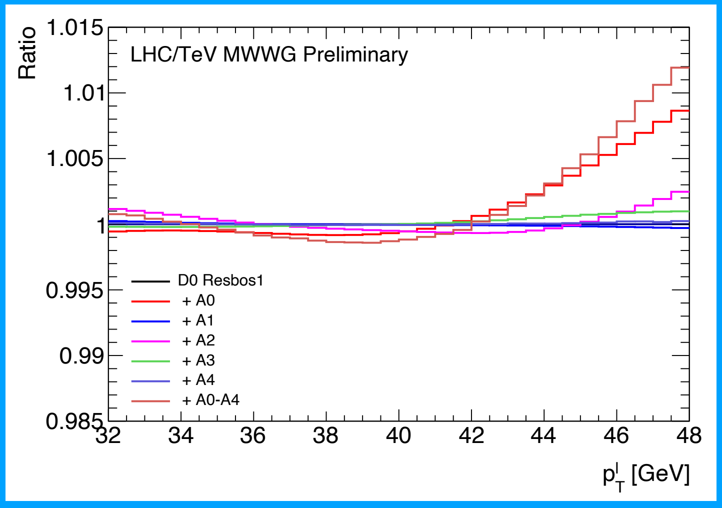

ATLAS reweights coefficients to DYNNLO prediction

LHCb models coefficients with DYTURBO and a scale factor from data for the A_3 coefficient

W boson production

Parton distributions impact the measurement through lepton acceptance

Restriction in η reduces the fraction of low-p_T leptons

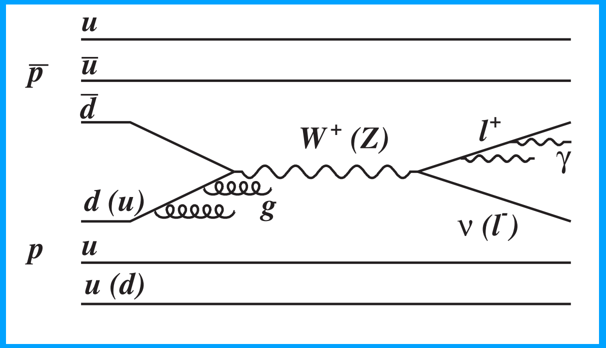

ATLAS uses the CT10 PDF set

LHCb uses the average of NNDF31, CT18, and MSHT20

D0 uses CTEQ6 (1/fb) and CTEQ6.6 (4.3/fb)

Dataset	NNPDF31	NNPDF40	MMHT14	MSHT20	CT18NNLO	ABMP16	CT10	cteq6	cteq66
CDF Z rapidity	24|28 / 28	28|30 / 28	30|31 / 28	32|32 / 28	27|27 / 28	31|31 / 28	29|33 / 28	33|29 / 28	31|32 / 28
CDF W asymmetry	11|57 / 13	14|17 / 13	12|13 / 13	28|27 / 13	11|35 / 13	21|43 / 13	14|22 / 13	14|21 / 13	16|18 / 13
D0 Z rapidity	22|22 / 28	23|23 / 28	23|23 / 28	24|23 / 28	22|22 / 28	22|22 / 28	22|22 / 28	22|22 / 28	22|22 / 28
D0 $We\nu$ lepton asymmetry	22|32 / 13	23|29 / 13	52|51 / 13	42|40 / 13	19|32 / 13	26|24 / 13	20|33 / 13	20|22 / 13	22|26 / 13
D0 $W\mu\nu$ lepton asymmetry	12|14 / 10	12|16 / 10	11|14 / 10	11|13 / 10	12|13 / 10	11|12 / 10	11|13 / 10	12|13 / 10	11|12 / 10
ATLAS peak CC Z rapidity	13|18 / 12	13|17 / 12	58|89 / 12	17|19 / 12	11|77 / 12	18|32 / 12	14|25 / 12	21|214 / 12	18|29 / 12
ATLAS W^- lepton rapidity	12|18 / 11	12|15 / 11	33|33 / 11	16|17 / 11	9.9|28 / 11	14|17 / 11	10|25 / 11	21|38 / 11	14|44 / 11
ATLAS W^+ lepton rapidity	8.9|13 / 11	8.6|11 / 11	15|21 / 11	12|13 / 11	9.4|16 / 11	10|12 / 11	11|28 / 11	12|59 / 11	12|59 / 11
Correlated χ^2	76|110	63|83	212|236	91|102	43|251	86|108	52|166	158|513	90|236
Log penalty χ^2	-0.62|-0.62	-0.58|-0.58	-1.62|-1.62	-2.89|-2.89	-1.68|-1.68	-2.72|-2.72	-3.94|-3.94	-7.70|-7.70	-4.37|-4.37
Total χ^2 / dof	200|312 / 126	195|242 / 126	445|509 / 126	270|283 / 126	163|499 / 126	236|300 / 126	179|364 / 126	306|923 / 126	231|472 / 126

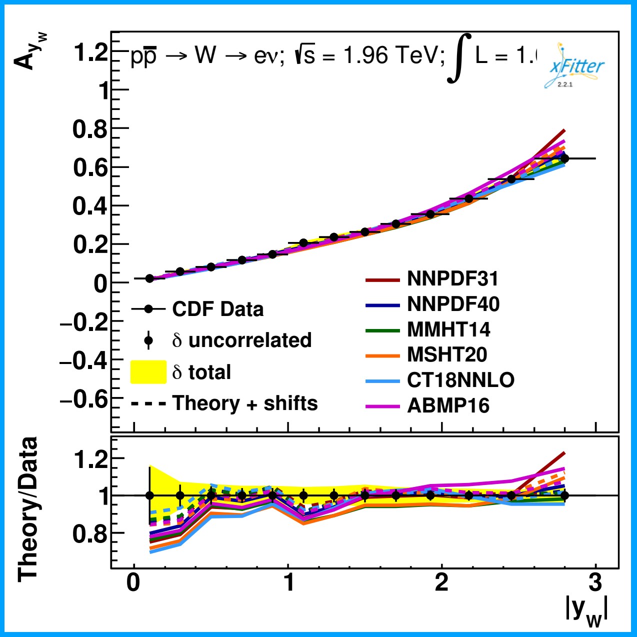

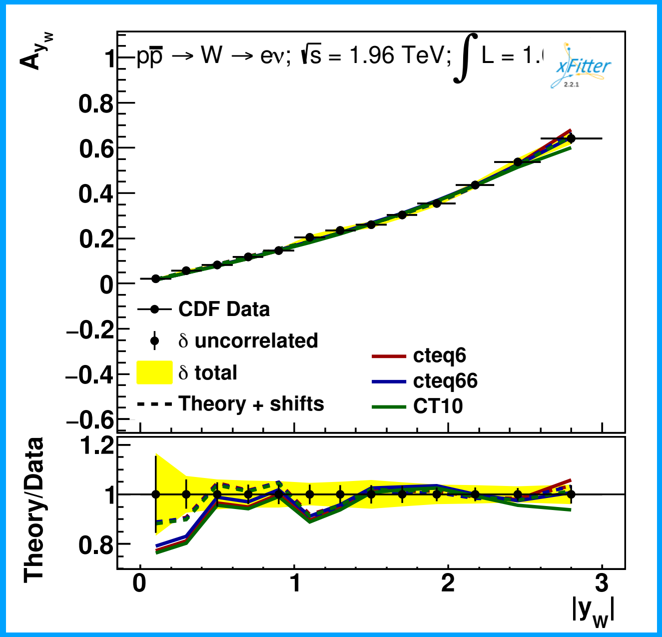

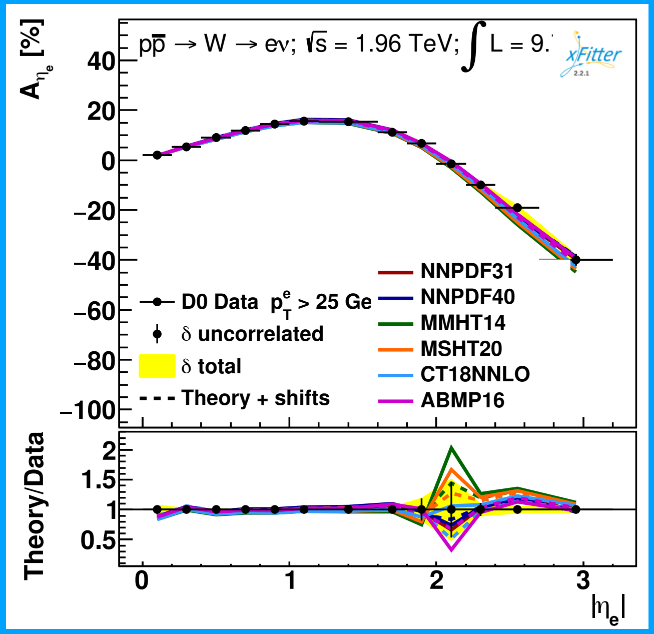

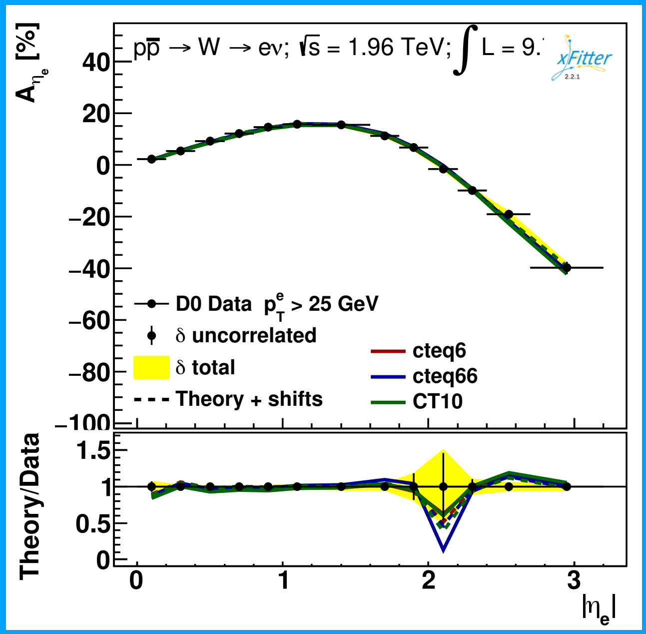

W boson candidates

W boson event selection
Require kinematics consistent with resonance production

Lepton identification
ATLAS, **LHCb** and **D0** require isolated charged leptons

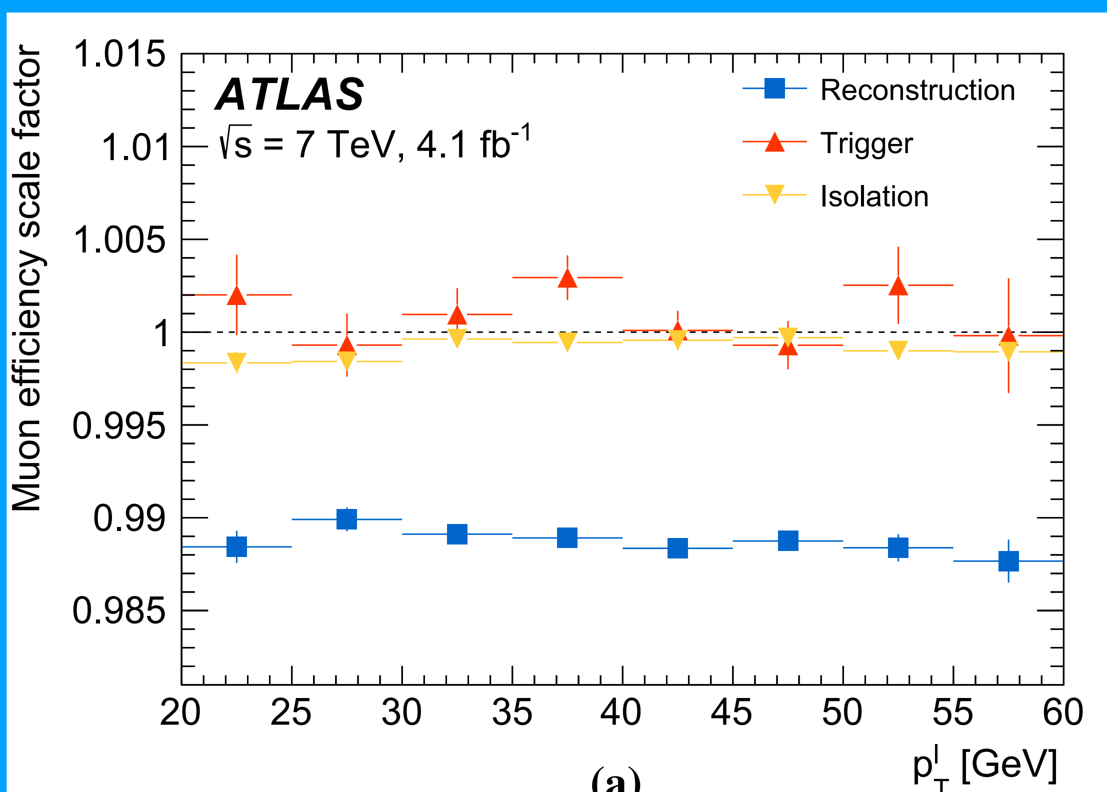

ATLAS
7.8 M $W \to \mu\nu$ candidates
5.9 M $W \to e\nu$ candidates

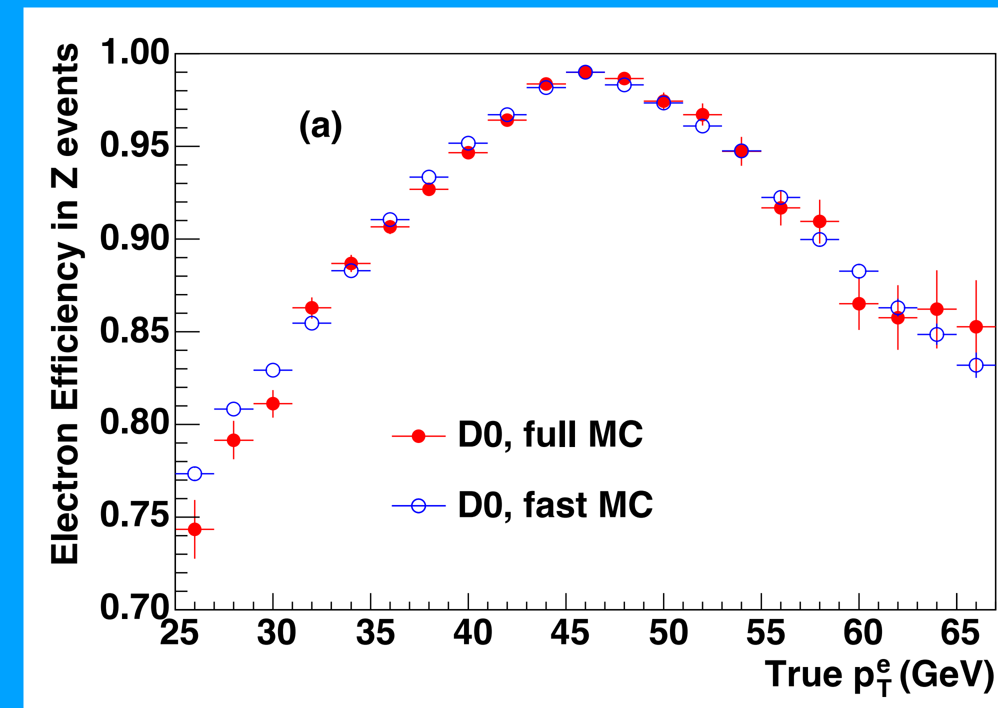

D0
1.7 M $W \to e\nu$ candidates

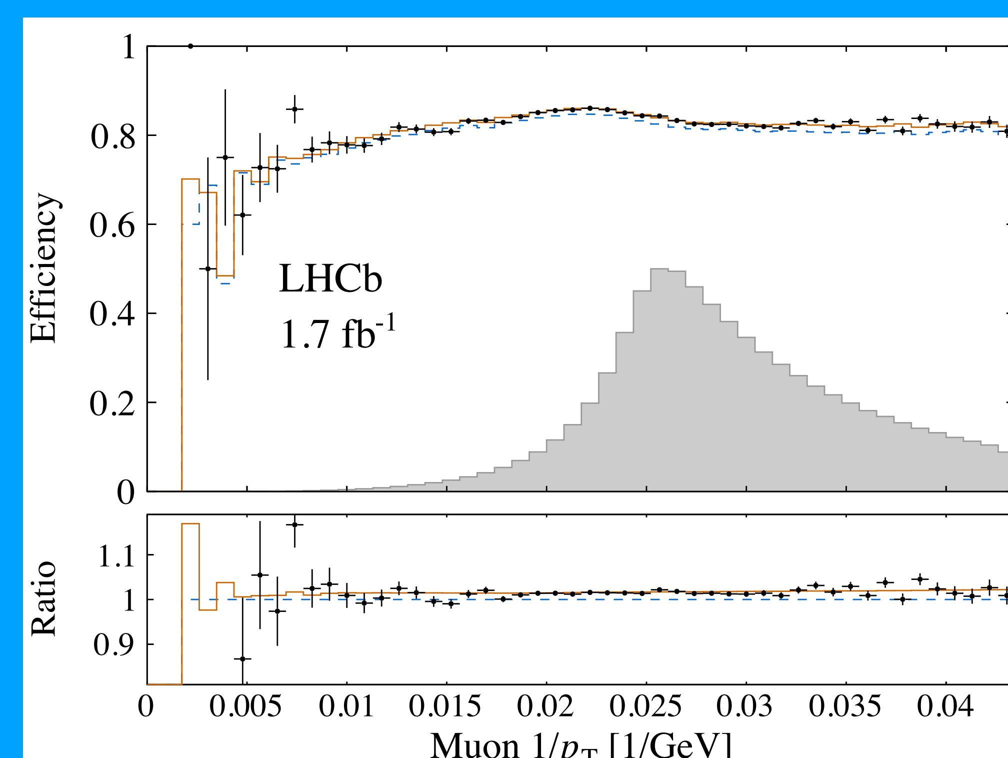

LHCb
2.4 M $W \to \mu\nu$ candidates

Backgrounds

Most challenging background comes from hadrons misreconstructed as leptons

ATLAS: 0.5-1.7%
D0: 1%
LHCb: 1.5%

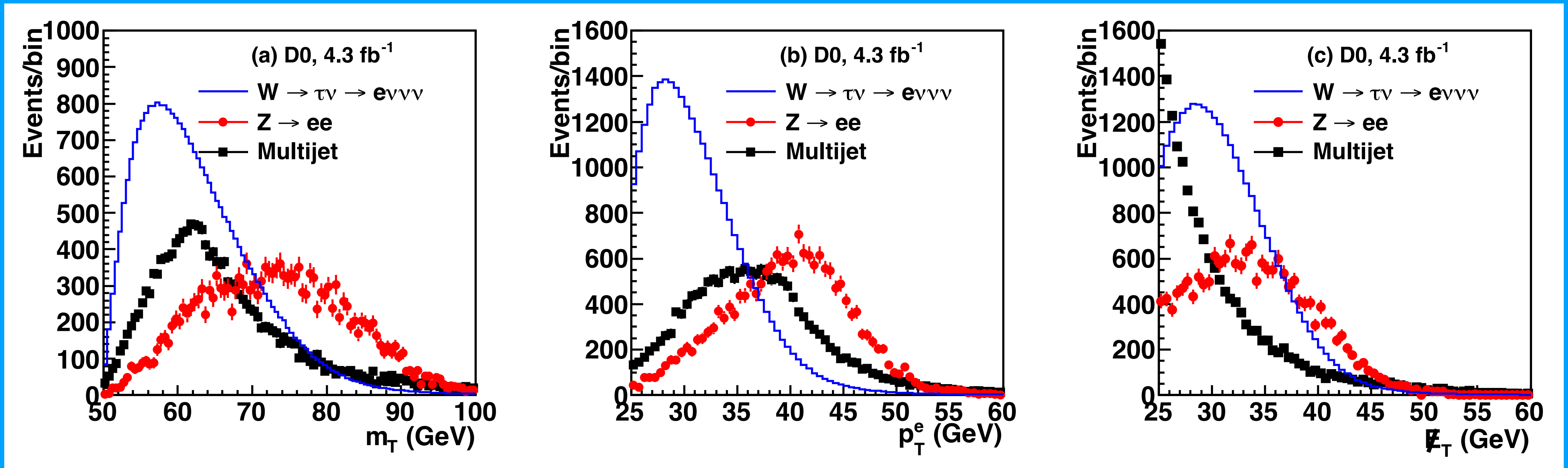

Estimated by fitting a background sample to a kinematic distribution in data

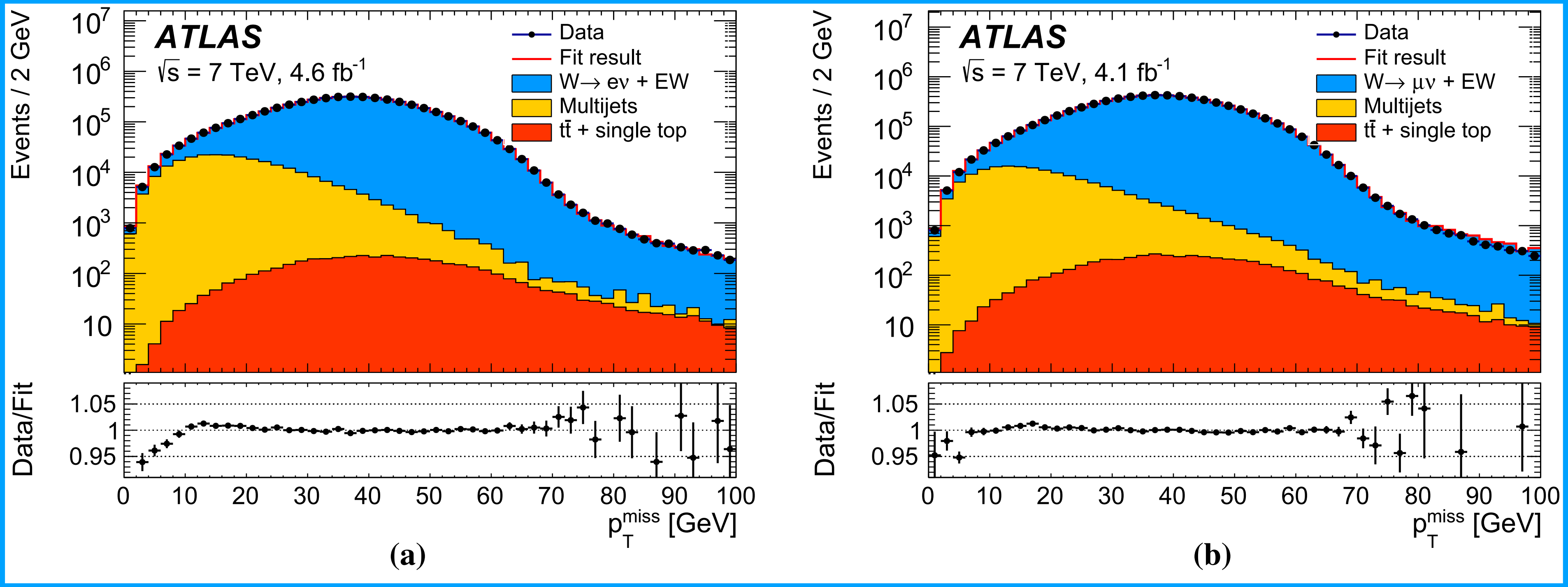

W boson mass measurements

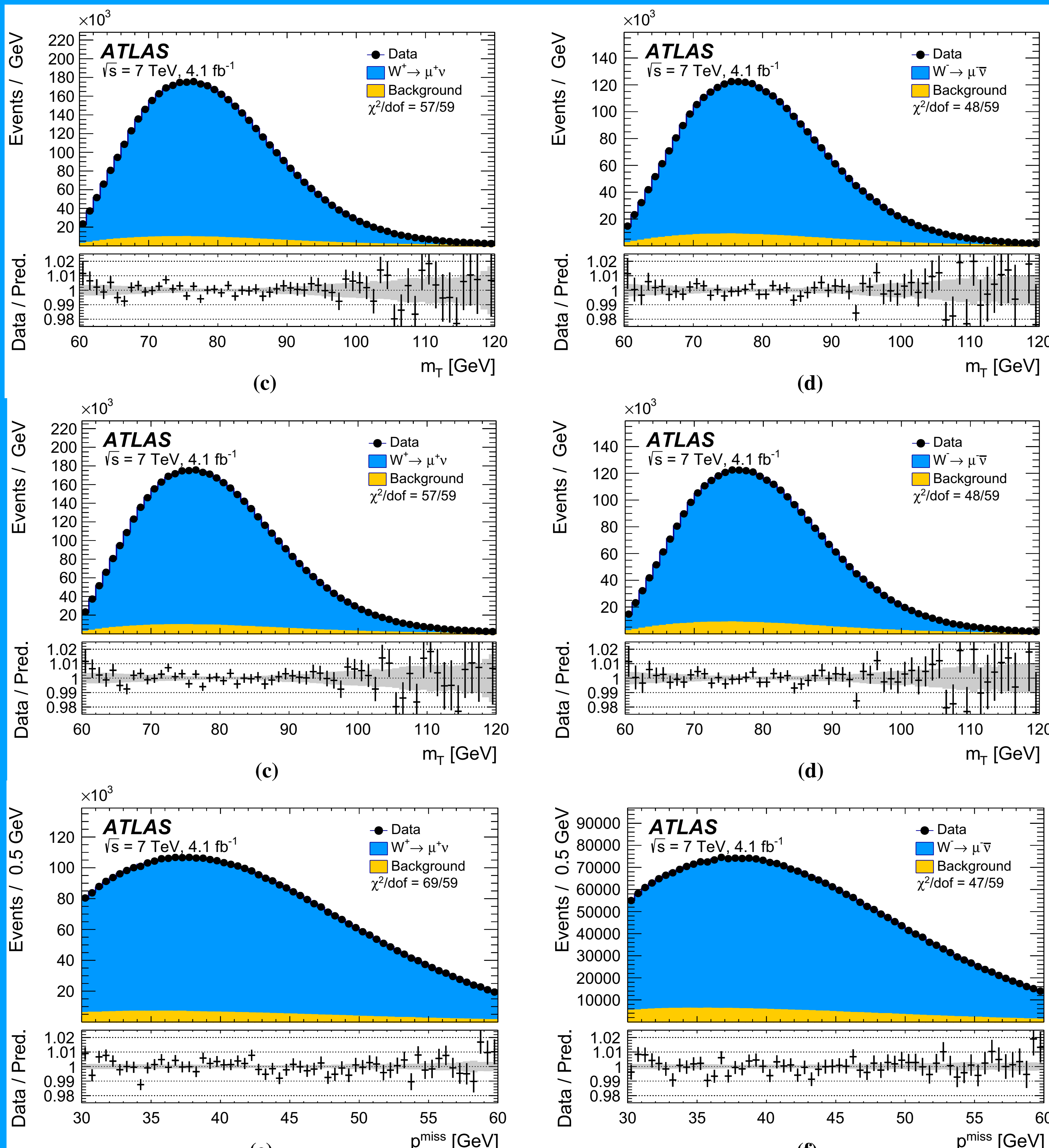

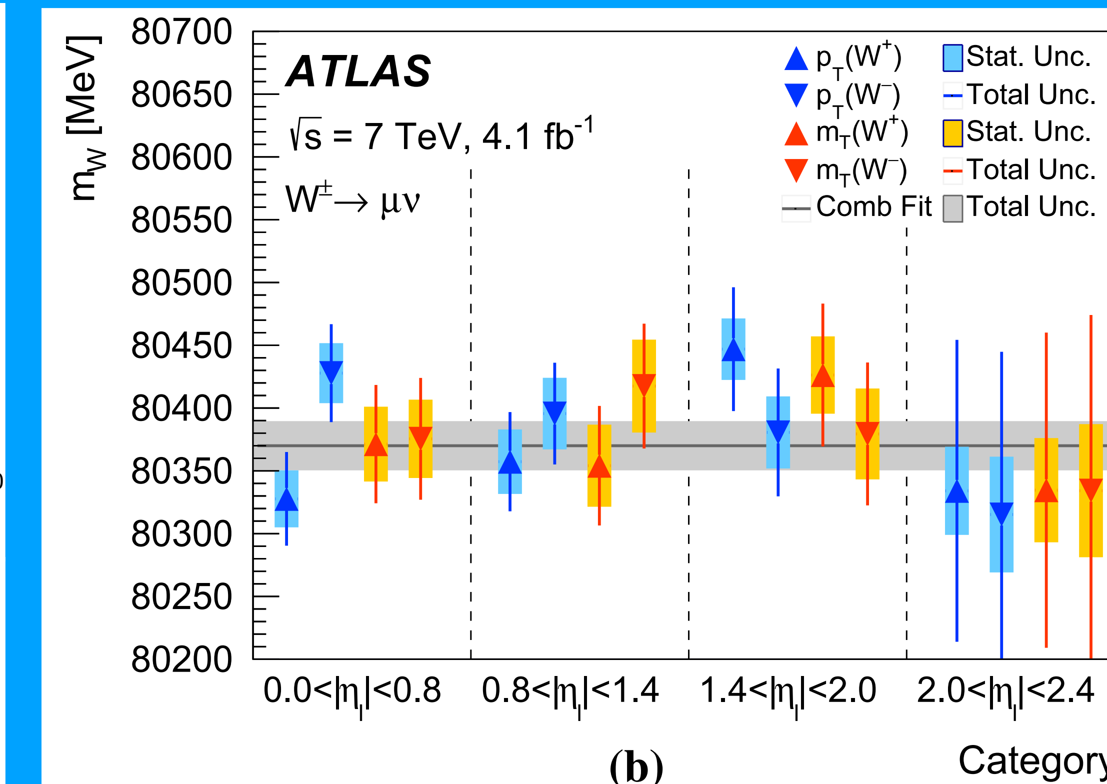

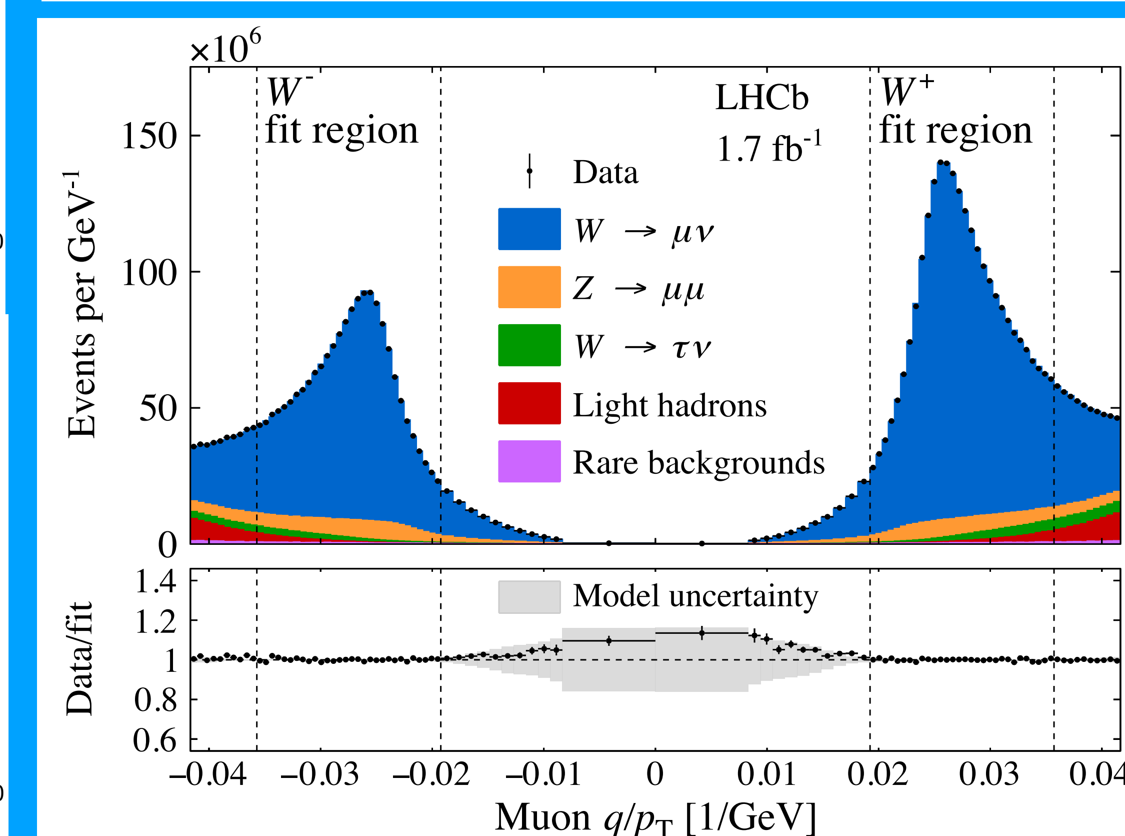

W boson mass measurements

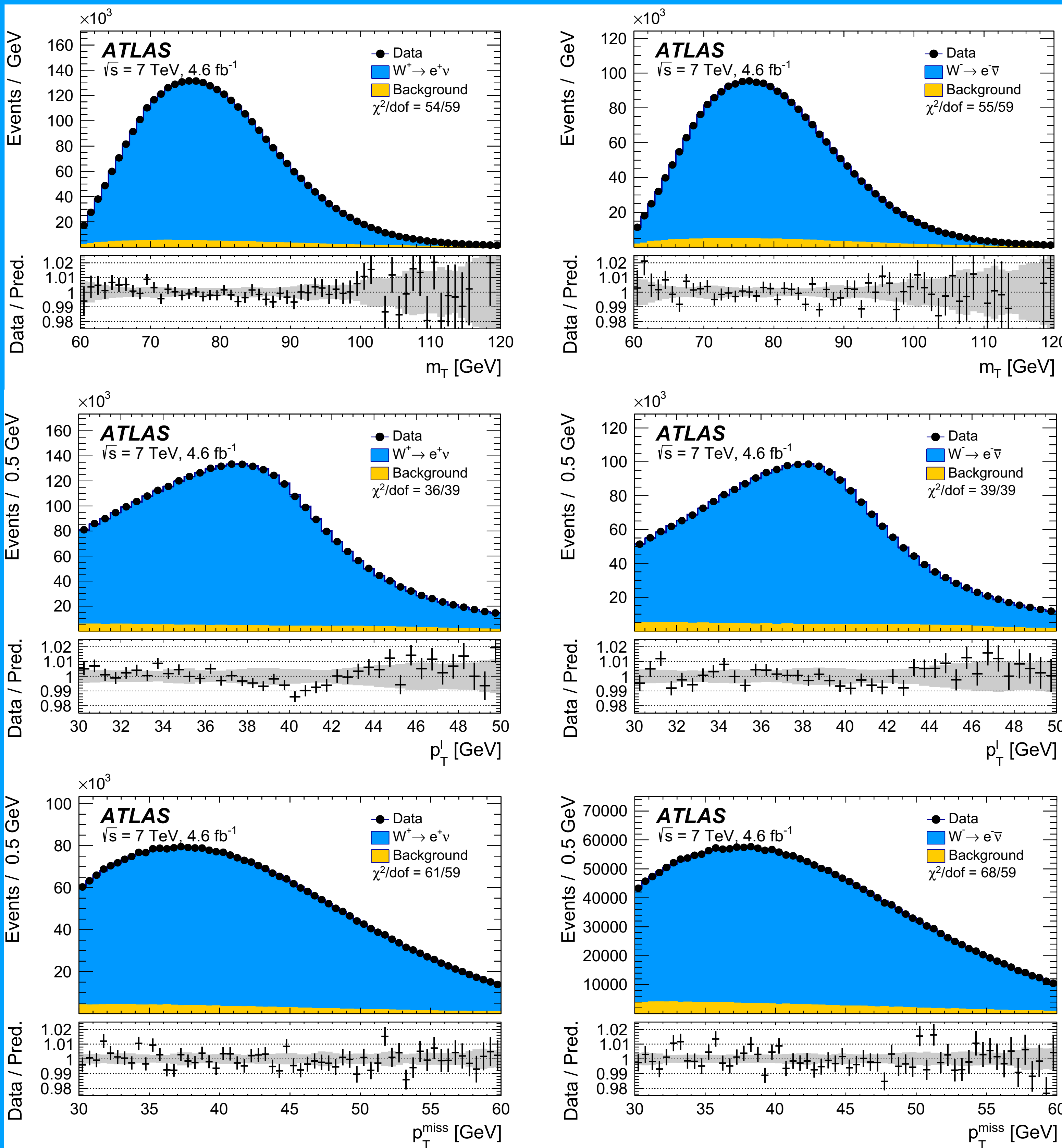

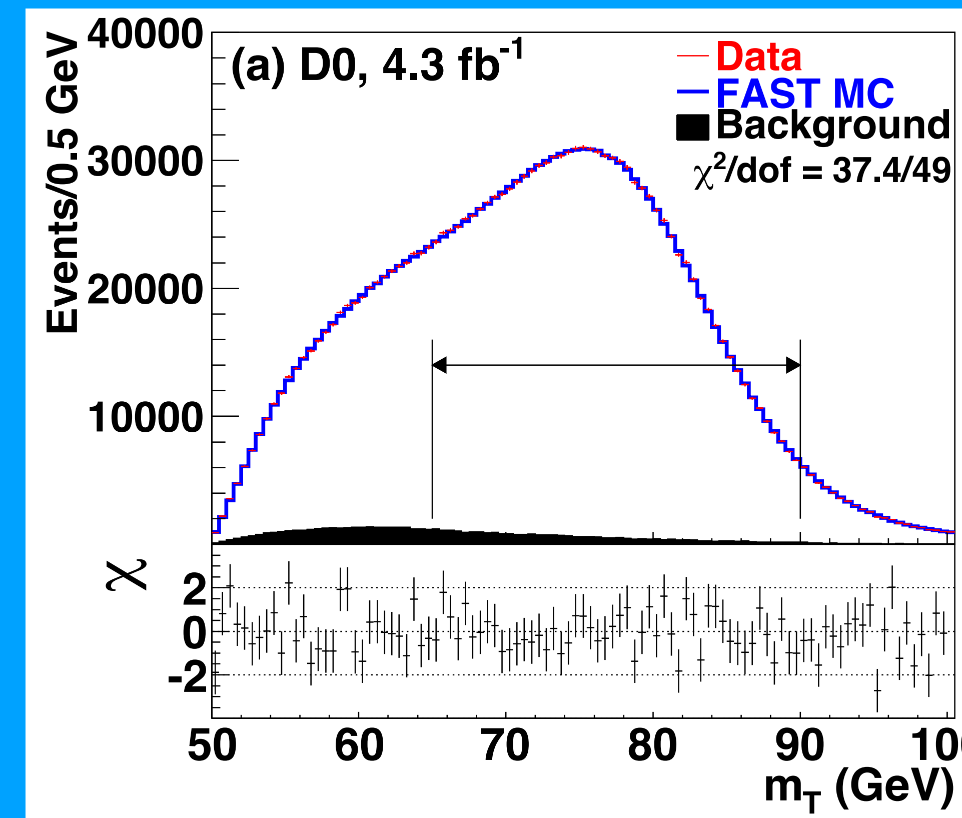

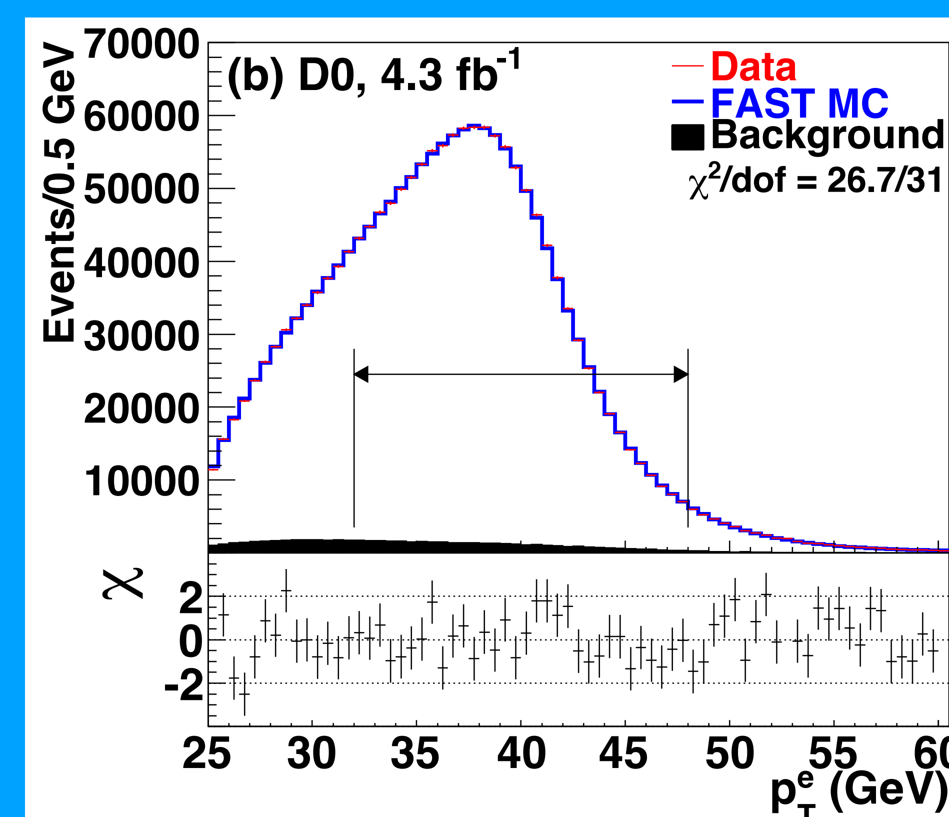

Validation of W boson mass measurements

ATLAS

Decay channel	$W \to e\nu$		$W \to \mu\nu$		Combined	
Kinematic distribution	p_T^ℓ	m_T	p_T^ℓ	m_T	p_T^ℓ	m_T
Δm_W [MeV]						
$\langle\mu\rangle$ in [2.5, 6.5]	8 ± 14	14 ± 18	-21 ± 12	0 ± 16	-9 ± 9	6 ± 12
$\langle\mu\rangle$ in [6.5, 9.5]	-6 ± 16	6 ± 23	12 ± 15	-8 ± 22	4 ± 11	-1 ± 16
$\langle\mu\rangle$ in [9.5, 16]	-1 ± 16	3 ± 27	25 ± 16	35 ± 26	12 ± 11	20 ± 19
u_T in [0, 15] GeV	0 ± 11	-8 ± 13	5 ± 10	8 ± 12	3 ± 7	-1 ± 9
u_T in [15, 30] GeV	10 ± 15	0 ± 24	-4 ± 14	-18 ± 22	2 ± 10	-10 ± 16
$u_\parallel^\ell < 0$ GeV	8 ± 15	20 ± 17	3 ± 13	-1 ± 16	5 ± 10	9 ± 12
$u_\parallel^\ell > 0$ GeV	-9 ± 10	1 ± 14	-12 ± 10	10 ± 13	-11 ± 7	6 ± 10
No p_T^{miss}-cut	14 ± 9	-1 ± 13	10 ± 8	-6 ± 12	12 ± 6	-4 ± 9

LHCb

Subset	χ^2_{tot}/ndf	δm_W [MeV]
Polarity $= -1$	92.5/102	–
Polarity $= +1$	97.3/102	-57.5 ± 45.4
$\eta > 3.3$	115.4/102	–
$\eta < 3.3$	85.9/102	$+56.9 \pm 45.5$
Polarity $\times\ q = +1$	95.9/102	–
Polarity $\times\ q = -1$	98.2/102	$+16.1 \pm 45.4$
$\lvert\phi\rvert > \pi/2$	98.8/102	–
$\lvert\phi\rvert < \pi/2$	115.0/102	$+66.7 \pm 45.5$
$\phi < 0$	91.8/102	–
$\phi > 0$	103.0/102	-100.5 ± 45.3

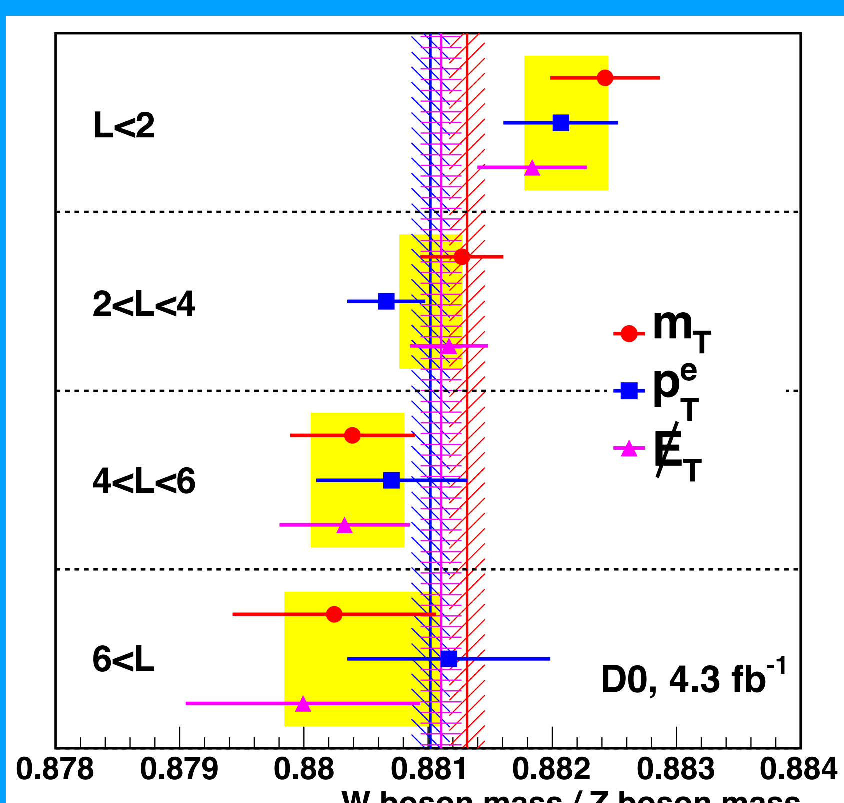

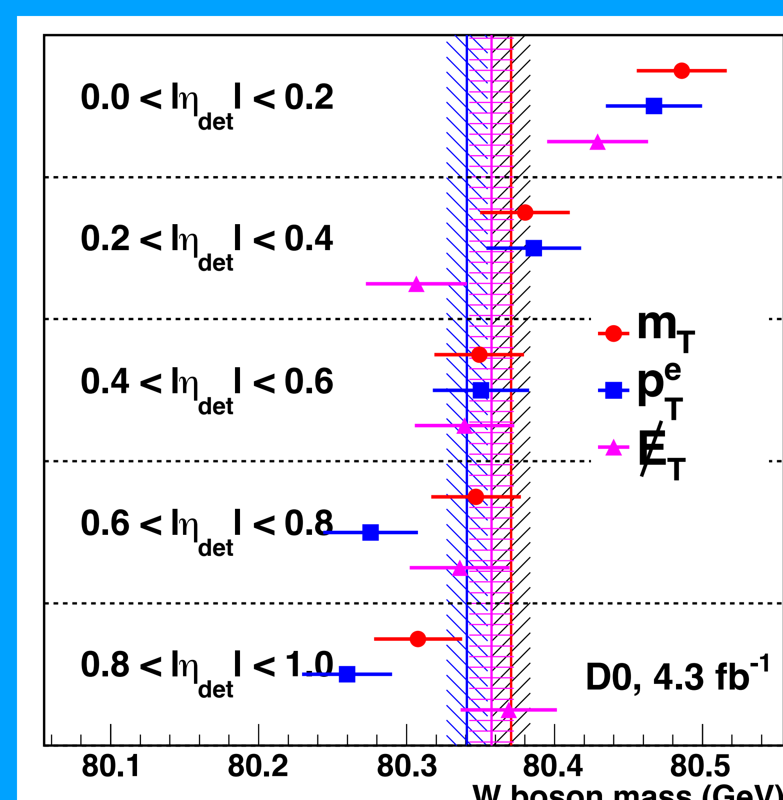

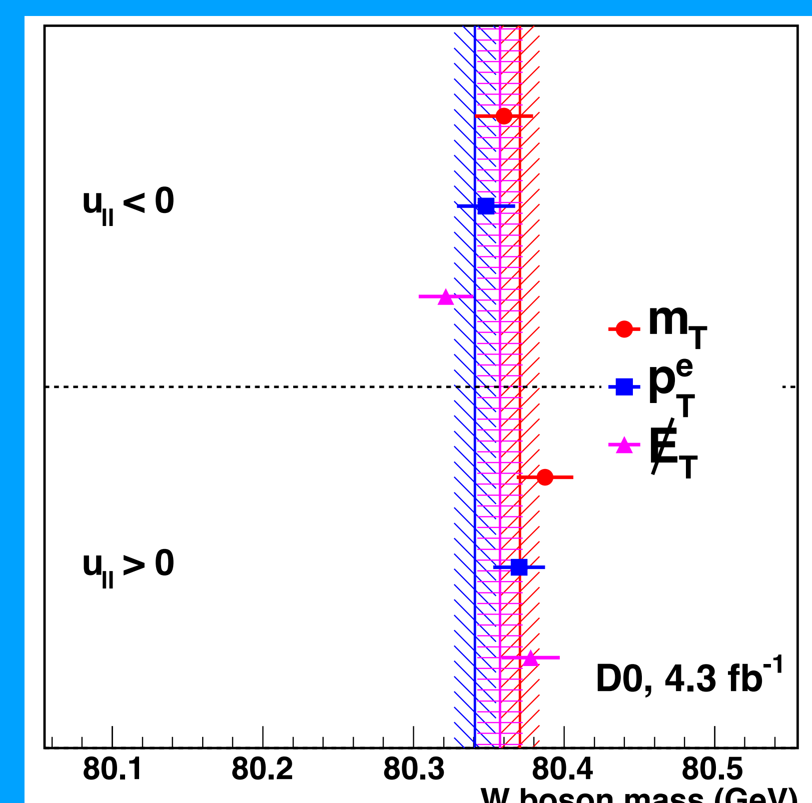

W boson mass measurements

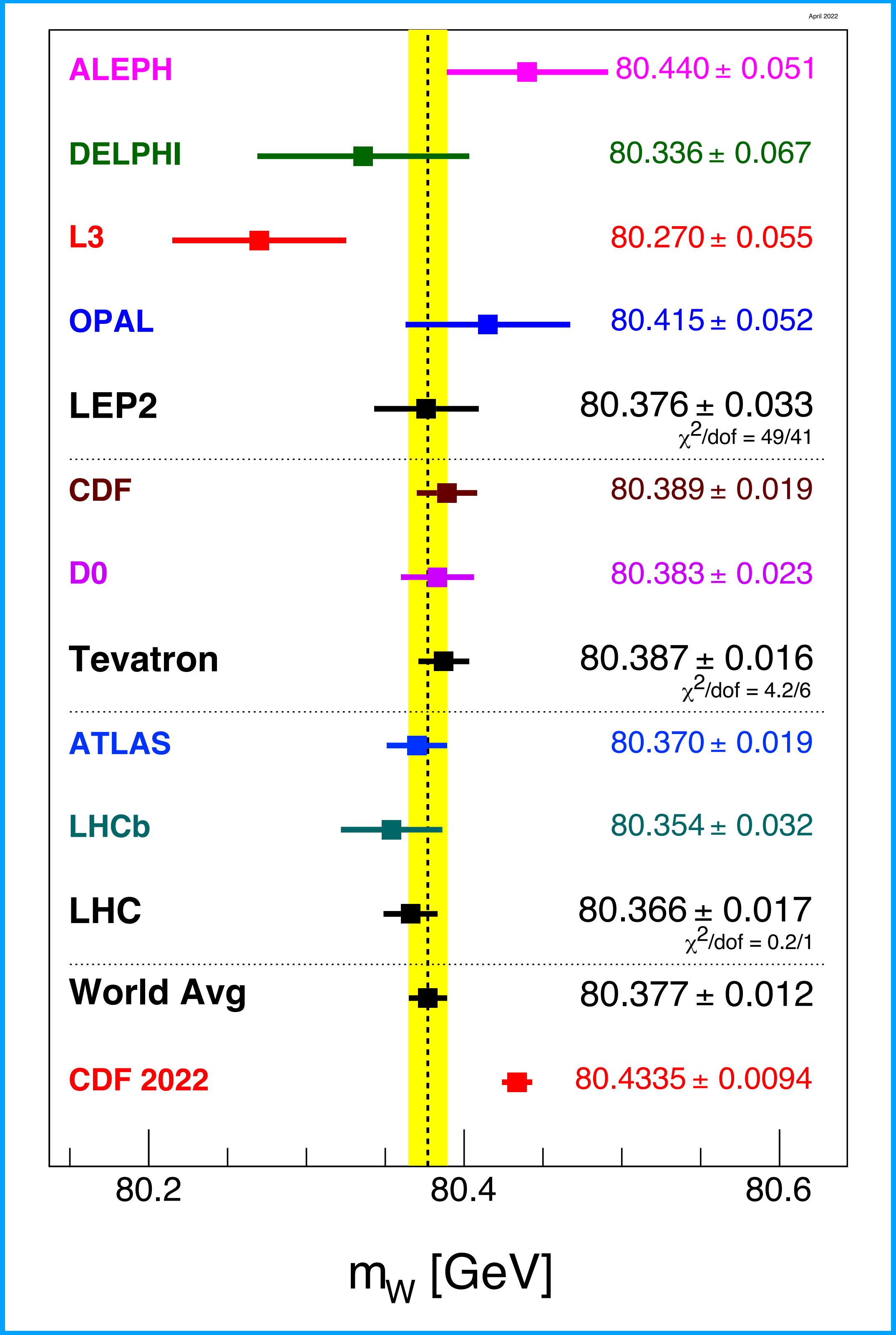

PDG (2022)

Summary

Hadron-collider W boson mass measurements are the most precise

Multiple measurements internally consistent with cross-checks

Small effects can be important

Future LHC measurements can be made more robust
e.g. Z mass measurement & efficiency checks with W leptons or varied isolation

Many effects can be tested with low-pileup runs & runs at different energies

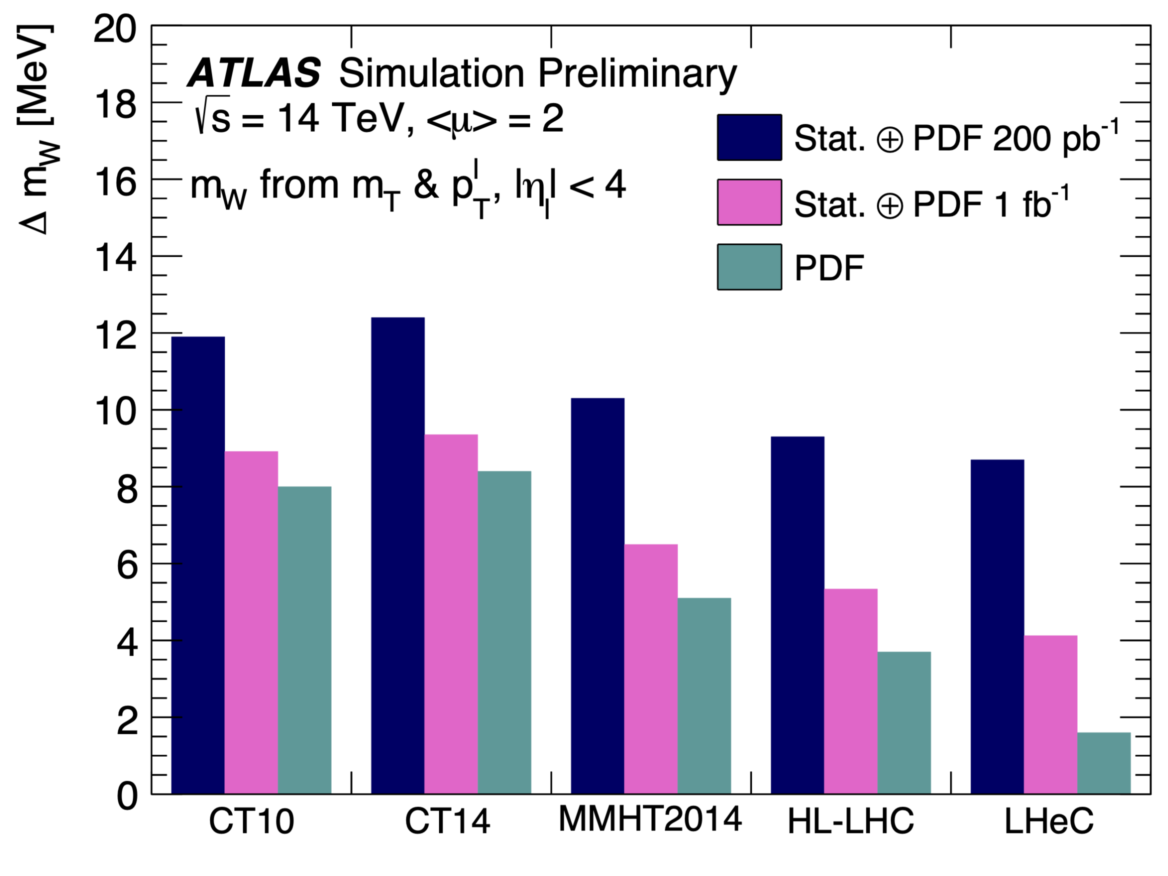

Backup

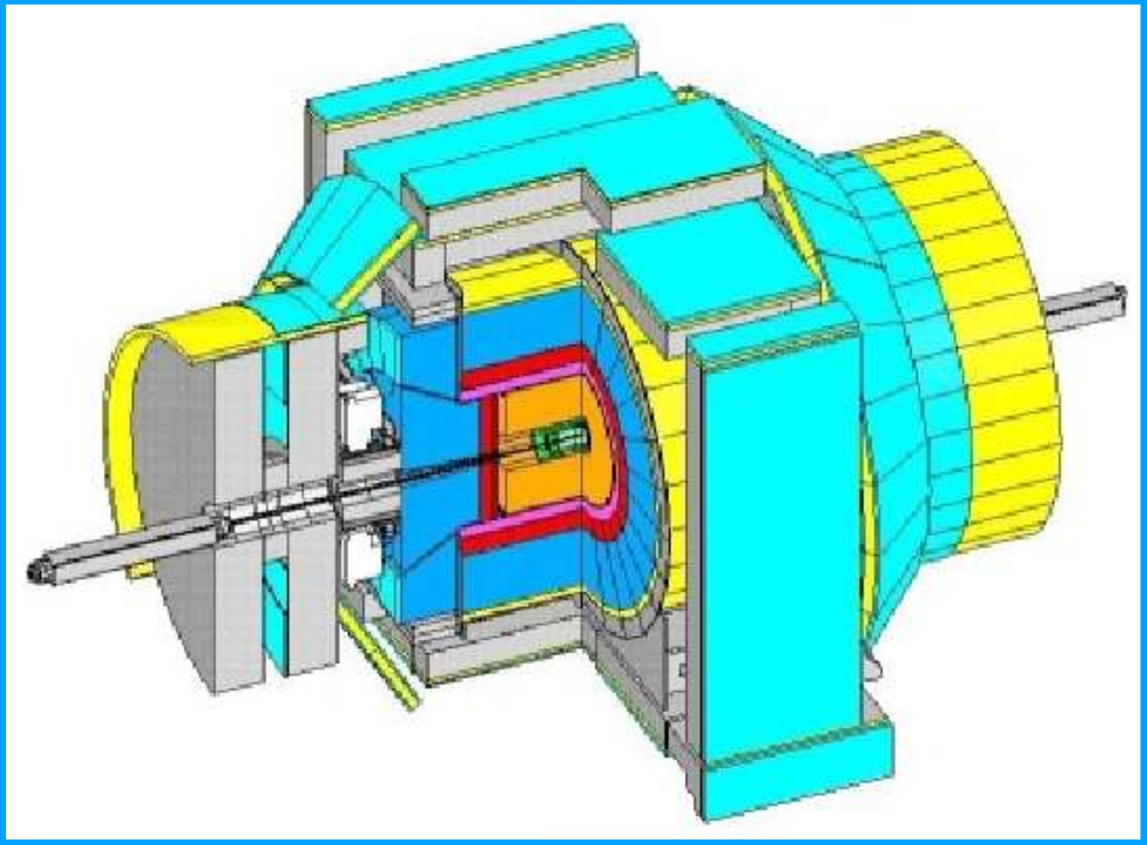

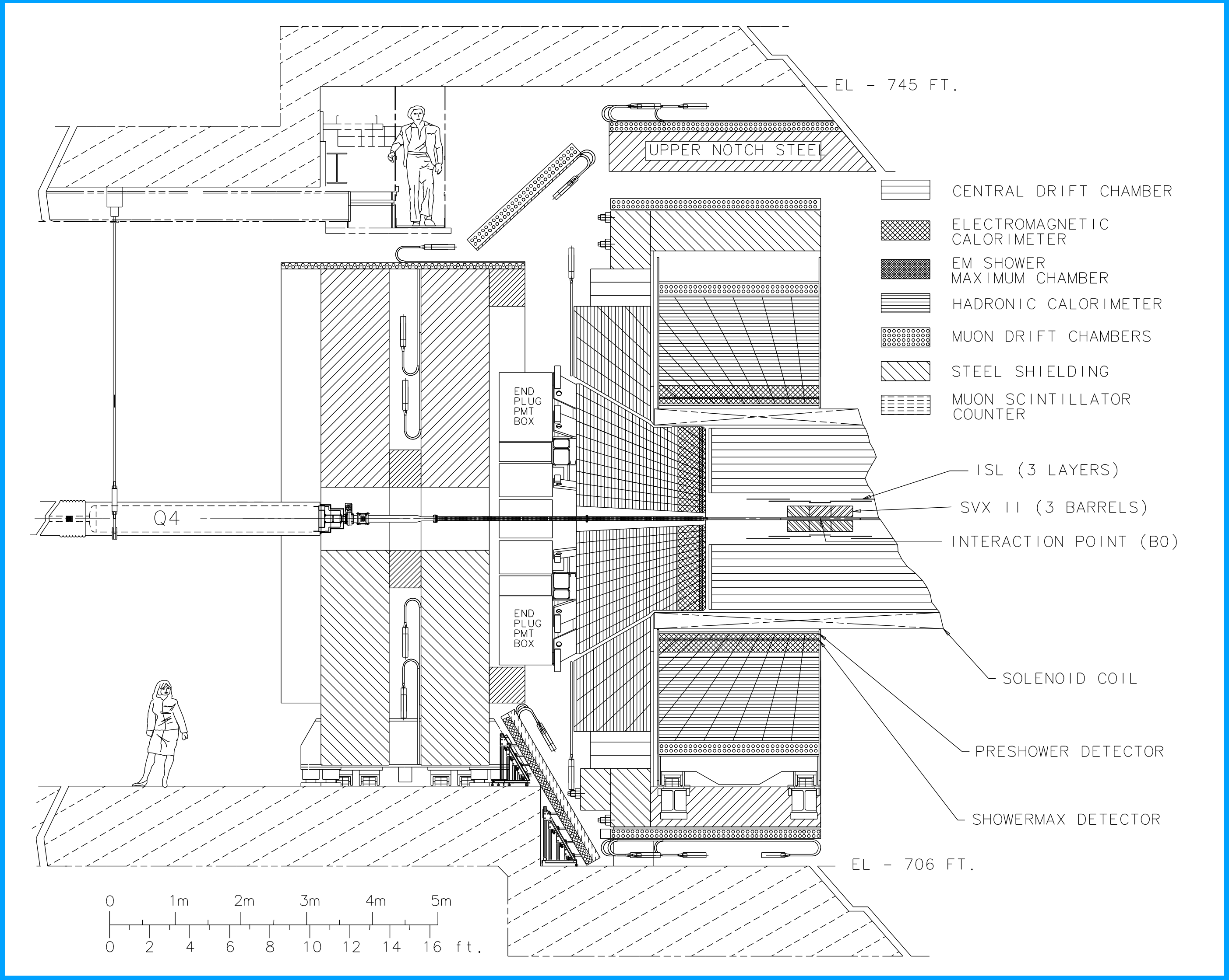
EL - 745 FT.
UPPER NOTCH STEEL
CENTRAL DRIFT CHAMBER
ELECTROMAGNETIC CALORIMETER
EM SHOWER MAXIMUM CHAMBER
HADRONIC CALORIMETER
MUON DRIFT CHAMBERS
STEEL SHIELDING
MUON SCINTILLATOR COUNTER
END PLUG PMT BOX
ISL (3 LAYERS)
SVX II (3 BARRELS)
Q4
INTERACTION POINT (B0)
END PLUG PMT BOX
SOLENOID COIL
PRESHOWER DETECTOR
SHOWERMAX DETECTOR
EL - 706 FT.
0 1m 2m 3m 4m 5m
0 2 4 6 8 10 12 14 16 ft.

W boson mass measurement

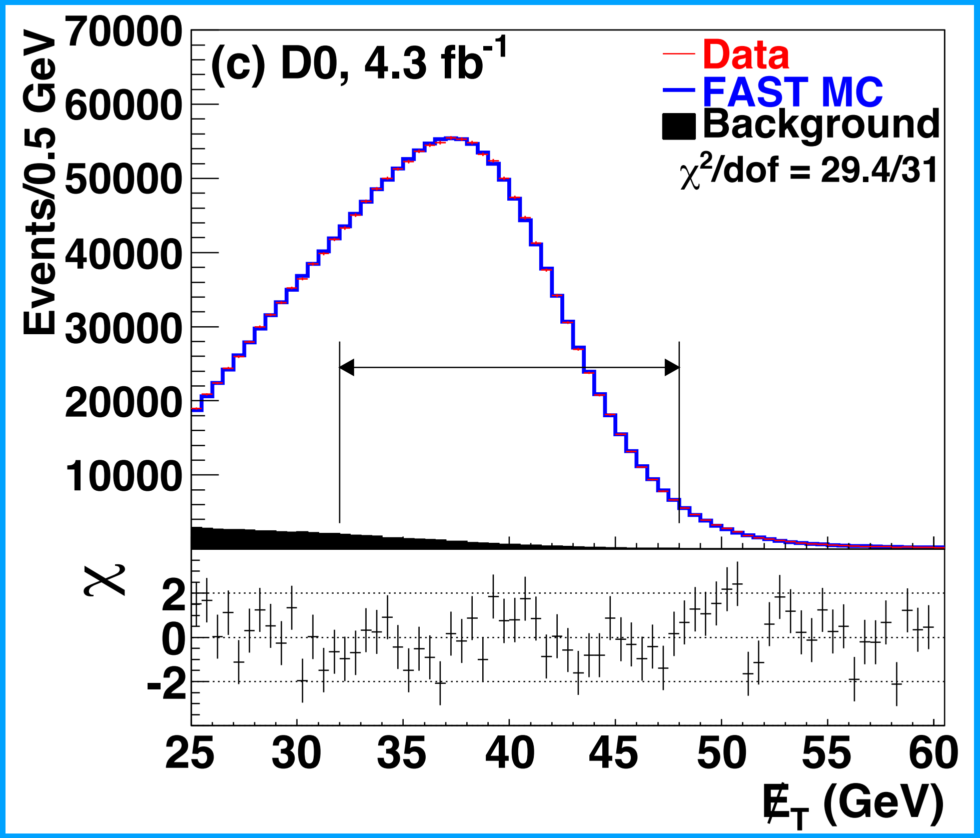

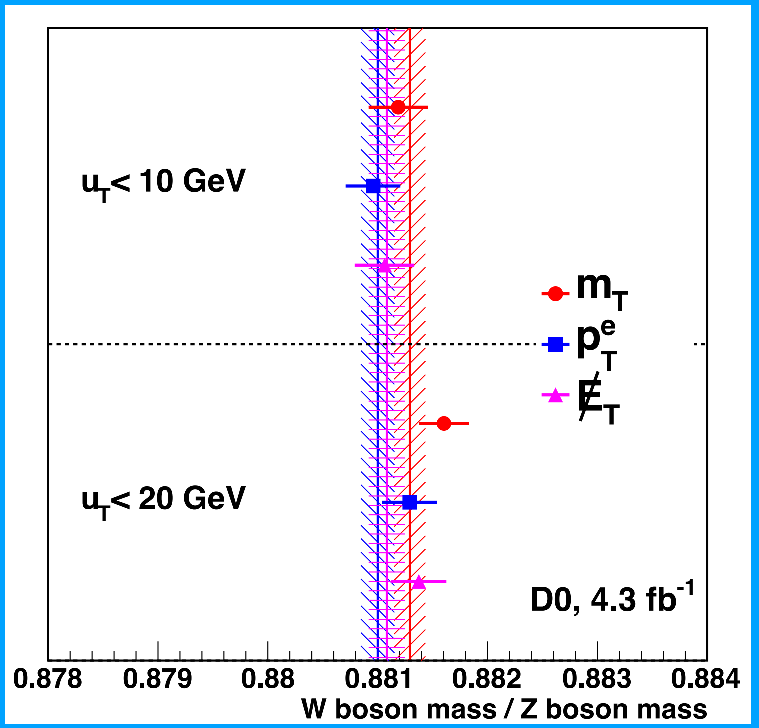

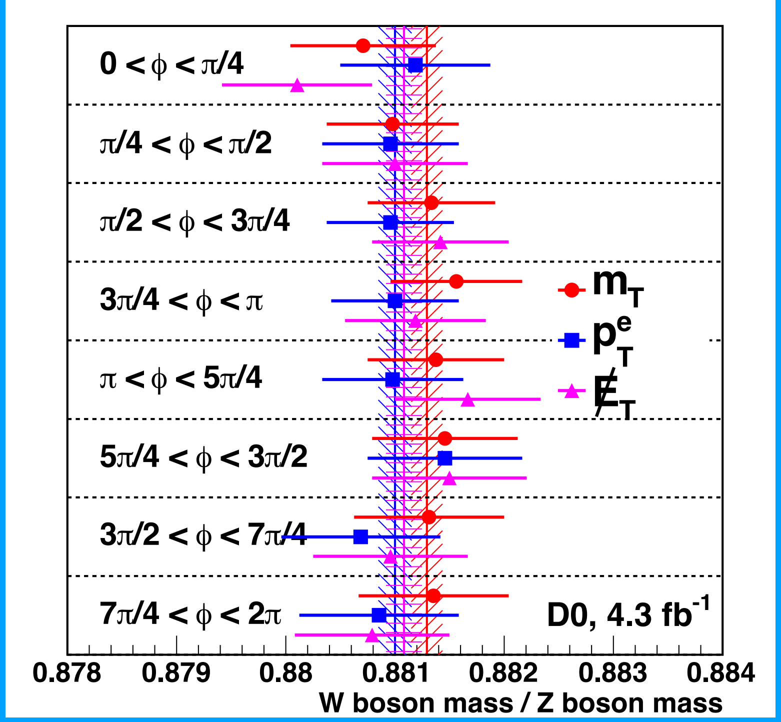

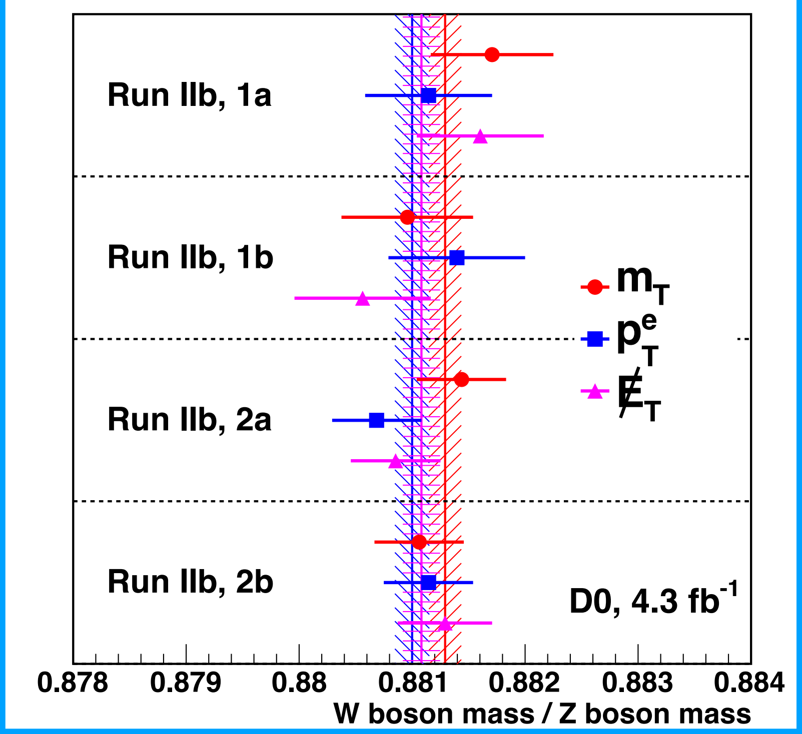

W boson polarization

$$
\begin{aligned}
\frac{d\sigma}{d\Omega} = \frac{d\sigma}{dm\, dp_{\mathrm{T}}\, dy} \Big[\; (1+\cos^2\theta) \quad &+ \quad \frac{1}{2} A_0 (1 - 3\cos^2\theta) + A_1 \sin 2\theta \cos\phi \\
&+ \quad \frac{1}{2} A_2 \sin^2\theta \cos 2\phi + A_3 \sin\theta \cos\phi \\
&+ \quad A_4 \cos\theta + A_5 \sin^2\theta \sin 2\phi \\
&+ \quad A_6 \sin 2\theta \sin\phi + A_7 \sin\theta \sin\phi \; \Big] ,
\end{aligned}
$$

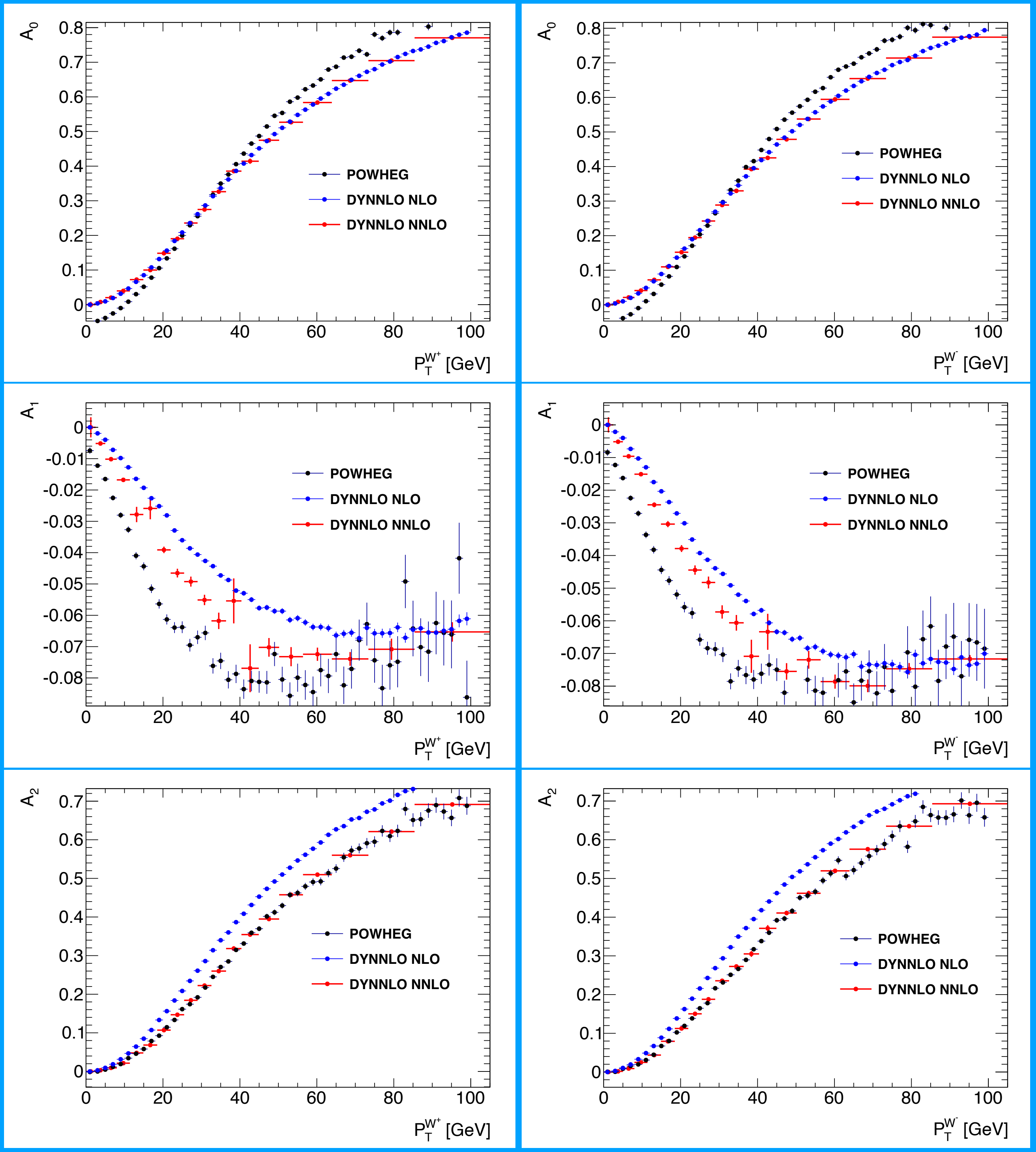

Initial state LO & NLO

W^+ initial	Type	Pythia LO	Madgraph LO	Madgraph NLO
u dbar	v-v	81.7%	82.0%	82.7%
dbar u	s-s	8.9%	9.0%	8.8%
u sbar	v-s	1.6%	1.9%	1.8%
sbar u	s-s	0.3%	0.3%	0.3%
c sbar	s-s	2.9%	2.9%	-
sbar c	s-s	2.9%	2.9%	-
c dbar	s-v	0.7%	0.7%	-
dbar c	s-s	0.2%	0.2%	-
u g	v-g		-	3.7%
g dbar	g-v		-	1.8%
g u	g-s		-	0.4%
dbar g	s-g		-	0.5%
g sbar	g-s		-	0.02%
sbar g	s-g		-	0.02%

Recoil

CDF

Parameter	Description	Source	m_T	p_T^ℓ	p_T^ν
a	average response	Fig. S23	−1.6	−2.9	−0.2
b	response non-linearity	Fig. S23	−0.8	−2.0	0.7
Response			1.8	3.5	0.7
N_V	spectator interactions	Fig. S24	0.5	−3.2	3.6
s_{had}	sampling resolution	Fig. S24	0.3	0.3	0.8
$f^4_{\pi^0}$	EM fluctuations at low u_T	Fig. S25	−0.3	−0.2	−1.0
$f^{15}_{\pi^0}$	EM fluctuations at high u_T	Fig. S25	−0.3	−0.3	−0.2
α	angular resolution at low u_T	Fig. S26	1.4	0.1	2.5
β	angular resolution at intermediate u_T	Fig. S26	0.2	0.1	0.7
γ	angular resolution at high u_T	Fig. S26	0.3	0.3	0.7
f^a_2	average dijet component	Fig. S27	0.1	−1.1	0.8
f^s_2	variation of dijet component with u_T	Fig. S27	−0.1	−0.2	−0.1
k_ξ	average dijet resolution	Fig. S28	−0.1	0.1	−0.3
δ_ξ	fluctuations in dijet resolution	Fig. S28	−0.2	0.2	−1.1
A_ξ	higher-order term in dijet resolution	Fig. S28	0.1	−1.0	0.7
μ_ξ	—"—	Fig. S28	−0.5	−0.4	−0.9
ϵ_ξ	—"—	Fig. S28	0.1	−0.2	0.4
S^+_ξ	—"—	Fig. S28	0.5	−0.4	1.4
S^-_ξ	—"—	Fig. S28	−0.3	−0.2	−0.5
q_ξ	—"—	Fig. S28	−0.2	0.0	0.2
Resolution			1.8	3.6	5.2

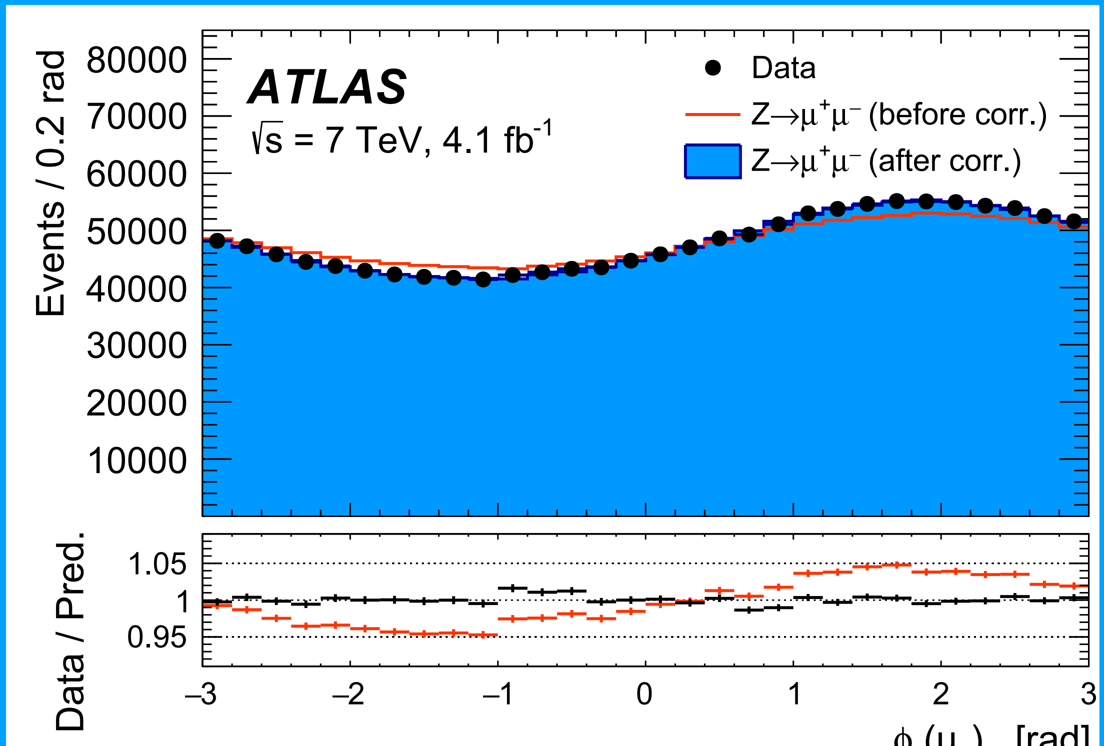

(b)

CDF II measurement of the W boson mass

4x the integrated luminosity of the previous measurement

Higher $\langle \mu \rangle$: peaks at 3

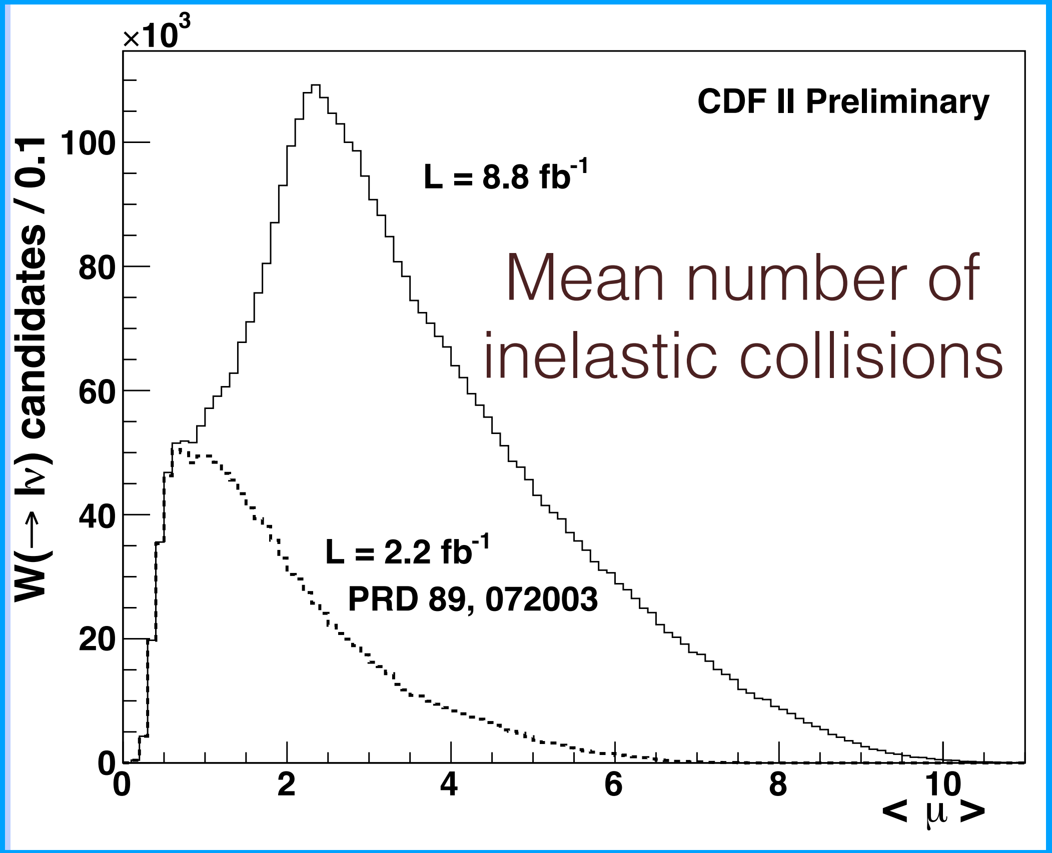

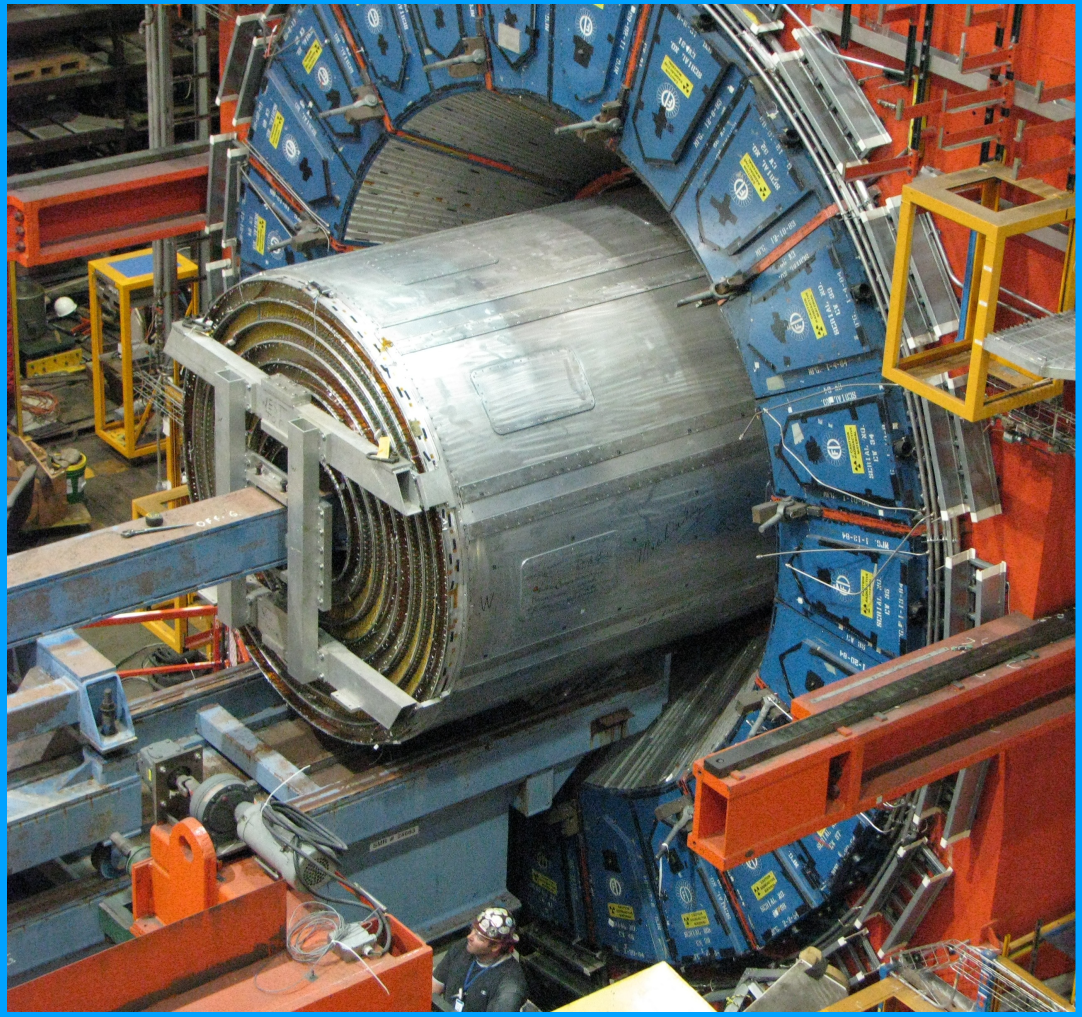

CDF II detector consists of

silicon vertex detector

large drift chamber

coarse calorimeter towers

outer muon chambers

Detector simulation

Developed custom simulation for analysis
Models ionization energy loss, multiple scattering, bremsstrahlung, photon conversion, Compton scattering

Acceptance map for muon detectors

Parameterized GEANT4 model of electromagnetic calorimeter showers
Includes shower losses due to finite calorimeter thickness

Kotwal & CH, NIMA 729, 25 (2013)

Hit-level model of central outer tracker
Layer-by-layer resolution functions and efficiencies

Material map of inner silicon detector
Includes radiation lengths and Bethe-Bloch terms

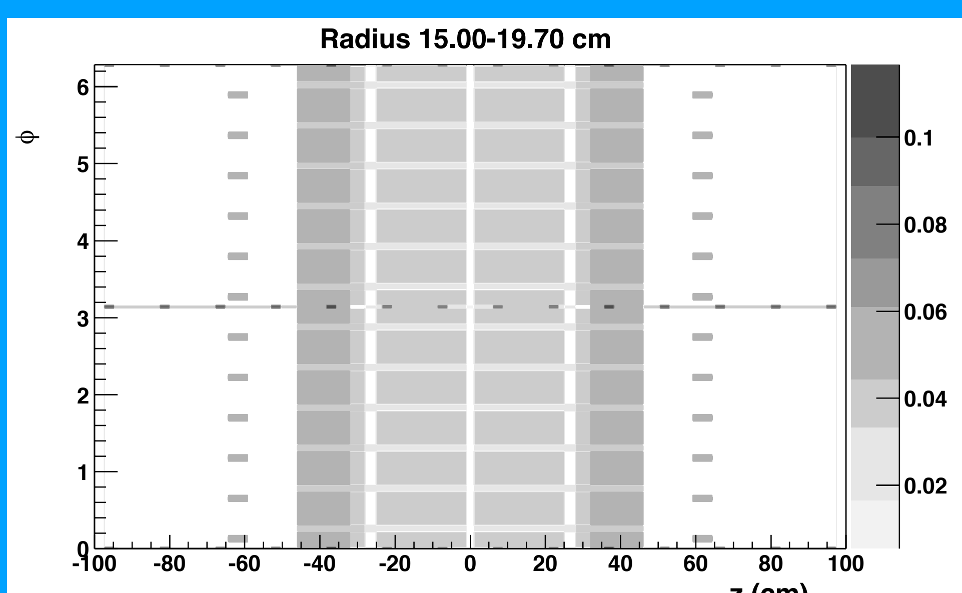

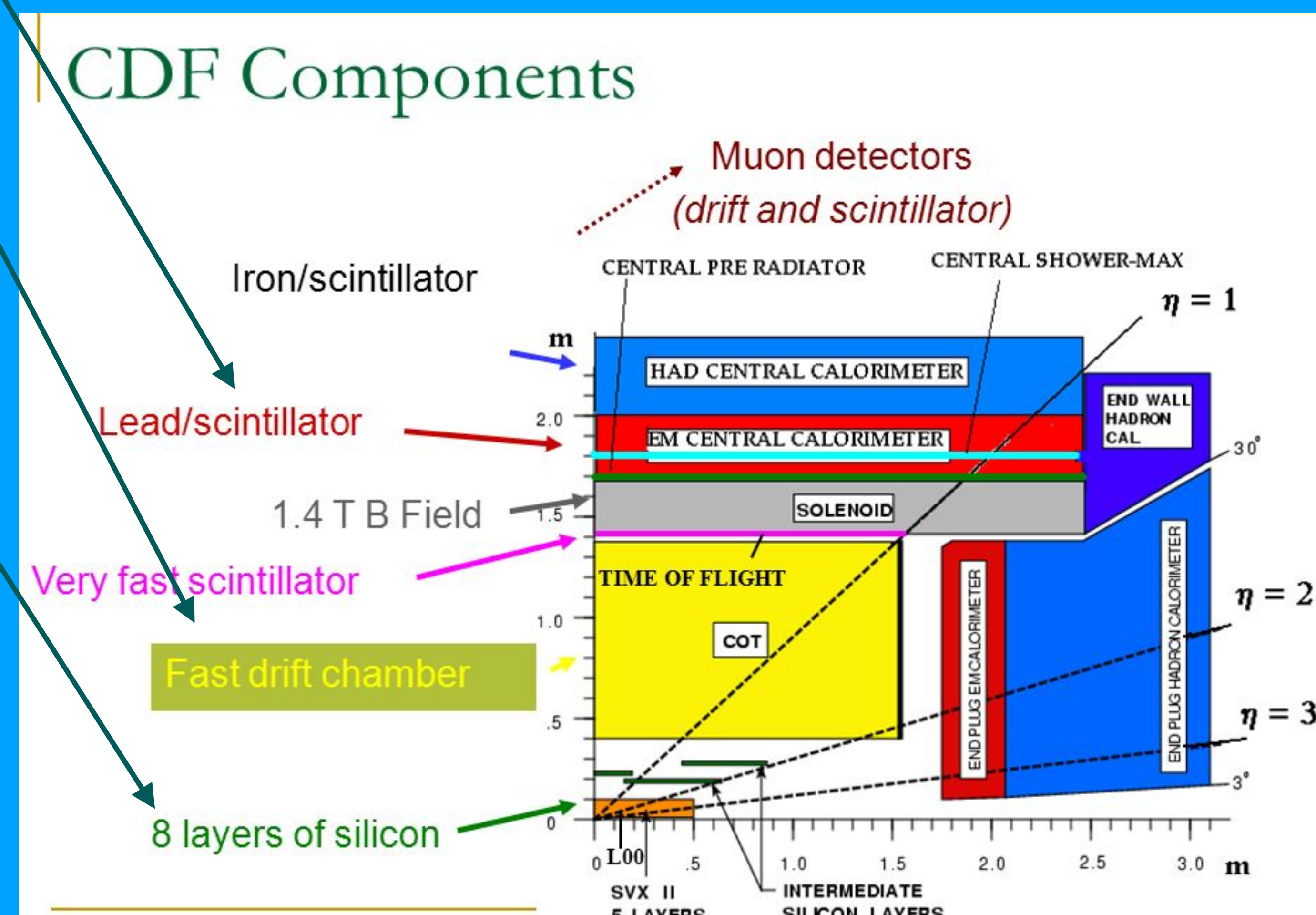

Background fractions

Source	Fraction (%)	δM_W (MeV) m_T fit	p_T^μ fit	p_T^ν fit
$Z/\gamma^* \to \mu\mu$	7.37 ± 0.10	1.6 (0.7)	3.6 (0.3)	0.1 (1.5)
$W \to \tau\nu$	0.880 ± 0.004	0.1 (0.0)	0.1 (0.0)	0.1 (0.0)
Hadronic jets	0.01 ± 0.04	0.1 (0.8)	-0.6 (0.8)	2.4 (0.5)
Decays in flight	0.20 ± 0.14	1.3 (3.1)	1.3 (5.0)	-5.2 (3.2)
Cosmic rays	0.01 ± 0.01	0.3 (0.0)	0.5 (0.0)	0.3 (0.3)
Total	8.47 ± 0.18	2.1 (3.3)	3.9 (5.1)	5.7 (3.6)

Source	Fraction (%)	δM_W (MeV) m_T fit	p_T^e fit	p_T^ν fit
$Z/\gamma^* \to ee$	0.134 ± 0.003	0.2 (0.3)	0.3 (0.0)	0.0 (0.6)
$W \to \tau\nu$	0.94 ± 0.01	0.6 (0.0)	0.6 (0.0)	0.6 (0.0)
Hadronic jets	0.34 ± 0.08	2.2 (1.2)	0.9 (6.5)	6.2 (−1.1)
Total	1.41 ± 0.08	2.3 (1.2)	1.1 (6.5)	6.2 (1.3)

Uncertainties

Source	Uncertainty (MeV)
Lepton energy scale	3.0
Lepton energy resolution	1.2
Recoil energy scale	1.2
Recoil energy resolution	1.8
Lepton efficiency	0.4
Lepton removal	1.2
Backgrounds	3.3
p_T^Z model	1.8
p_T^W/p_T^Z model	1.3
Parton distributions	3.9
QED radiation	2.7
W boson statistics	6.4
Total	9.4

Source of systematic	m_T fit			p_T^ℓ fit			p_T^ν fit		
uncertainty	Electrons	Muons	Common	Electrons	Muons	Common	Electrons	Muons	Common
Lepton energy scale	5.8	2.1	1.8	5.8	2.1	1.8	5.8	2.1	1.8
Lepton energy resolution	0.9	0.3	-0.3	0.9	0.3	-0.3	0.9	0.3	-0.3
Recoil energy scale	1.8	1.8	1.8	3.5	3.5	3.5	0.7	0.7	0.7
Recoil energy resolution	1.8	1.8	1.8	3.6	3.6	3.6	5.2	5.2	5.2
Lepton $u_{\|\|}$ efficiency	0.5	0.5	0	1.3	1.0	0	2.6	2.1	0
Lepton removal	1.0	1.7	0	0	0	0	2.0	3.4	0
Backgrounds	2.6	3.9	0	6.6	6.4	0	6.4	6.8	0
p_T^Z model	0.7	0.7	0.7	2.3	2.3	2.3	0.9	0.9	0.9
p_T^W/p_T^Z model	0.8	0.8	0.8	2.3	2.3	2.3	0.9	0.9	0.9
Parton distributions	3.9	3.9	3.9	3.9	3.9	3.9	3.9	3.9	3.9
QED radiation	2.7	2.7	2.7	2.7	2.7	2.7	2.7	2.7	2.7
Statistical	10.3	9.2	0	10.7	9.6	0	14.5	13.1	0
Total	13.5	11.8	5.8	16.0	14.1	7.9	18.8	17.1	7.4

Electron momentum calibration

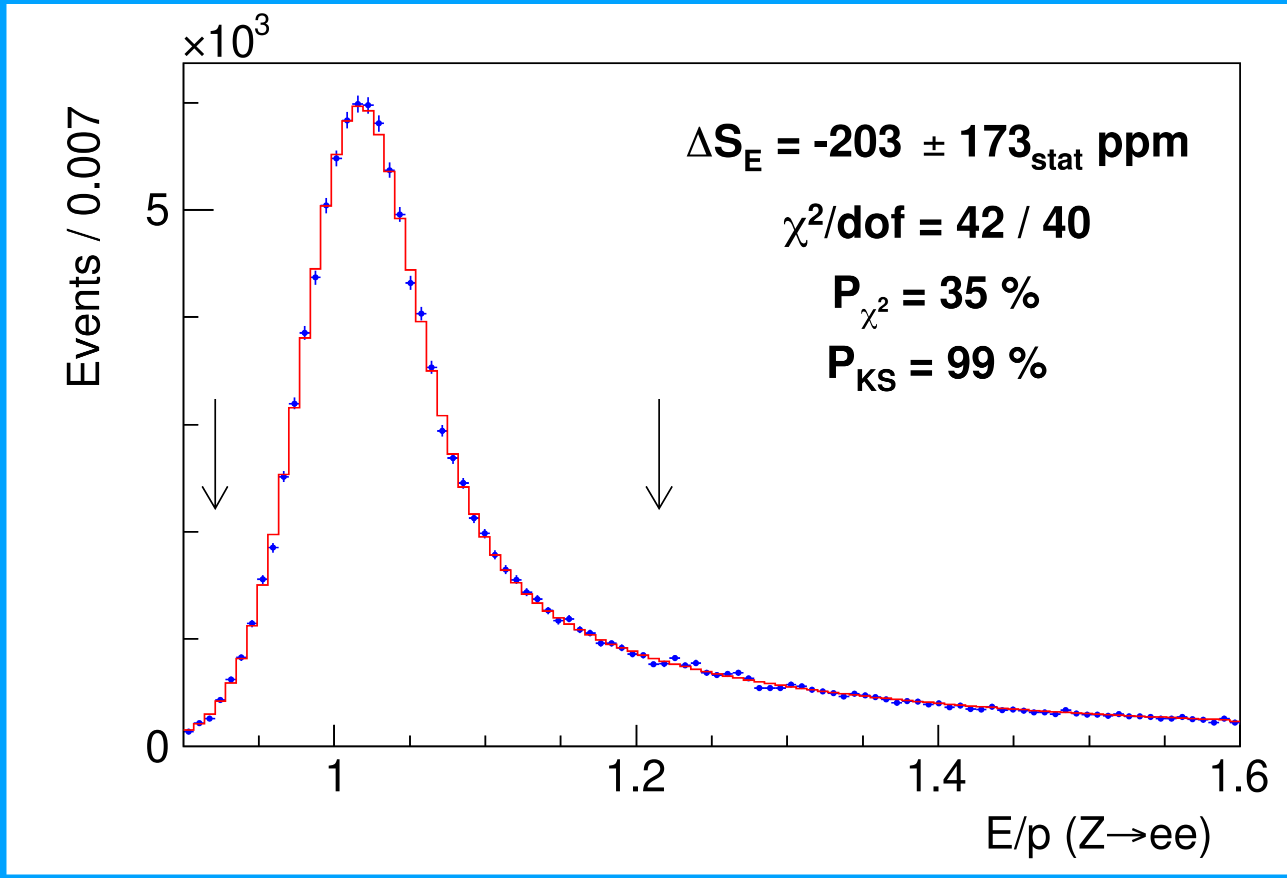

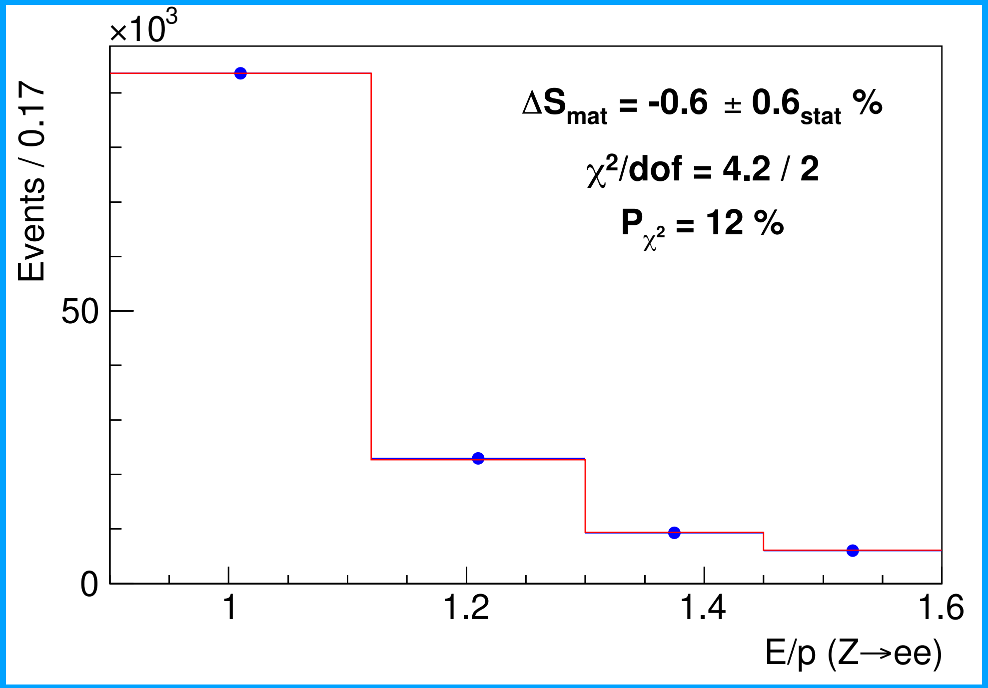

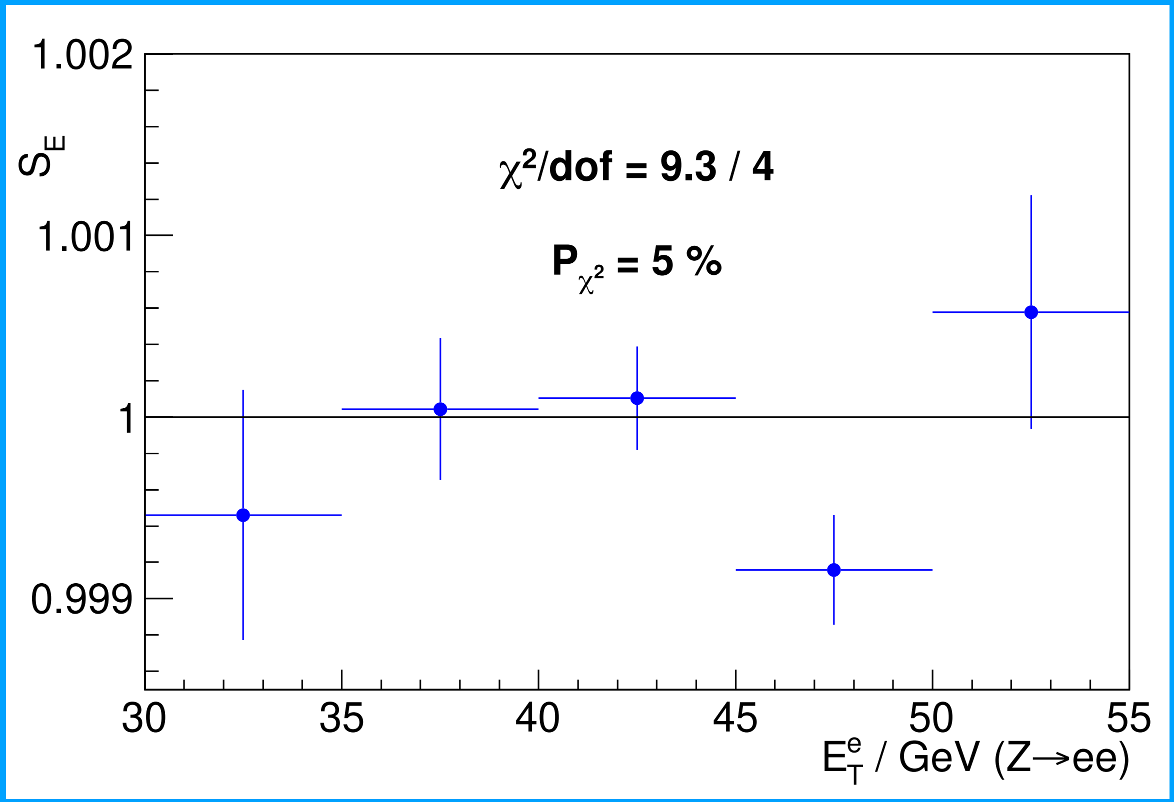

Recoil in W & Z events

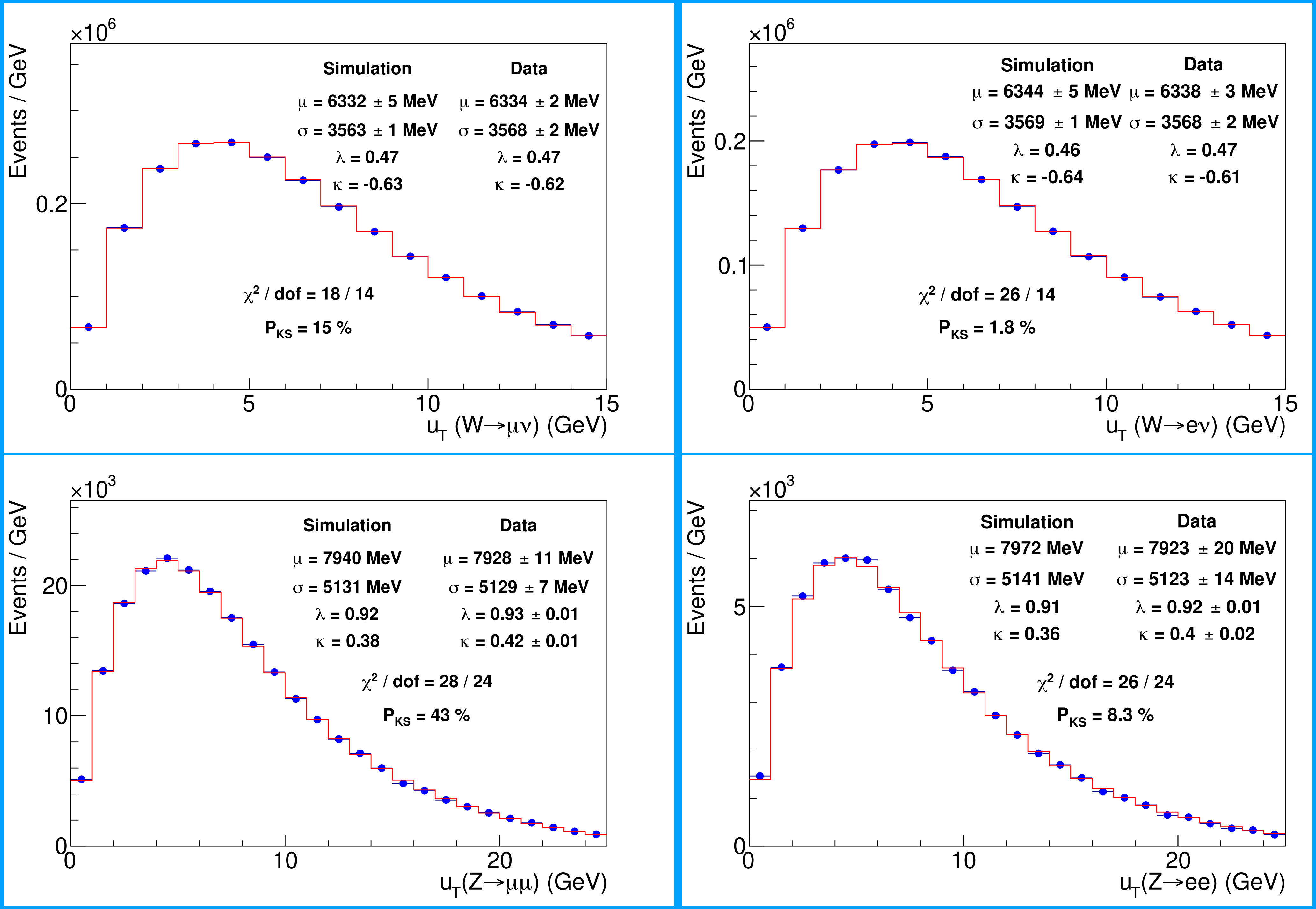

Recoil projections in W events

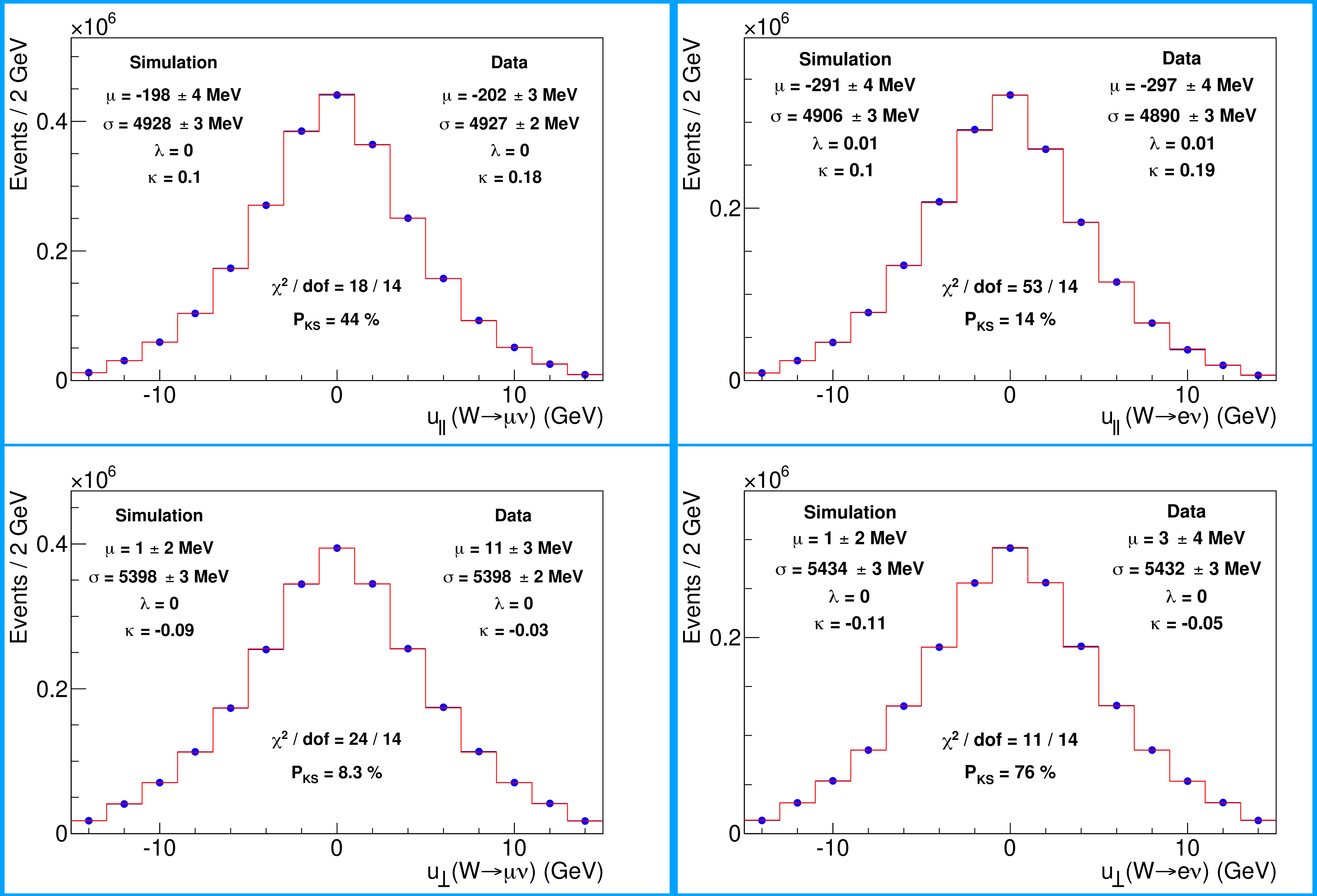

Recoil reconstruction in muon channel

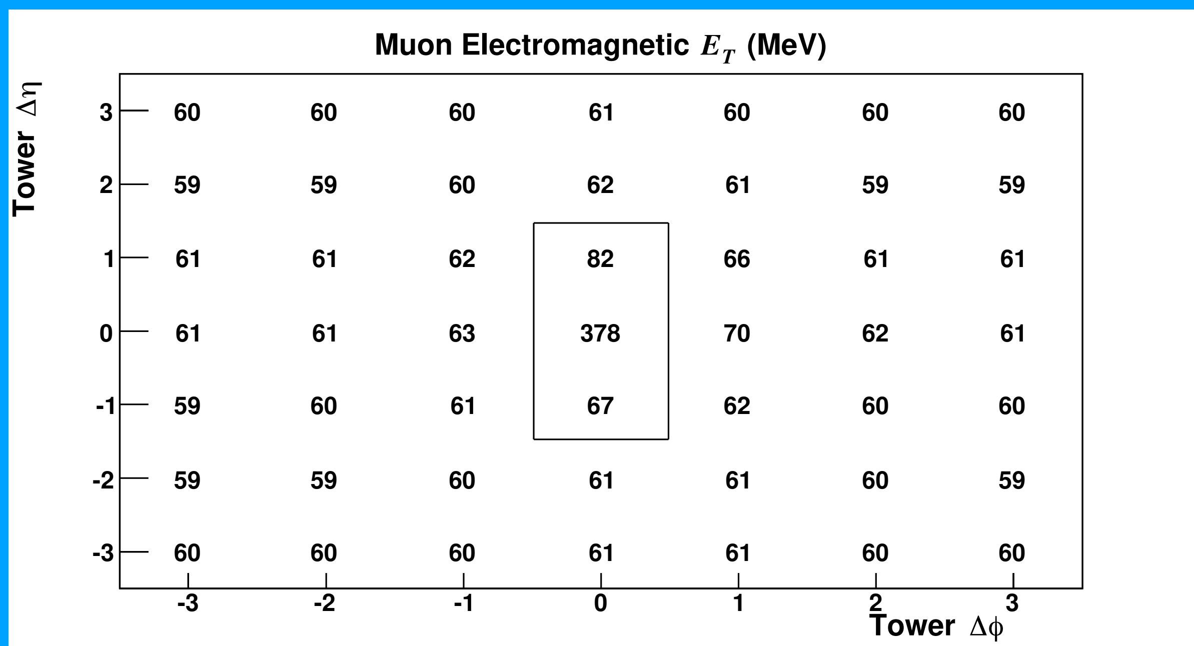

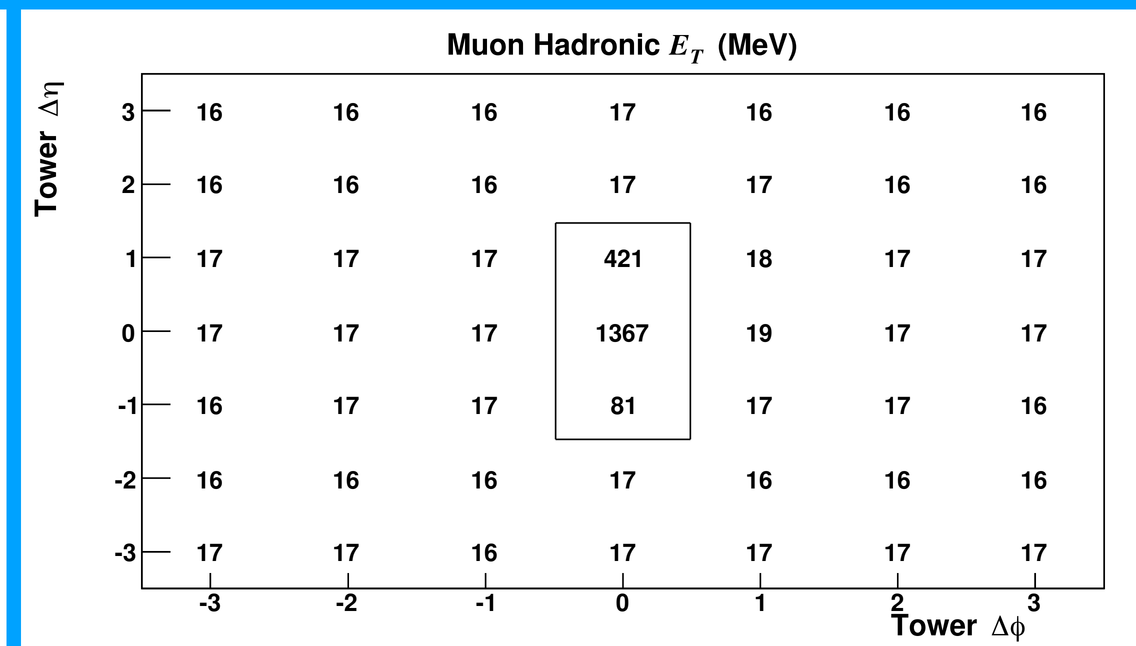

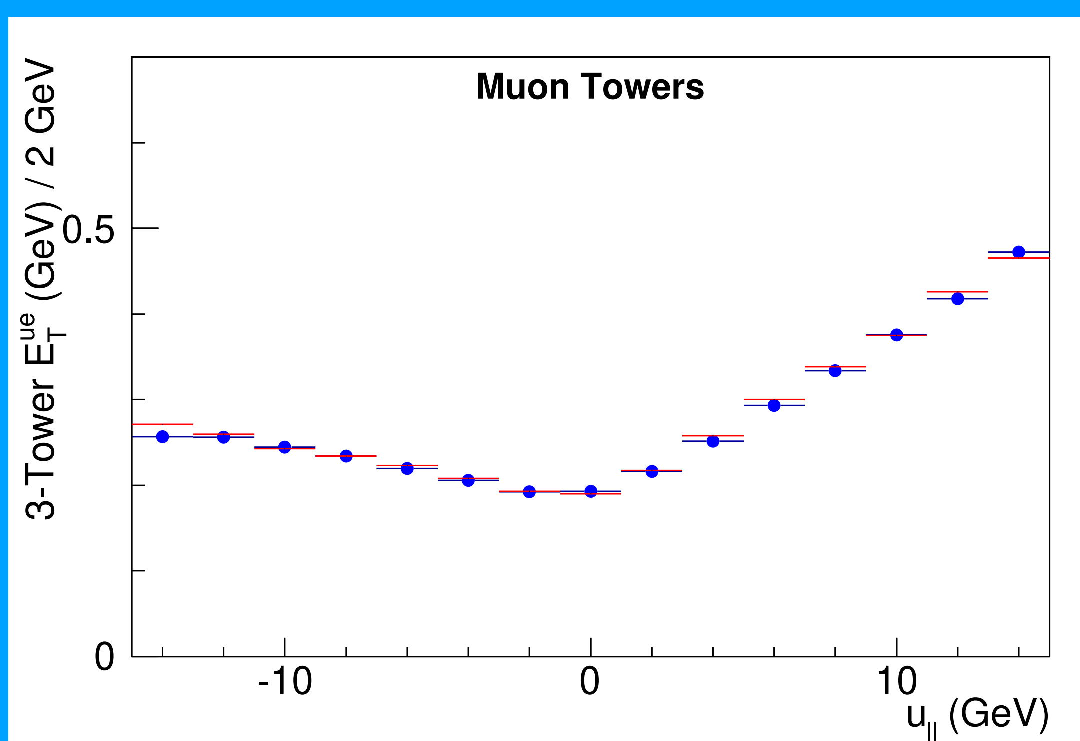

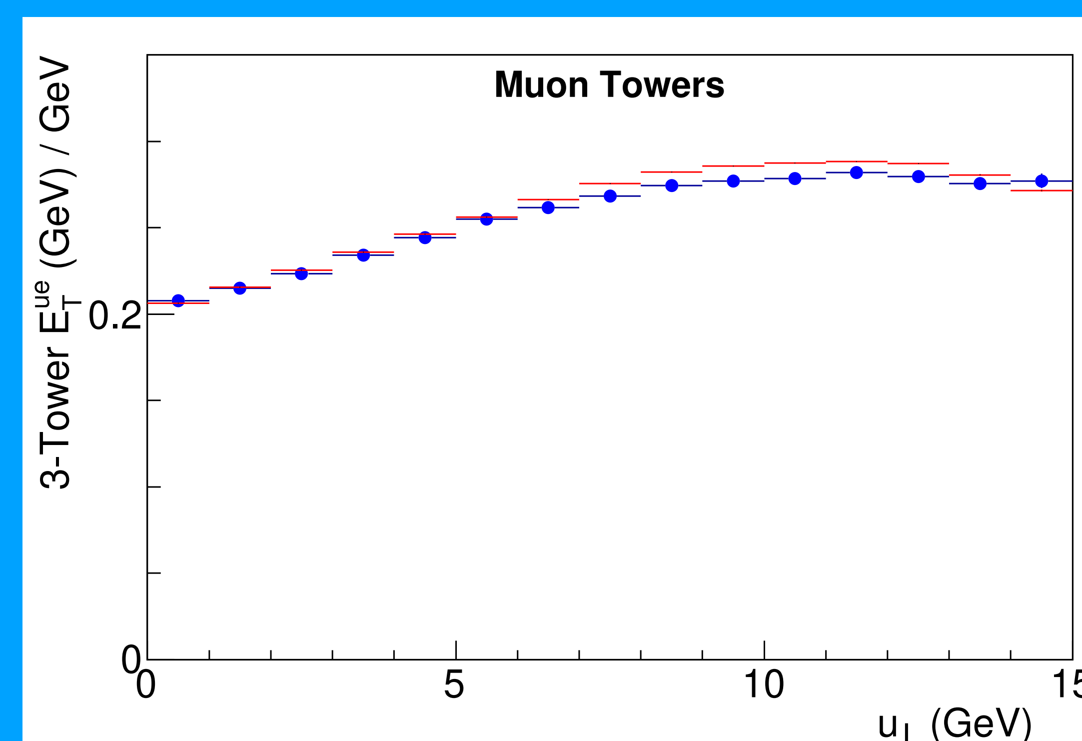

Electron momentum calibration

First step is to transfer the track calibration to the calorimeter (E/p) using W & Z decays

Parameterize calorimeter shower deposition and leakage based on GEANT4
Determine small calorimeter thickness corrections using region of low E/p in data
Fit calorimeter scale as a function of E_T to correct for any remaining energy dependence

Tower	Thickness (x_0)	Number of lead sheets
0	17.9	30
1	18.2	30
2	18.2	29
3	17.8	27
4	18.0	26
5	17.7	24
6	18.1	23
7	17.7	21
8	18.0	20

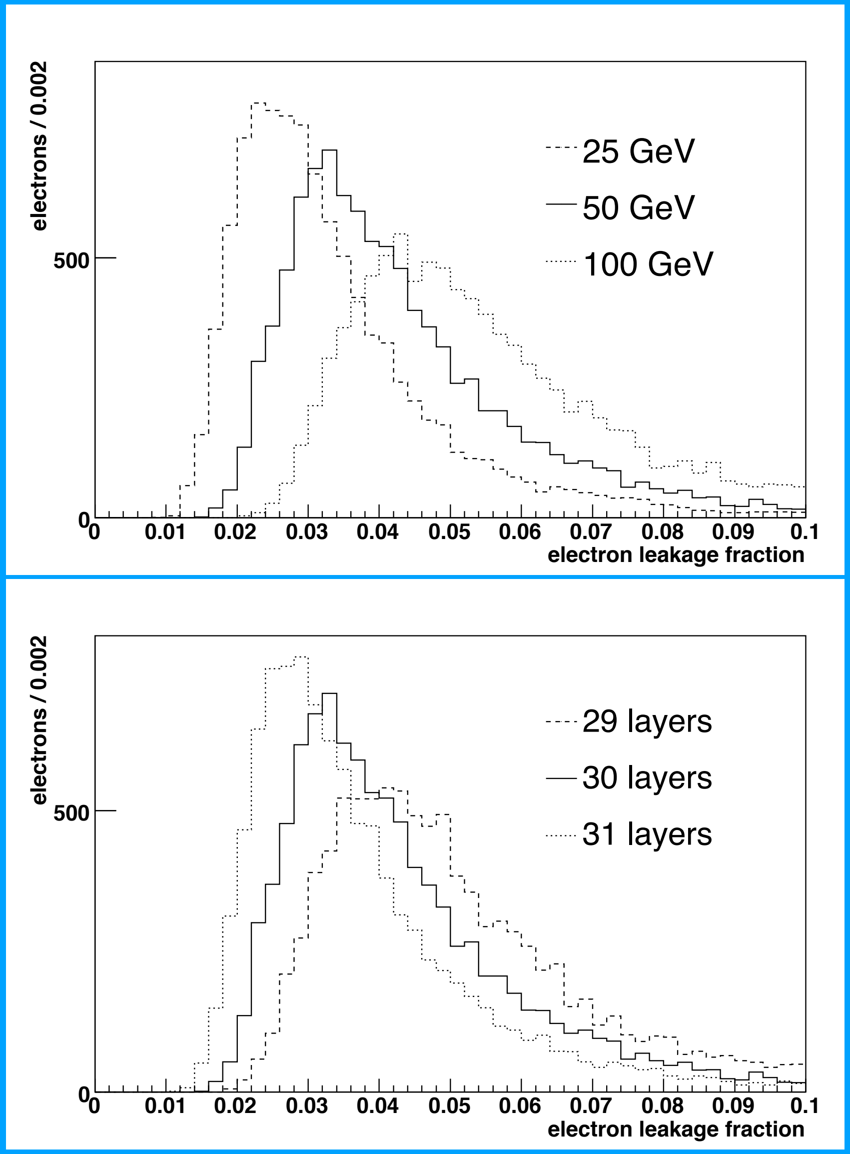

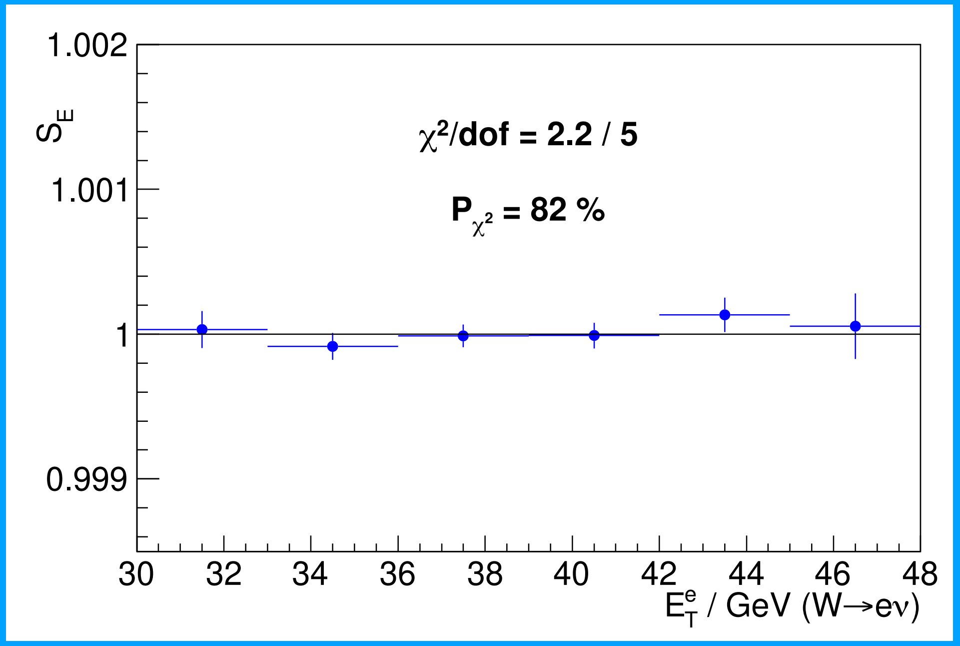

Kotwal & CH, NIMA 729, 25 (2013)

Electron momentum calibration

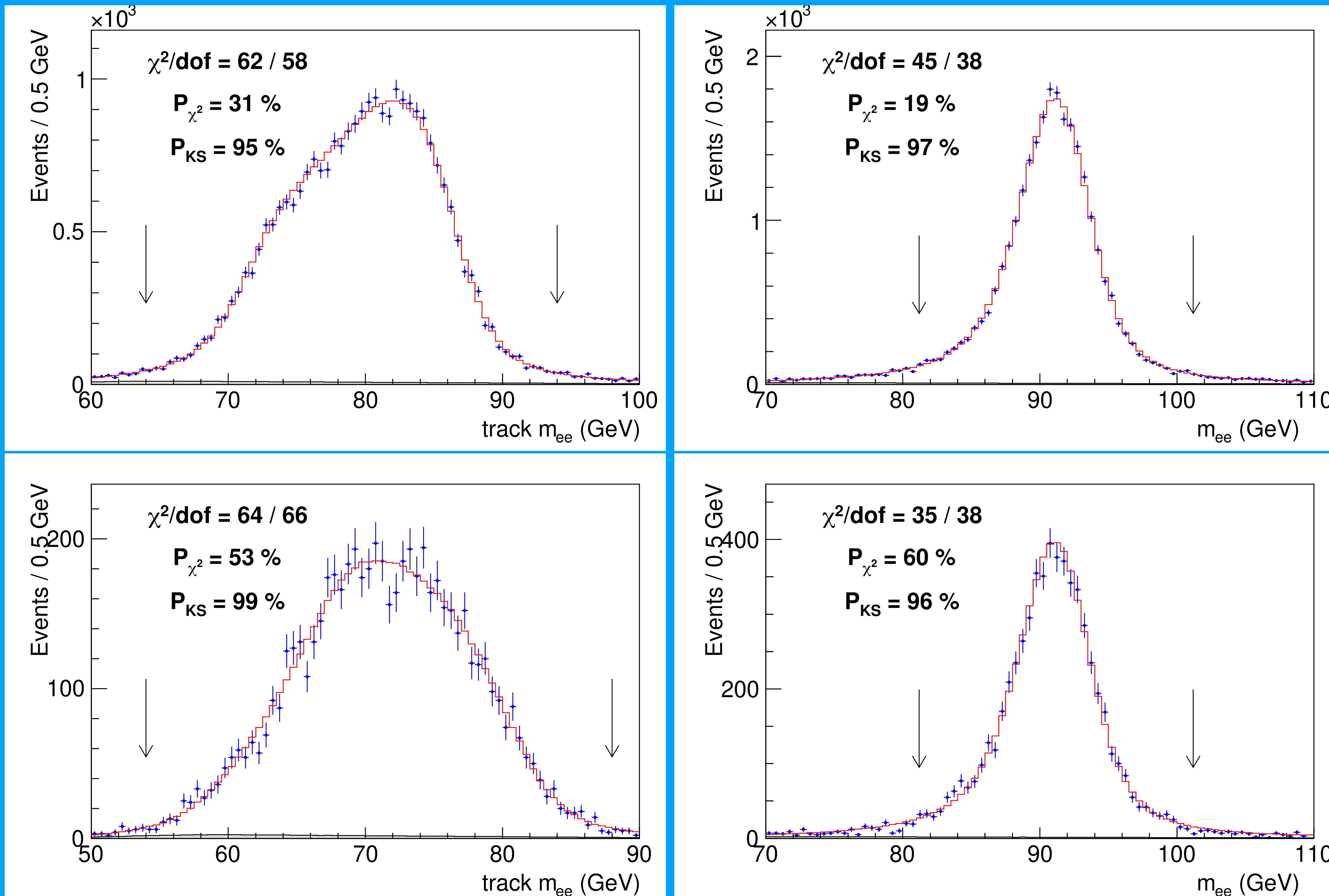

Z mass fits using tracker or calorimeter

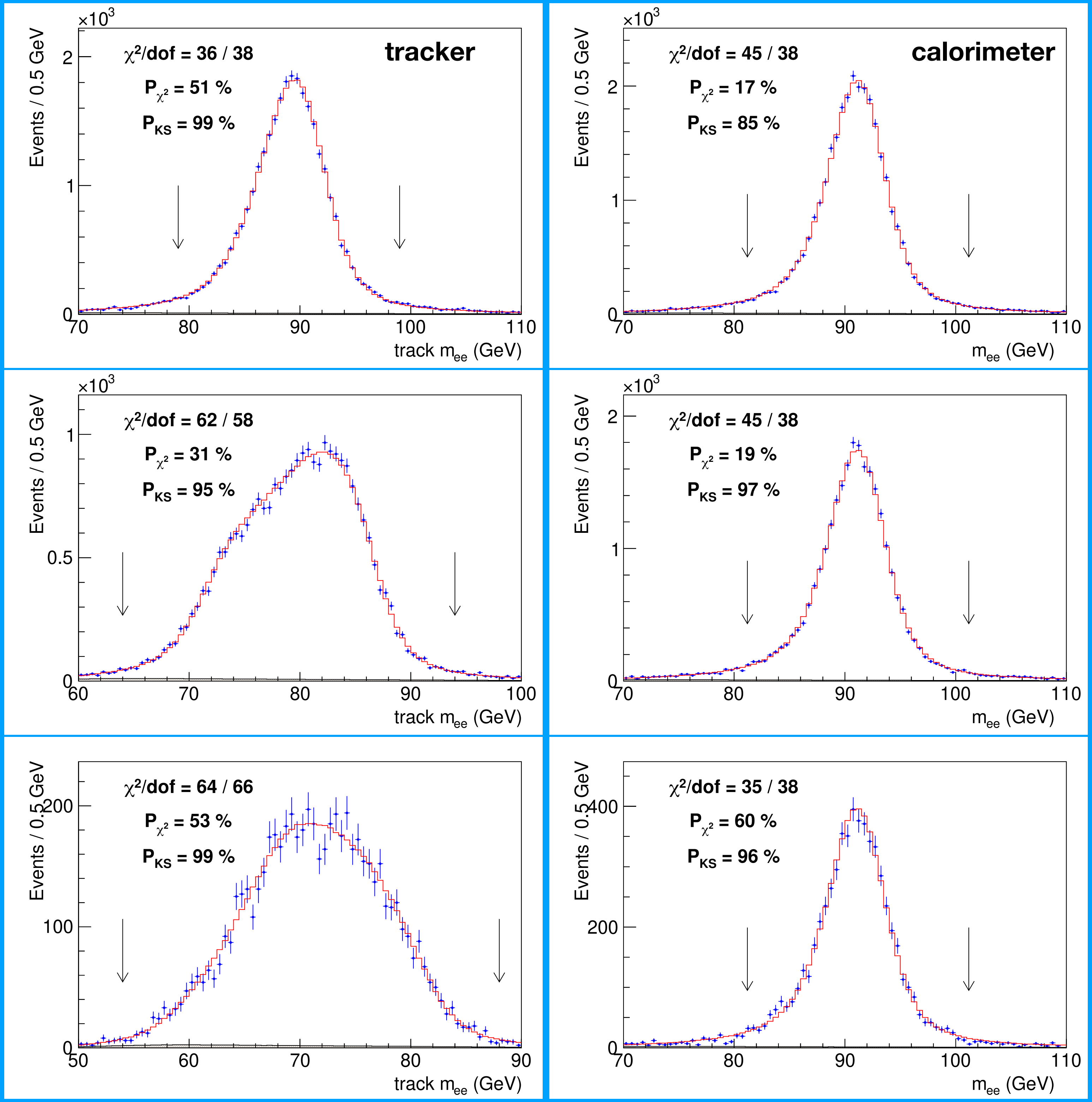

Electrons	Calorimeter	Track
$E/p < 1.1$ only	$91\,190.9 \pm 19.7$	$91\,215.2 \pm 22.4$
$E/p > 1.1$ and $E/p < 1.1$	$91\,201.1 \pm 21.5$	$91\,259.9 \pm 39.0$
$E/p > 1.1$ only	$91\,184.5 \pm 46.4$	$91\,167.7 \pm 109.9$

Muon momentum calibration

Source	J/ψ (ppm)	Υ (ppm)	Correlation (%)
QED	1	1	100
Magnetic field non-uniformity	13	13	100
Ionizing material correction	11	8	100
Resolution model	10	1	100
Background model	7	6	0
COT alignment correction	4	8	0
Trigger efficiency	18	9	100
Fit range	2	1	100
$\Delta p/p$ step size	2	2	0
World-average mass value	4	27	0
Total systematic	29	34	16 ppm
Statistical NBC (BC)	2	13(10)	0
Total	29	36	16 ppm

Muon momentum calibration

Third step is to calibrate the scale using Υ decays to muons

Compare fit results with and without constraining the track to the collision point

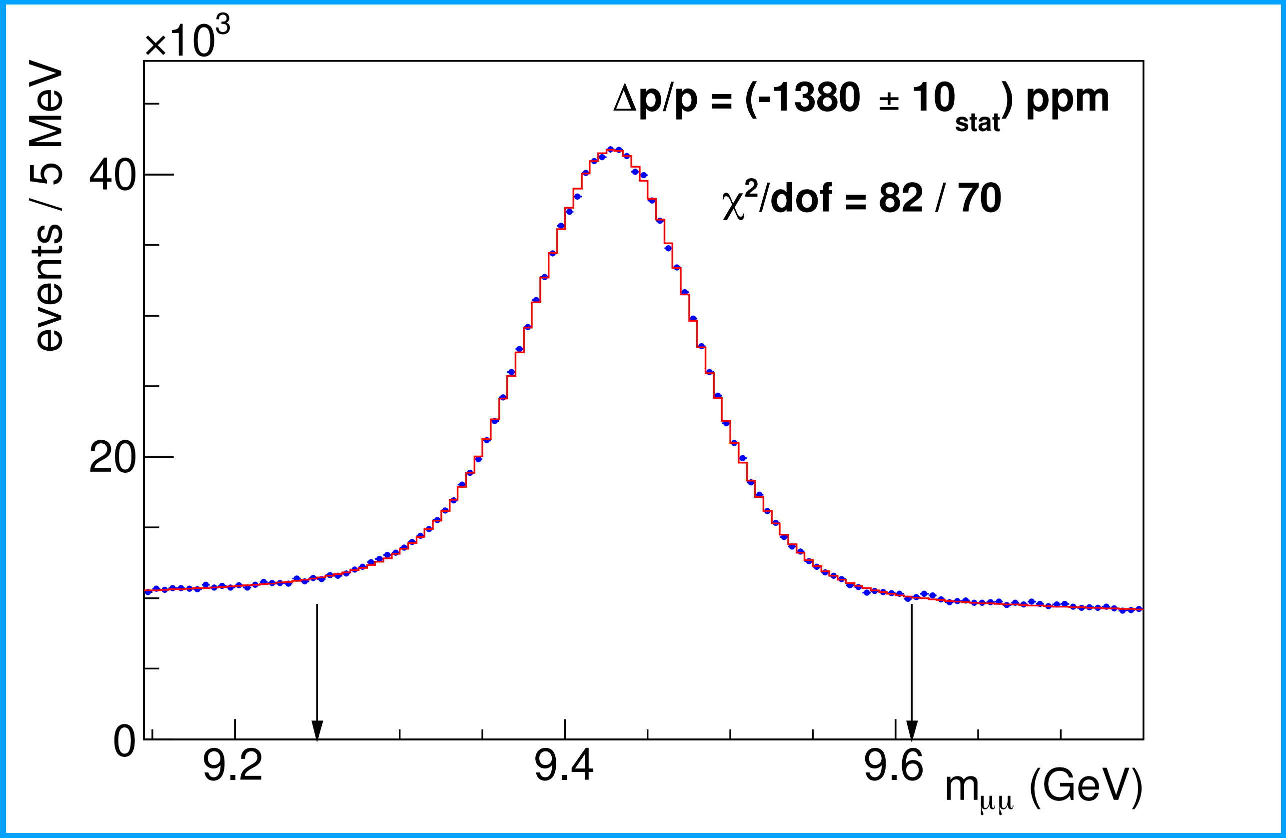

with constraint

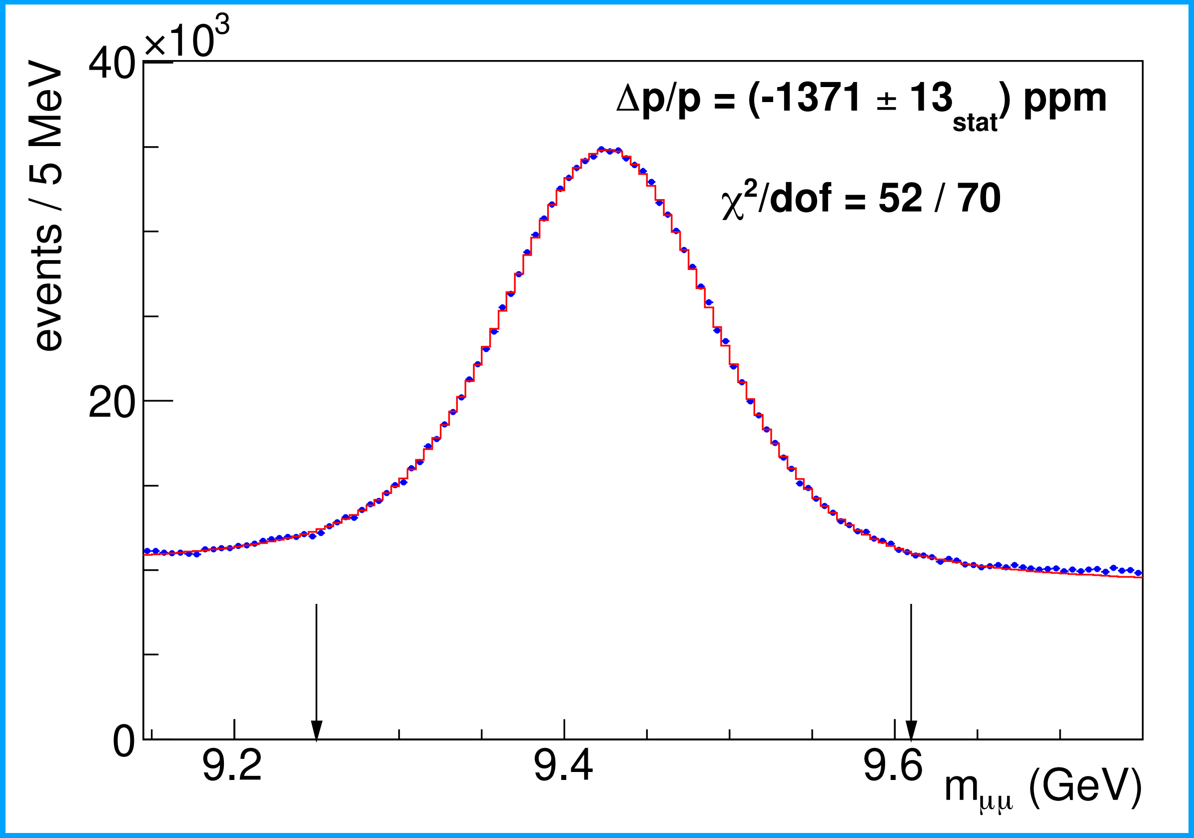

without constraint

Track momentum calibration

Residual tracker misalignments studied using difference in E/p between electrons and positrons

Correction as a function of polar angle applied to measured tracks from W and Z decays

Linear dependence on cot theta would cause a bias in the m_W mass fit

No linear correction required, statistical precision from E/p constrains the bias to <0.8 MeV

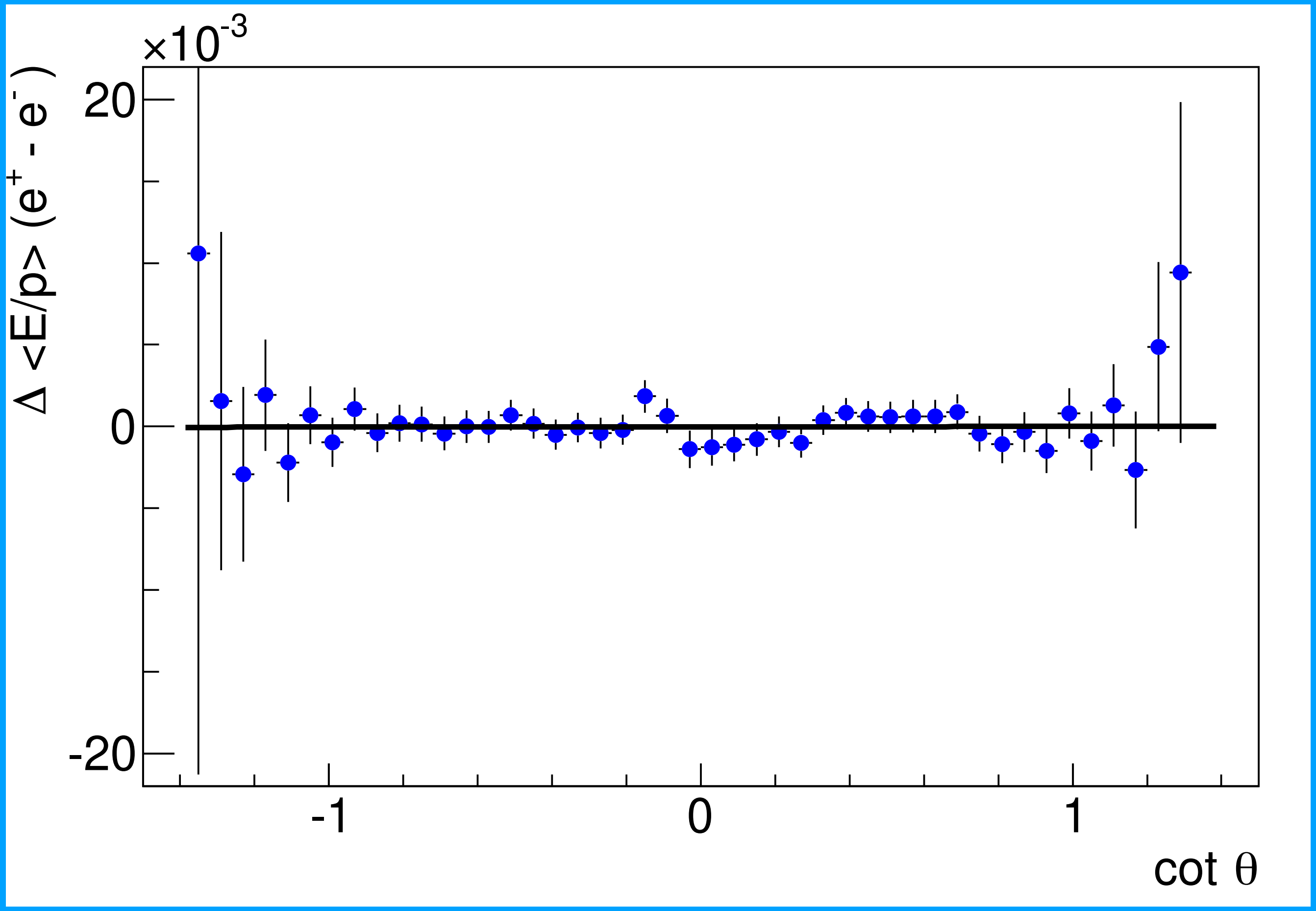

Measurement updates

Method or technique	impact
Detailed treatment of parton distribution functions	+3.5 MeV
Resolved beam-constraining bias in CDF reconstruction	+10 MeV
Improved COT alignment and drift model [65]	uniformity
Improved modeling of calorimeter tower resolution	uniformity
Temporal uniformity calibration of CEM towers	uniformity
Lepton removal procedure corrected for luminosity	uniformity
Higher-order calculation of QED radiation in J/ψ and Υ decays	accuracy
Modeling kurtosis of hadronic recoil energy resolution	accuracy
Improved modeling of hadronic recoil angular resolution	accuracy
Modeling dijet contribution to recoil resolution	accuracy
Explicit luminosity matching of pileup	accuracy
Modeling kurtosis of pileup resolution	accuracy
Theory model of p_T^W/p_T^Z spectrum ratio	accuracy
Constraint from p_T^W data spectrum	robustness
Cross-check of p_T^Z tuning	robustness

Muon momentum calibration

Second step is to correct for biases unconstrained by alignment procedure

Use data from resonance decays to muons and electrons

CDF: Correct curvature as function of polar angle using electrons from $W \to e\nu$ and $Z \to ee$ decays
Use J/ψ, Υ, and Z decays to correct for tracker length, field nonuniformities, endplate twists, and amount of material upstream of drift chamber

ATLAS: Correct curvature using electrons from $W \to e\nu$ decays and muons from Z decays
Magnetic field direction tested using J/ψ and kaon decays

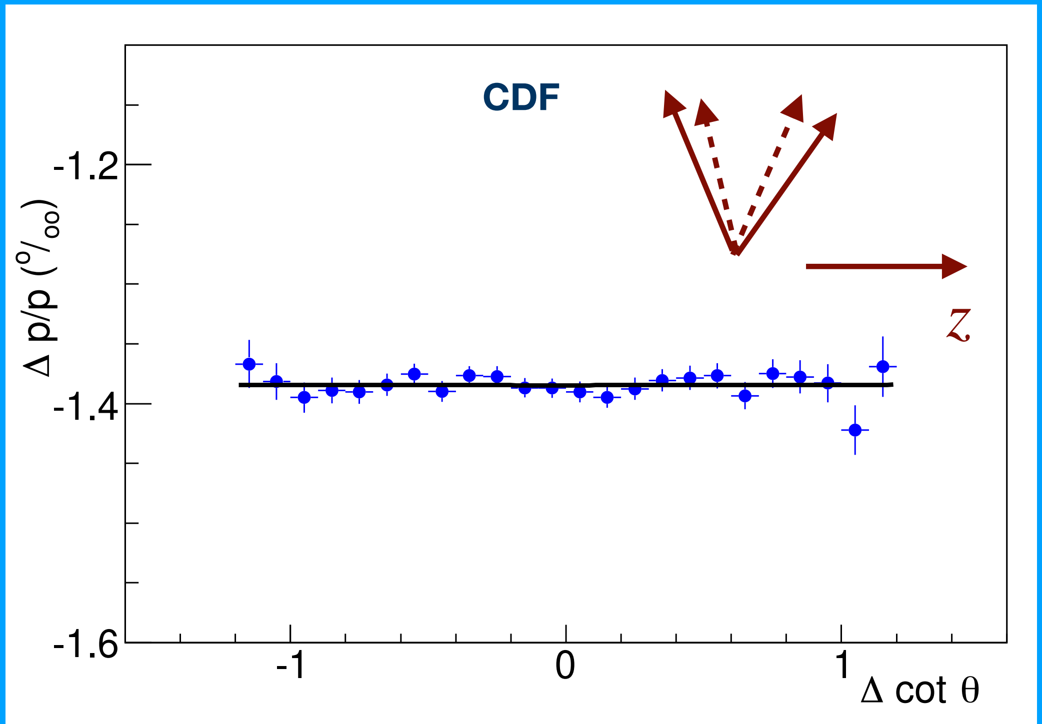

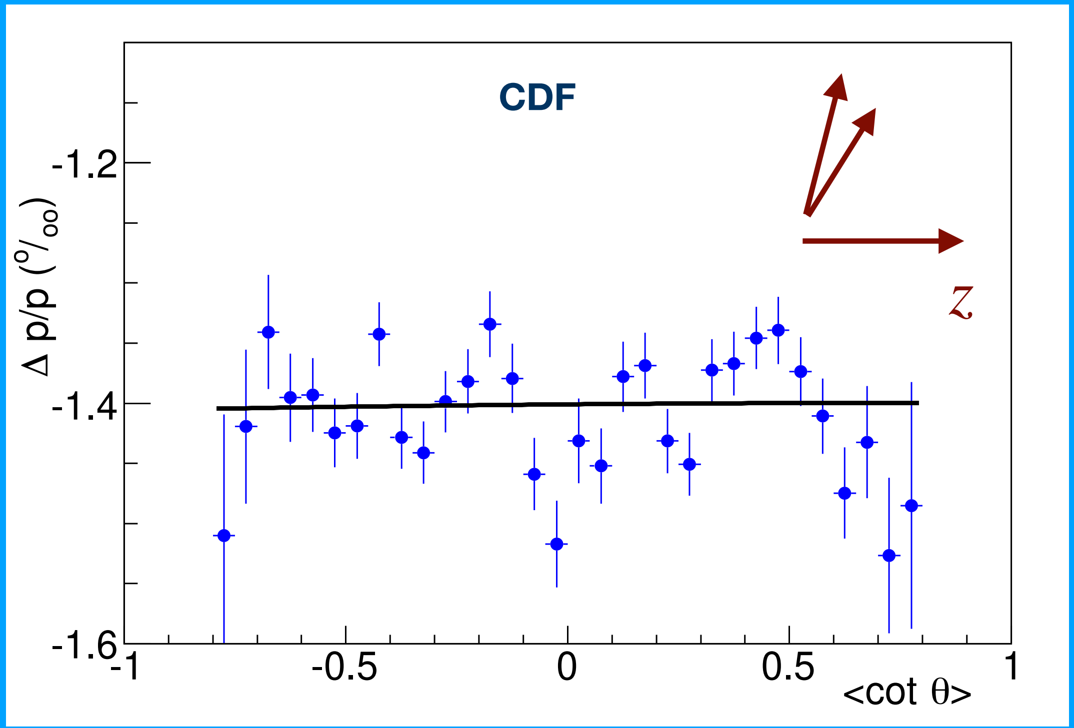

Muon momentum calibration

CDF measures the Z boson mass in the muon decay channel to be

$$M_Z = 91\ 192.0 \pm 6.4_{stat} \pm 4.0_{sys}\ \text{MeV}$$

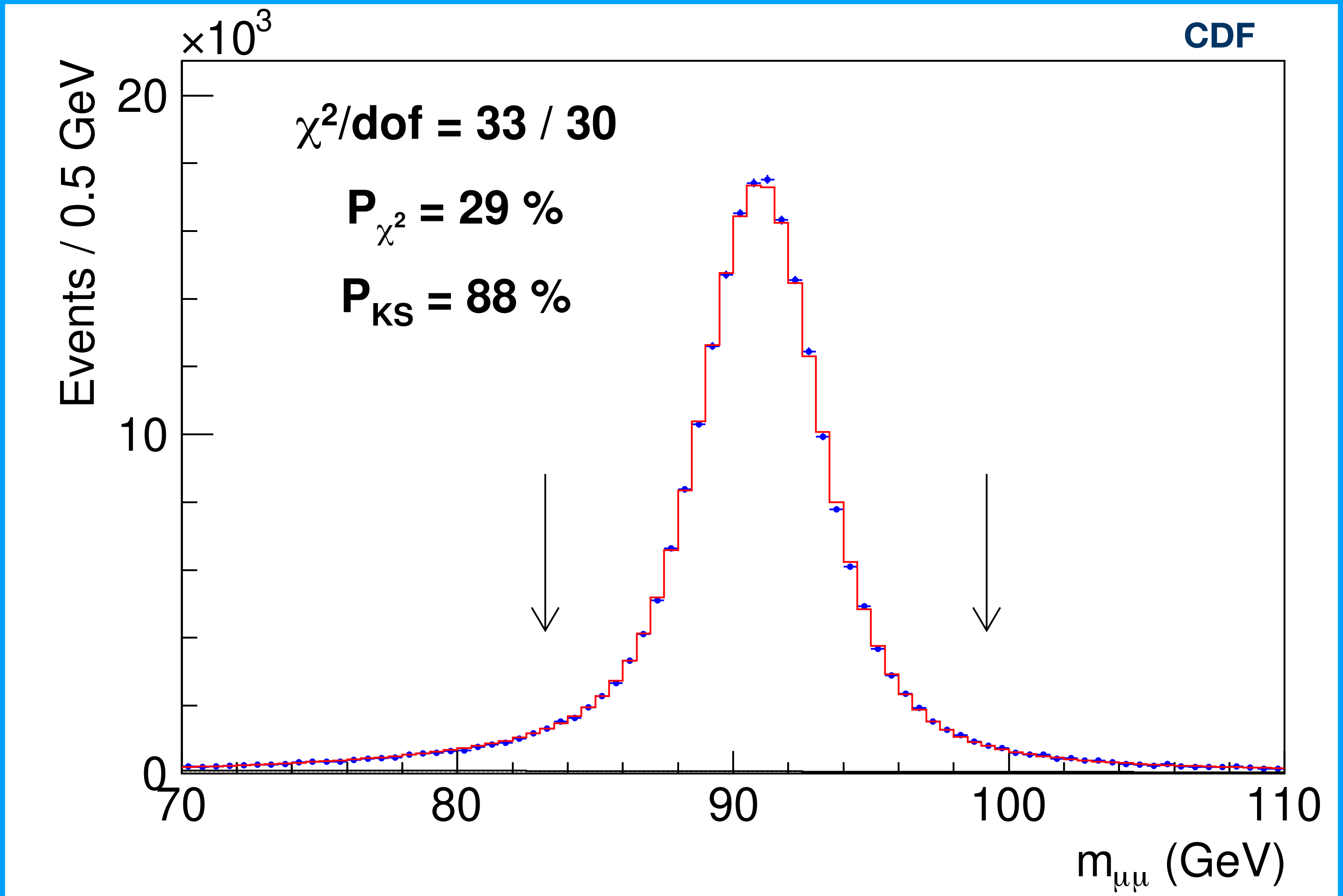

The most precise measurement of the Z boson mass at a hadron collider
Uncertainty is 3.6 times that of LEP

Electron momentum calibration

CDF measures the Z boson mass in the electron decay channel to be

$$M_Z = 91\ 194.3 \pm 13.8_{stat} \pm 7.6_{sys}\ \text{MeV}$$

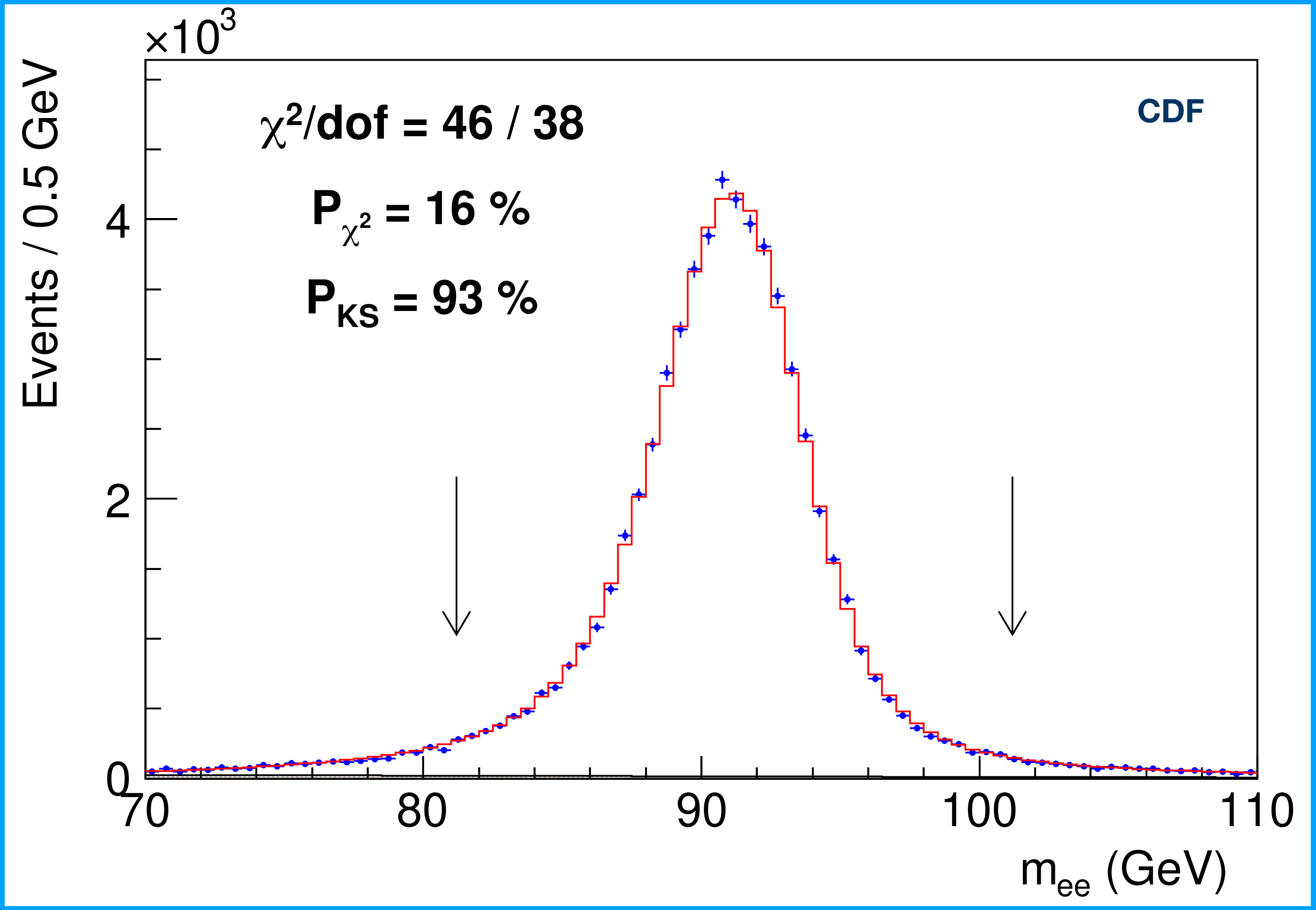

Electroweak boson masses

Higgs field potential

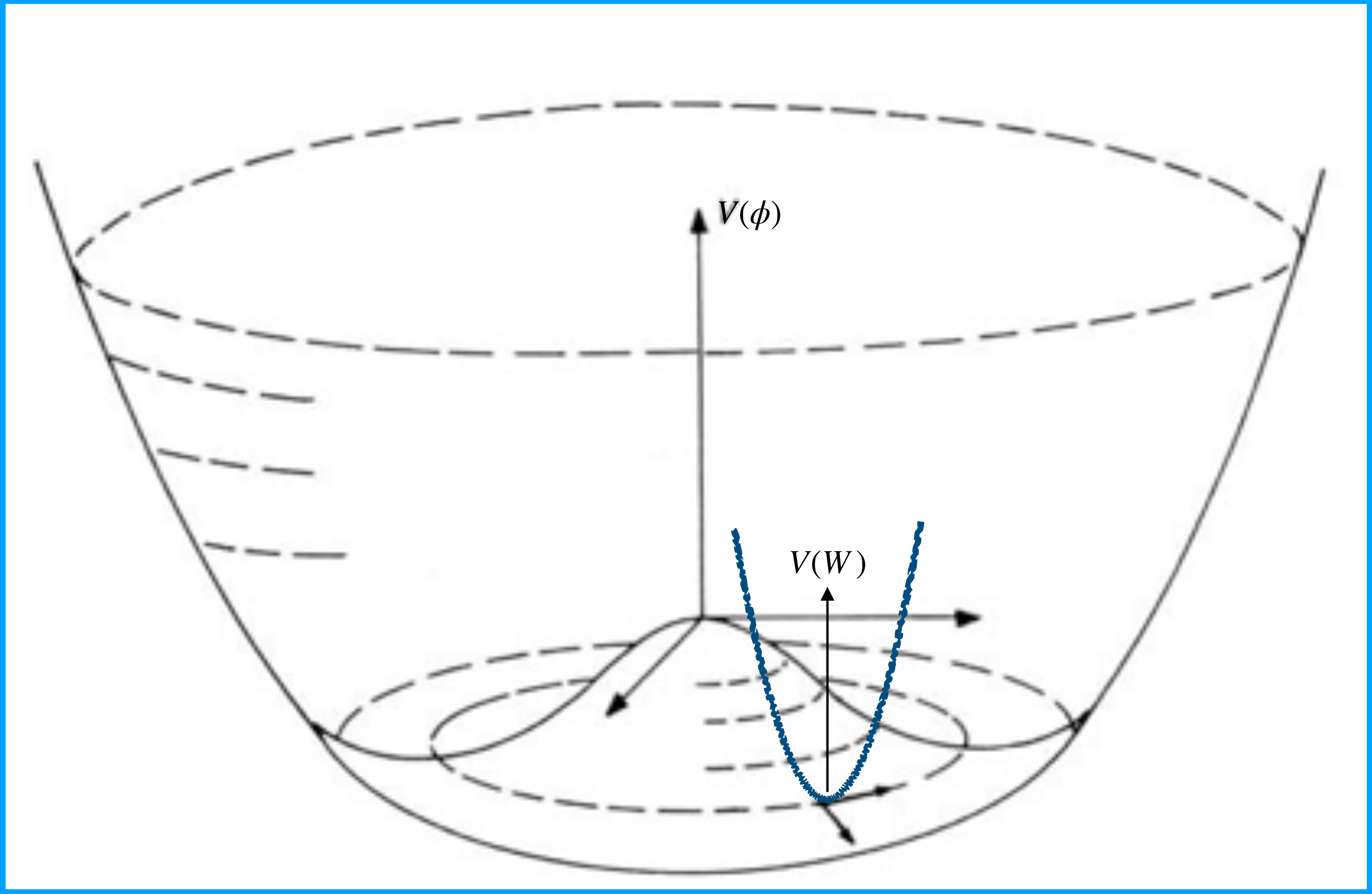

$m_H = v\sqrt{2\lambda} = 125$ GeV

$\lambda \approx 0.1$

Gauge field potential

$$V = -\frac{g^2 v^2}{8}[(W_\mu^+)^2 + (W_\mu^-)^2] - \frac{v^2(g^2 + g'^2)}{8} Z^\mu Z_\mu$$

$m_W = \frac{v}{2} g$

$m_Z = \frac{v}{2}\sqrt{g^2 + g'^2}$

$v = 246$ GeV and $g = 0.64$:

$m_W = 78.7$ GeV

Electroweak boson masses

Gauge boson masses

$$m_Z = \frac{v}{2}\sqrt{g^2 + g'^2}$$

$$m_W = \frac{v}{2} g$$

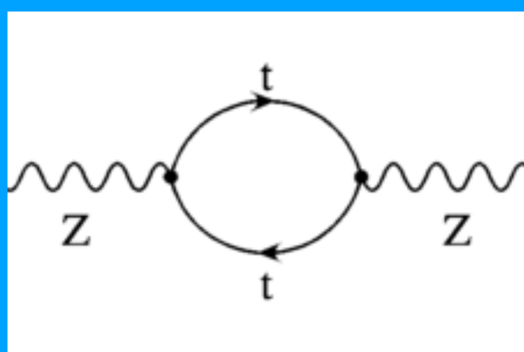

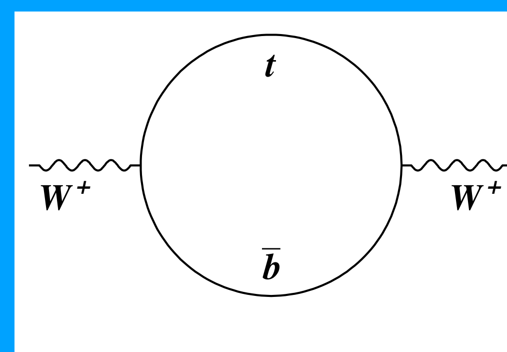

$$m_W^2 = \frac{\hbar^3}{c} \frac{\pi \alpha_{EM}}{\sqrt{2} G_F (1 - m_W^2/m_Z^2)(1 - \Delta r)}$$

$$\Delta r_{tb} = \frac{c}{\hbar^3} \frac{-3 G_F m_W^2}{8\sqrt{2}\pi^2 (m_Z^2 - m_W^2)} \times \left[m_t^2 + m_b^2 - \frac{2 m_t^2 m_b^2}{m_t^2 - m_b^2} \ln(m_t^2/m_b^2) \right]$$

SM calculation of W boson mass yields
81358 ± 4 MeV

Erler & Freitas
PDG (2022)

Higgs boson mass

$$m_H = v\sqrt{2\lambda}$$

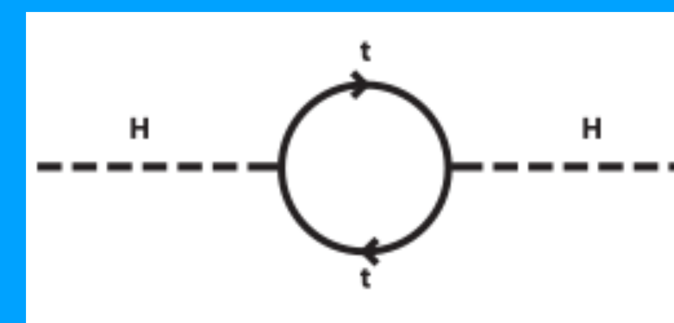

Naively integrating to a cutoff scale Λ:

$$\Delta m_H = \frac{3 g^2 m_t^2}{16 \pi^2 m_W^2} \Lambda^2$$

If there is no new physics up to scale Λ then we have 'fine-tuning' to cancel the quantum corrections

1% fine tuning: $\Lambda = 6.6$ TeV

Motivates TeV-scale new physics

W boson mass

The W boson mass is the most sensitive observable to sources of ‘naturalness’

Classic example: **Supersymmetry**

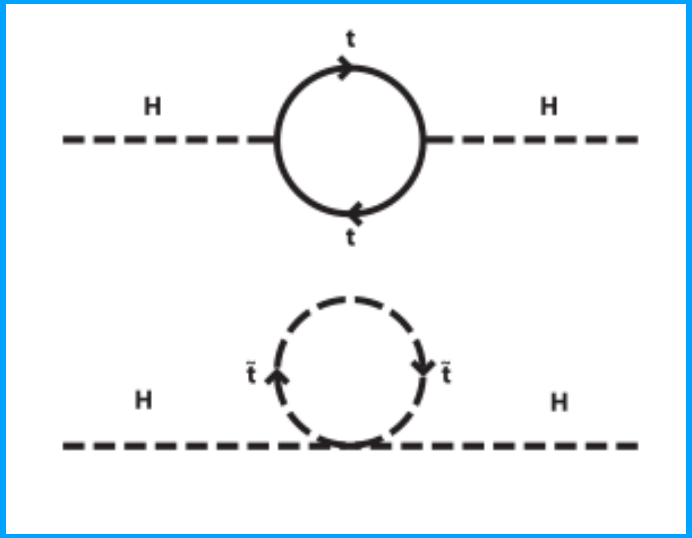

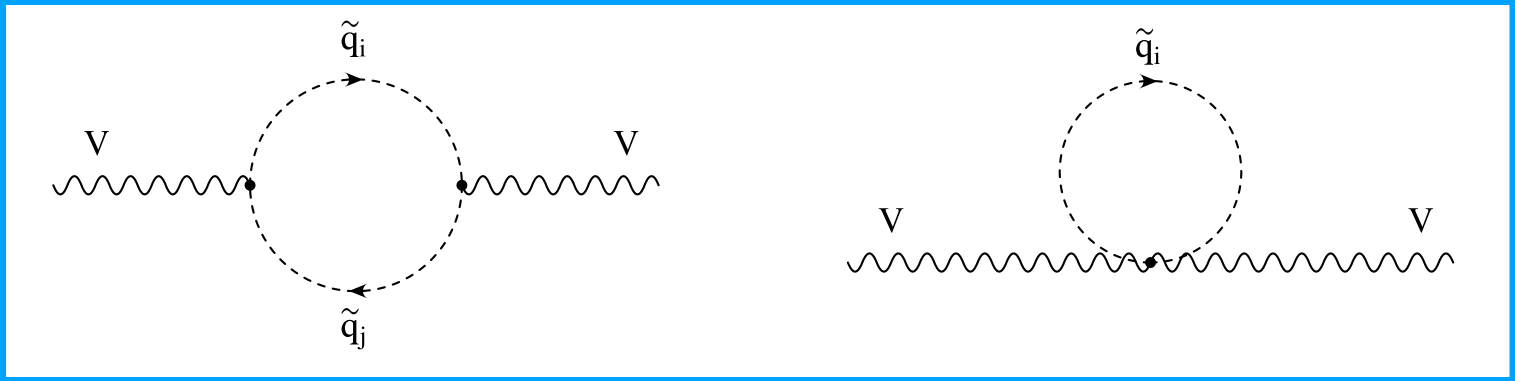

Mass splittings in supersymmetric isospin doublets:
different mass shifts for W & Z bosons

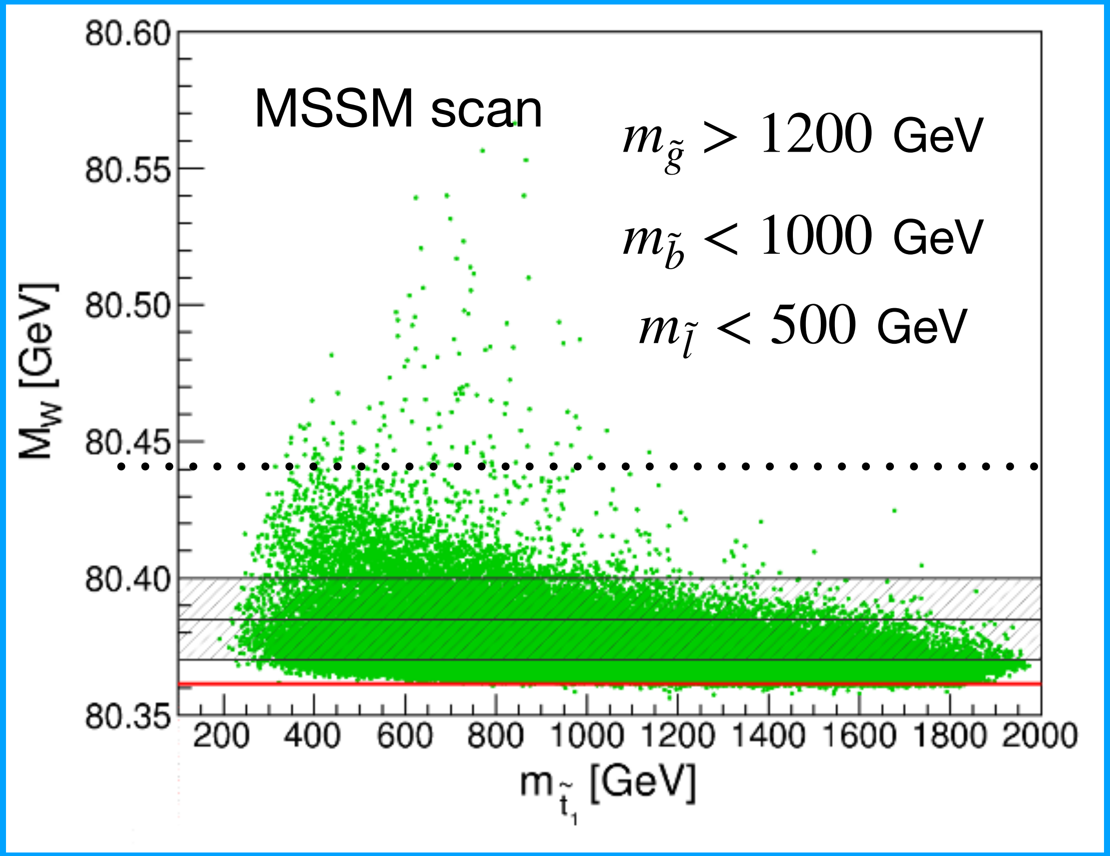

Heinemeyer, Hollik, Weiglein, Zeune
JHEP 12 (2013) 084

W boson mass

The SM effective field theory parameterizes high-scale effects

$$\mathcal{L}_{SMEFT} = \mathcal{L}_{SM} + \mathcal{L}^{(5)} + \mathcal{L}^{(6)} + \mathcal{L}^{(7)} + \cdots, \qquad \mathcal{L}^{(d)} = \sum_{i=1}^{n_d} \frac{C_i^{(d)}}{\Lambda^{d-4}} Q_i^{(d)} \quad \text{for } d > 4.$$

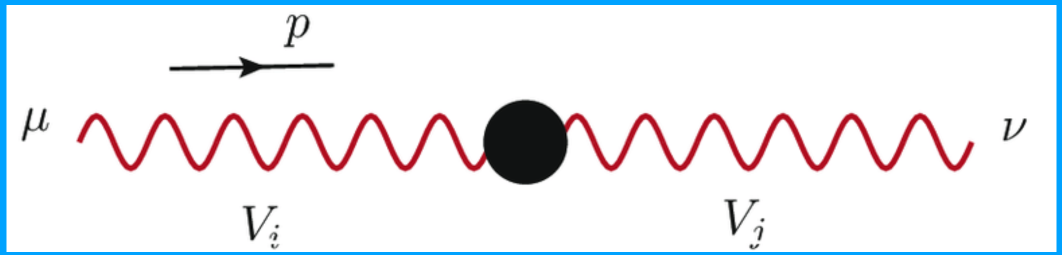

$$\frac{\delta m_W}{m_W} = \left(0.34 c_{HD} + 0.72 c_{HWB} + 0.37 c_{Hl3} - 0.19 c_{ll1}\right) \frac{v^2}{\Lambda^2}$$

I. Brivio and M. Trott, Phys. Rep. 793 (2019) 1

For $\delta m_W / m_W = 0.1\ \%$ and c_{HD}=1, $\Lambda = 4.5$ TeV

e.g. Z' boson

For $\delta m_W / m_W = 0.1\ \%$ and c_{HWB}=1, $\Lambda = 6.6$ TeV

e.g. compositeness

Smaller $c_i \rightarrow$ smaller Λ